Electronic Supplementary Information for

Investigation of the structure and dynamics of Gallium binding to high-affinity peptides elucidated by multi-scale simulation, quantum chemistry, NMR and ITC

Corey Taylor,[*a] Nora Schönberger,[b] Alice Laníková,[c,d] Michael Patzschke,[a] Björn Drobot,[e] Lukáš Žídek[c,d] and Franziska Lederer[*b]

[a] *Department of Chemistry of the f-elements, Institute of Resource Ecology (IRE), Helmholtz-Zentrum Dresden-Rossendorf, Bautzner Landstraße 400, 01328, Dresden, Germany. Tel: +49 351 260 3328*

[b] *Helmholtz Institute Freiberg for Resource Technology, Helmholtz-Zentrum Dresden-Rossendorf, BautznerLandstraße 400, 01328 Dresden, Germany.*

[c] *Central European Institute of Technology (CEITEC), Masaryk University, Kamenice 753/5, Brno, 625 00, Czech Republic.*

[d] *National Centre for Biomolecular Research, Faculty of Science, Masaryk University, Kamenice 753/5, Brno, 625 00, Czech Republic.*

[e] *Department of Biogeochemistry, Institute of Resource Ecology (IRE), Helmholtz-Zentrum Dresden-Rossendorf, Bautzner Landstraße 400, 01328, Dresden, Germany. Tel: Tel: +49 351 260 2427.*

5 Methods

5.1 Isothermal Titration Calorimetry

A MicroCal Peaq-ITC (Malvern Instruments, Worcestershire, UK) with 200 μL sample cell and 40 μL titration syringe was used to determine the thermodynamic parameters of the peptide-Ga^{3+} interactions. Thermograms were recorded in 19x2 μL injection steps and evaluated with the MicroCal PEAQ-ITC Software V 1.3 (Microcal-Malvern Panalytical, Malvern, UK). The heat change in the sample cell was measured in relation to a water-filled reference cell, which was obtained by stepwise titration of a Ga^{3+} solution to a peptide solution in the sample cell. Experiments were performed in 150 mM NaCl at pH 3.0, adjusted with either 80 mM acetate buffer (77.2 mM acetic acid, 2.8 mM sodium acetate, pH 3.0) or 1 mM HCl.

For the titration, 3.6 mM Ga^{3+} ($Ga(NO_3)_3$-xH_2O, Alfa Aeser Kandel AG, Landau, Germany) and between 190 - 280 μM peptide (DGpeptides Co.,Lt; Hangzhou, CN) were used in the corresponding buffer. To determine the background heat, control experiments were performed in which the corresponding metal solution was titrated in buffer without peptide.

5.2 Molecular dynamics simulation

Three-dimensional structures for both peptides were prepared with UCSF Chimera[38] from the sequences HTCHIQSCDHLA and NYLPHQSSSPSRC for peptide M3 and C3.15, respectively. Structures were energy minimised with CHARMM 43b2[39] using Steepest Descent[40] (SD) and conjugate gradient[41] (CONJ) minimisation. The system was solvated and neutralising ions added with CHARMM-GUI[42] with parameter and topology files generated at each stage. A cubic TIP3[43] water box with edge distance of 10Å was generated to ensure complete coverage of the peptide. Na^+ and Cl^- counter ions were added to an concentration of 150mM. Periodic boundary conditions were applied.

Solvent-exposed histidines would be very likely doubly-protonated at biological pH and the same would be expected at low pH. Histidines were therefore prepared for simulation by ensuring both nitrogens for each histidine (Nδ and Nε) were protonated. To ensure the correct protonation state for any other ionisable residue, the software tool PROPKA[44] was used to output a structure for both peptides commensurate with a pH of 3.0. In each case, the structure outputted by PROPKA was used for subsequent simulations.

Classical simulations were conducted on both peptides in the absence of Ga^{3+}. All simulations were conducted with CHARMM 43b2 using the CHARMM36m[45] force field. For equilibration steps, a harmonic constraint of 24 Kcal/mol/Å^2 was first applied to peptide backbone atoms. This was followed by short minimisations of 50 steps each (SD/Adopted Basis Newton-Raphson[46]) to relax the structure. An equilibration simulation of time step 1fs was run for 250ps at a temperature of 303.15K. The Vertlet[47] integrator and SHAKE[48] algorithms were used in concert with the Nose-Hoover[49] thermostat to ensure a constant temperature. Checks were conducted of pressure, temperature, etc. to ensure stability prior to production simulations.

Constant-pressure (NVT) production simulations were run with Langevin dynamics and time step of 2fs for a total of 50ns with restarts every 1ns. GPU-accelerated simulations were performed with the CHARMM/OpenMM (v7.3.1) interface[50]. A constant pressure of 1 atm was maintained with the Monte Carlo barostat included with OpenMM. Pressure Particle Mesh Ewald summation[51] was used with non-bonded interaction cut-offs set at 11Å. The Leapfrog[52] integration algorithm was used. SHAKE was again switched on. Each simulation was performed with three replicates to ensure a significant hypergeometric p-value.

Post-processing of trajectories was conducted using CPPTRAJ[53] in the Ambertools[54] suite. The *hbond* module was used to calculate time-series and summary data for solute:solute and solute:solvent interactions with default program cutoffs applied with respect to hydrogen bond parameters (distance: < 3 Å, angle $> 135^\circ$). Heirarchical agglomerative clustering was used with clustering stopped when either 5 clusters or ε=4.0 was reached. Root-Mean Square Deviation (RMSD) from starting structures were calculated and plotted. LOcally EStimated Scatterplot (LOESS) smoothing[55] was applied to plots with a smoothing parameter value, α, of 0.75.

QMMM simulations were conducted with CHARMM 38b2 and Turbomole 7.3.1[56] via the CHARMM/Turbomole interface[57].

The 'QM' region for each peptide was initially delineated by all peptide atoms within 5Å of its Ga^{3+} ion. All waters within its 1st and 2nd solvation shell after equilibration were also included. Where the boundary between QM and MM regions intersects with a covalent bond, monovalent link atoms along the direction of the bond were used. Bonds cut in this fashion were C-C bonds in the peptide, typically a Cα-Cβ bond.

The quantum chemical portion of the QMMM calculation was calculated via a Density Functional Theorem (DFT) hybrid functional at the B3LYP[58–61]/def2-SVP[62] level of theory. Point charge embedding was used to ensure that forces acting on the MM region by the QM region were included in the Hamiltonian evaluated as part of the DFT calculation. The D3 dispersion correction method[63] as well as Resolution of the Identity[64] (RI) and multipole accelerated RI-J[65] approximations were used. Equilibration steps were as for classical simulations.

Equilibration steps were run for 5000 steps where the centre-of-mass positions of the Ga^{3+}, acetate anion (ACET) and nearby residues were constrained via spherical harmonic potentials of force constant 200 kcal.mol^{-1} for salt-bridge interactions and 100 kcal.mol^{-1} for non-bonded interactions. This was to ensure appropriate starting positions for production simulations as the MM force field tended to overestimate the strength of ionic interactions with the Ga^{3+} ion. Absent this step, the result was placement of interaction partners in energetically unfavourable positions, well within van der Waals radius for each interaction partner (1.2-1.4 Å). Constraints ensured distances of 2.2-2.4 Å for all Ga^{3+} interaction partners prior to production simulation.

Production Langevin QMMM simulations were run with a time step of 1fs with the scalar friction coefficient (FBETA) set to 8.0 to assist in more thorough exploration of conformational space. Each simulation and three replicates was run in total for 25ps each. Upon energetic convergence of a stabilised binding position of the peptide with Ga^{3+} structures for both peptides were take as inputs for quantum chemical optimisation and further bonding analysis.

5.3 Quantum chemistry

Each converged structure was truncated to include waters within 5Å and residue atoms within 10 Å of the Ga^{3+} position. All quantum chemical calculations were conducted with Turbomole 7.3.1 using a DFT hybrid functional at the RI-B3LYP-D3/def2-SVP(C, O, N, H) and def2-TZVP(Ga) levels of theory. COnductor-like Screening MOdel[66] (COSMO) continuum solvation (ε=80) was used to account for solvent forces. Structures were fully optimised and vibrational frequencies calculated to ensure that stationary points were at their energetic minimum. Further frequency analysis was conducted with Molden[67].

All real-space analyses and post-processing of converged wave functions were conducted with MultiWFN v3.6[68].

Fuzzy Bond Order (FBO[69]) was preferred to Mayer bond order[70] as it is less dependent upon basis set size. Each calculated FBO (B_{AB}), an extension of the Mayer bond order, considers three-dimensional regions for given atoms A and B in 'fuzzy' atomic space as a function of the total density and spin density (**P**):

$$B_{AB} = 2\sum_{\mu,\nu}\left[(P^{\alpha}S^{A})_{\mu\nu}(P^{\alpha}S^{B})_{\nu\mu} + (P^{\beta}S^{A})_{\mu\nu}(P^{\beta}S^{B})_{\nu\mu}\right] \tag{1}$$

Where **S** is the overlap matrix of fuzzy atomic basis functions:

$$S^{A}_{\mu\nu} = \int W_A(r)\chi^{*}_{\mu}(r)\chi_{\nu}(r)dr \tag{2}$$

Multi-centre bond orders[71] can be calculated as essentially an extension of the Mayer bond order for more than two centres. In the three-centre case:

$$I_{ABC} = \sum_{a\in A}\sum_{b\in B}\sum_{c\in C}(PS)_{ab}(PS)_{bc}(PS)_{ca} \tag{3}$$

To ensure comparability of different multiple-centre bond order, the Multi-Center Index (MCI)[72], was computed via summation of all possible I_{ring} contributions, generalised from the Wiberg bond index[73], of all atoms in $\mathscr{A}$:

$$MCI(\mathscr{A}) = \frac{1}{2n}\sum_{\mathscr{P}(\mathscr{A})} I_{ring}(\mathscr{A}) \tag{4}$$

For the purposes of this study, a normalised form[74] of the MCI was used.

Molecular ESP (MESP) maps were created by mapping electrostatic potential values onto the area represented by electron density. Plots were created with an isovalue of ρ=0.5 with areas of potential represented with the BWR scheme (-ve ESP $\rightarrow$ +ve ESP). Plots of vdW surface ESP were generated from Turbomole output using MultiWFN's Quantitative Molecular Surface Analysis module where the electrostatic potential was calculated and mapped at vertices of the vdW surface (ρ=0.001). Surface and ESP maxima and minima were also calculated.

Reduced Density Gradient (RDG) methods were used to calculate and visualise weak interactions for each complex. The Non-Covalent Interaction (NCI) method[75] was used to calculate and plot RDG isosurfaces of magnitude 0.5 and grid size 0.116 Bohr. Further integrations of RDG isosurfaces with electron density as the integrand were conducted to further characterise weak interactions where regions of RGD < 0.5 were used to define regions where grids could be calculated. Grids in each domain were then used to calculate a real-space interatomic potential, q_{bind}, of extension distance 3.0 Bohr for domains taking into account the attractive and repulsive contributions to binding[76]:

$$q_{att} = \int_{\Omega(NCI)} \rho^n(\overrightarrow{r}) d\overrightarrow{r} \qquad \lambda_2(\overrightarrow{r}) < 0 \tag{5}$$

$$q_{rep} = \int_{\Omega(NCI)} \rho^n(\overrightarrow{r}) d\overrightarrow{r} \qquad \lambda_2(\overrightarrow{r}) > 0 \tag{6}$$

$$q_{bind} = -(q_{att} - q_{rep}) \tag{7}$$

Bonding analysis was conducted using Bader's Quantum Theory of Atoms-In-Molecules[77] (QTAIM). That all possible Critical Points (CPs) calculated during topology analysis were found was verified by the Poincaré-Hopf relationship. All CPs were calculated and analysed, corresponding to (3, -3) Atomic Critical Points (ACPs), (3, -1) Bond Critical Points (BCPs), (3, +1) Ring Critical Points (RCPs) and (3, +3) Cage Critical Points (CCPs) although only BCPs were used.

Real space functions were also calculated from the wave function. Real space functions exhibit one or more maxima, also known as attractors, that correspond to (3,-3) critical points. A given basin is a subspace of the whole space and contains an attractor. Delocalisation Indices[78] (DI), calculated from the integration of the Fermi hole density, are measures of the number of α and β electrons shared or exchanged between two atoms or basins:

$$DI = 2F(\Omega,\Omega') = 2[F^{\alpha}(\Omega,\Omega') + F^{\beta}(\Omega,\Omega')] = -2\sum_{ij}^{N} S_{ij}(\Omega)S_{ij}(\Omega') \tag{8}$$

where $S_{ij}(\Omega)$ is the overlap integral of α spin orbitals Φ_{i} and Φ_{j} over the atomic basin Ω and $F^{\alpha}(\Omega,\Omega')$ is the Fermi correlation for α electrons of atomic basin Ω delocalised into a nearby basin Ω':

$$F^{\alpha}(\Omega,\Omega') = \sum_{ij}^{N\alpha} NS_{ij}(\Omega)S_{ij}(\Omega') \tag{9}$$

The ellipticity of the electron density is defined as:

$$\varepsilon(r) = [\lambda_1(r)/\lambda_2(r)] - 1 \tag{10}$$

where λ_1 and λ_1 are the lowest and second lower eigenvalues, respectively, of the Hessian matrix of the density. At a given BCP, ε(r) is representative of the curvature of electronic density that is perpendicular to the bond itself and, hence, offers an indication at which atomic centre density is greatest.

A Taylor expansion of the spherically-averaged spin pair probability, the Electron Localisation Function (ELF[79]), can be used to define a simple measure of electronic localisation:

$$ELF(r) = \frac{1}{1 + [D(r)/D_0(r)]^2} \tag{11}$$

where, for a closed-shell system, the probability of finding an electron, D(r), with respect to the the position of a reference (uniform electron gas) electron, D_0(r), can be expressed in terms of the sums of molecular orbital contributions, φ, and density, ρ:

$$D(r) = \frac{1}{2}\sum_i \eta_i |\lambda\phi_i(r)|^2 - \frac{1}{8}\frac{|\lambda\rho(r)|^2}{\rho(r)} \tag{12}$$

$$D_0(r) = \frac{3}{10}(3\pi^2)^{\frac{2}{3}}\rho(r)^{\frac{5}{3}} \tag{13}$$

The ELF is constrained to be within a range of [0,1], where the upper limit corresponds to perfect localisation.

All representations of simulations and optimized structures were created with the Visual Molecular Dynamics (VMD) program version 1.9.3[80]. All plots and analyses were completed with the R statistical language[81] and the Tidyverse[82] using a colour blind-friendly palette for all plots (DOI: 10.5281/zenodo.3381072).

5.4 NMR spectroscopy

Samples of peptides M3 and C3.15 were prepared at the Helmholtz Institute Freiberg for Resource Technology, Biotechnology department in Dresden, Germany. Each sample consisted of 0.5 mM peptide with trifluoracetic acid, 150 mM NaCl and 0.02% NaN_3 in 10% D_2O. The samples with Ga^{3+} were of the same composition and contained 0.5 mM $Ga(NO_3)_3$. HCl was used to adjust pH to 3. Both peptides were not isotopically labelled. The measurements were carried out on the samples in 5 mm NMR tubes (600 μL).

All experiments were conducted on 850 MHz, 950 MHz and 600 MHz NMR Bruker Avance III spectrometers equipped with quadruple (triple - 950 MHz) resonance inverse cryoprobe with cooled ^{1}H and ^{13}C preamplifiers. For each peptide, there were three types experiments measured apart from the 1D proton spectra for sample control. The 2D ^{1}H-^{1}H NOESY and ^{1}H-^{13}C HSQC experiments were measured on 850 MHz and 950 MHz spectrometers, the 2D ^{1}H-^{1}H TOCSY on the 600 MHz spectrometer. The temperature was set to correspond to 25°C calibrated on the pure methanol sample with D_2O in coaxial arrangement by measuring the distance between proton peaks.

A pulse sequence of hsqcfpf3gpphwg of the standard Bruker library used for Heteronuclear Single Quantum Coherence (HSQC) experiments with water suppression achieved by a WATERGATE sequence. The acquisition mode in the indirect dimension was States-TPPI. Spectra were acquired with spectral widths set to 16 ppm in the direct dimension with the carrier frequency matching water resonance (at 4.7 ppm), and to 80 ppm in the indirect dimension with carrier frequency of 40 ppm. The time domain matrix consisted of 512 $\times$ 4096 complex data points. The total number of scans was 128 and recovery delay set to 1.2 s. The sequence used for decoupling was GARP.

A pulse sequence of dipsi2gpph19 was used for TOtal Correlation SpectroscopY (TOCSY) experiments with water suppression by the WATERGATE 3-9-19 sequence with gradients. The sequence used for the TOCSY mixing period was DIPSI-2. The acquisition mode in the indirect direction was States-TPPI. The spectra were acquired with spectral widths set to 16 ppm in the direct dimension and to 10 ppm in the indirect dimension, in both cases with the carrier frequency set to the water resonance. The time domain matrix consisted of 512 $\times$ 4096 complex data points. The TOCSY mixing time was set to 80 ms. The recovery delay was 2 s, the number of scans was 40.

A pulse sequence of noesygpph19 used for Nuclear Overhauser Effect SpectroscopY (NOESY) experiments. Parameters regarding acquisition modes were identical to that of the TOCSY measurements. The mixing time was set to 250 ms and the recovery delay was 1.5 s. The number of scans varied for each peptide, SDM-M3 peptide with and without Ga^{3+} was measured with 304 and 288 scans, C3.15 was measured with 128 scans in both cases.

Data post-processing was completed with NMRPipe[83], peak assignment using NMRFAM-Sparky[84]. Any other processing was completed with in-house scripts.

To compare dihedral angles (φ) with the J-coupling values, $^3J_{H^N\text{-}H^\alpha}$ constants were calculated for the dihedral angles of nine types of β-turns using the Karplus equation:

$$^3J(\theta) = A\cos^2\theta + B\cos\theta + C \tag{14}$$

where $\vartheta = \varphi$ - 60°, with published parameters[85] of A = 7.97, B = -1.26 and C = 0.63. Calculated $^3J_{H^N\text{-}H^\alpha}$ values are presented in Table S19.

6 Supplemental results

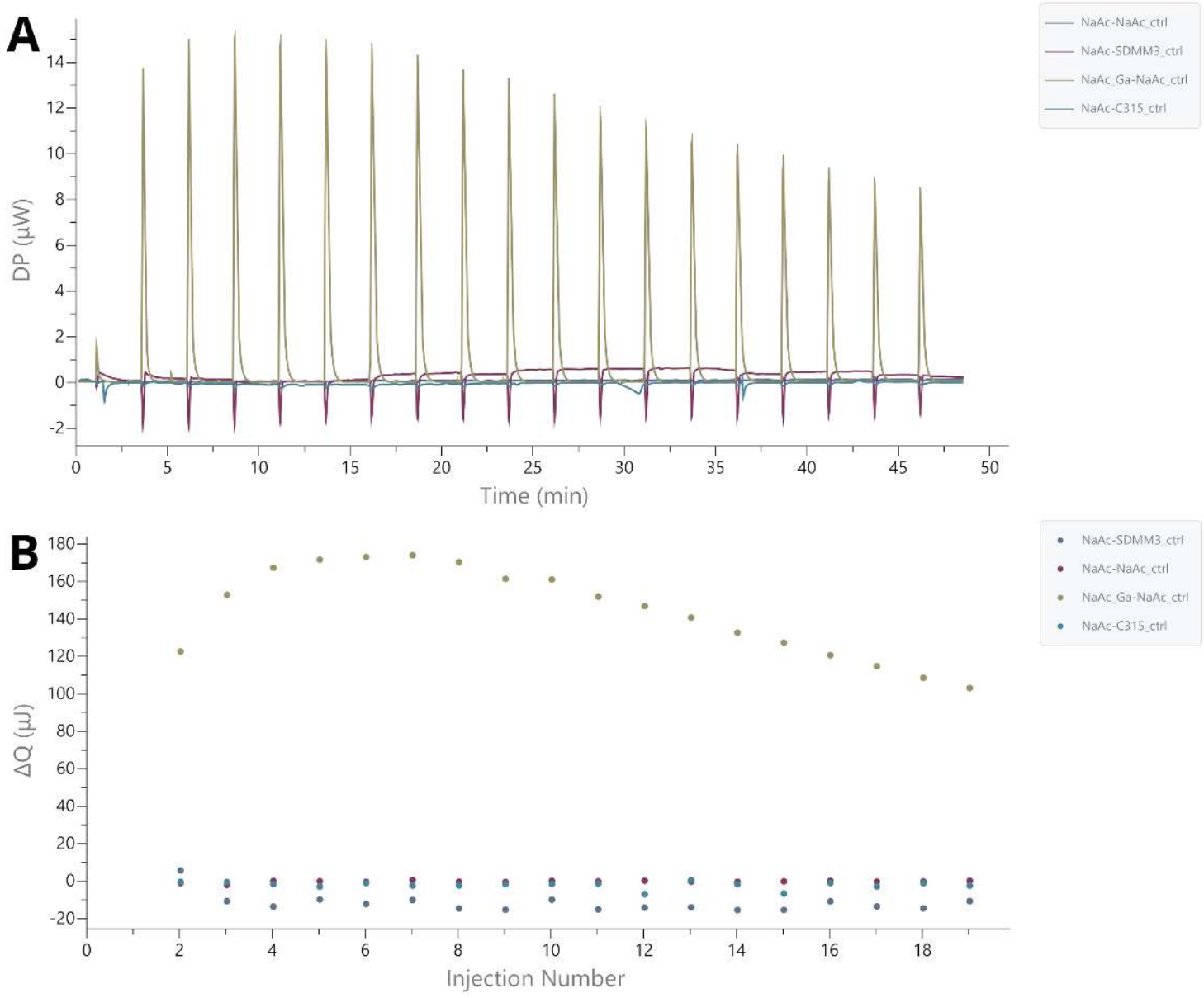

Fig. S1 Results from ITC control experiments involving sodium acetate buffer (NaAc) displaying (A) thermogram and (B) Wiseman plot describing the addition of buffer to buffer, buffer to peptides M3 and C3.15 and $Ga^{3+}$to buffer. These background data were used to construct the baseline corrected plots in Figures S3 and S4. Of note is a substantial energy increase upon the addition of Ga to ACET buffer, likely the result of the expected complexation of Ga by the acetate anion. No other notable energy changes were observed.

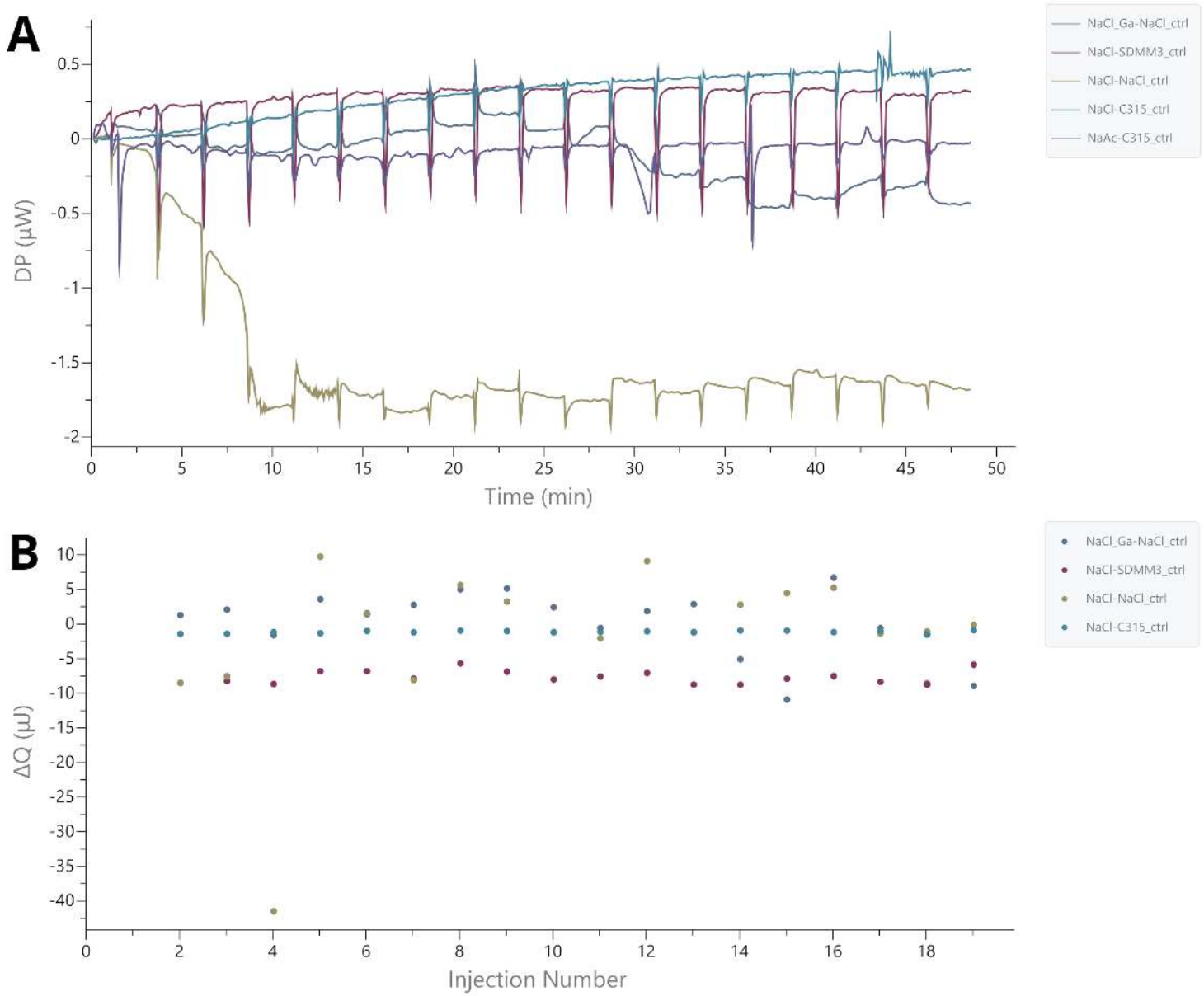

Fig. S2 Results from ITC control experiments involving sodium acetate buffer (NaCl) displaying (A) thermogram and (B) Wiseman plot describing the addition of buffer to buffer, buffer to peptides M3 and C3.15 and $Ga^{3+}$to buffer. No notable energy changes were observed.

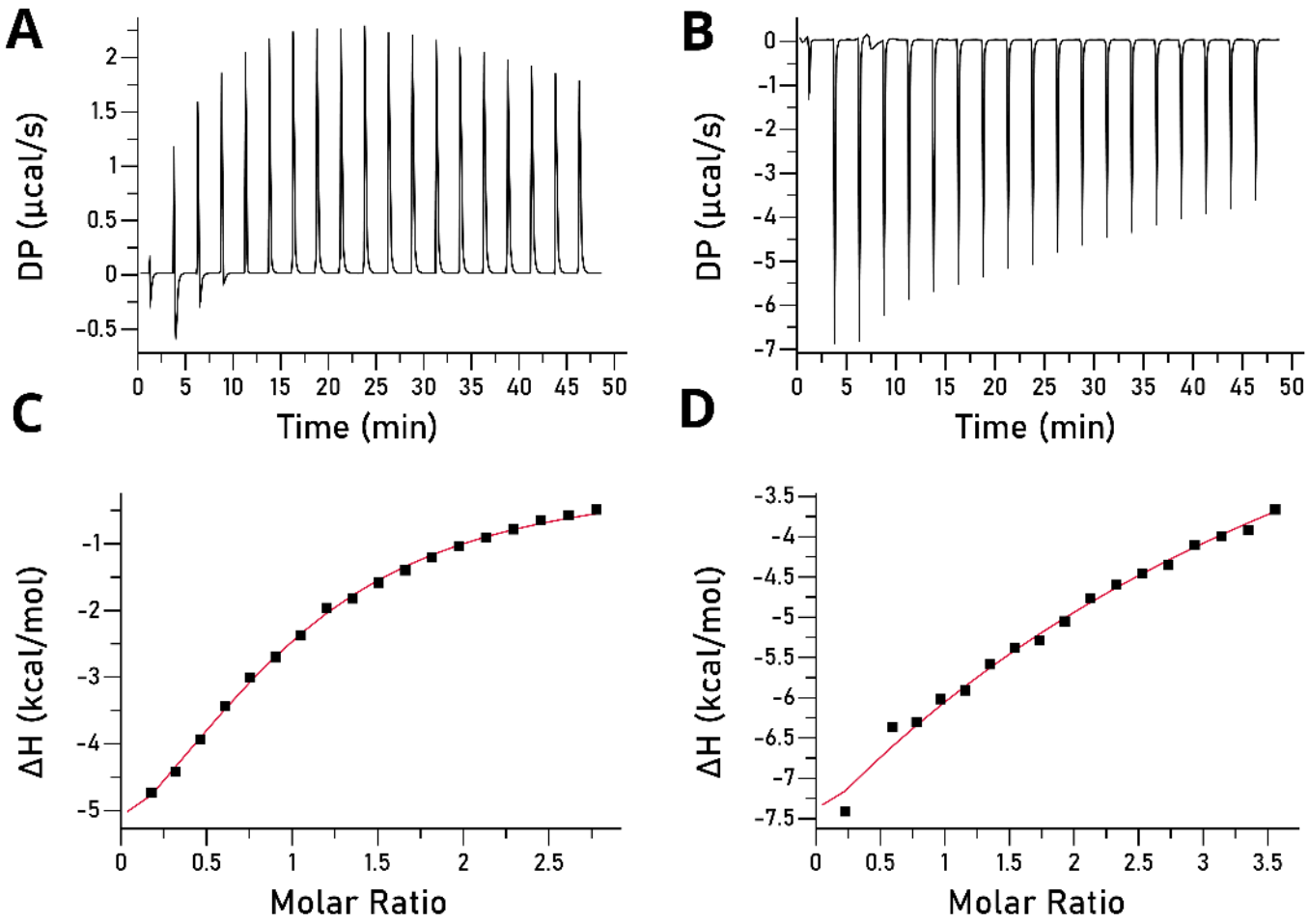

Fig. S3 Results from Isothermal Calorimetry (ITC) for peptide M3 displaying the baseline-corrected thermogram and Wiseman plot in the absence (A and C) and presence (B and D) of ACET.

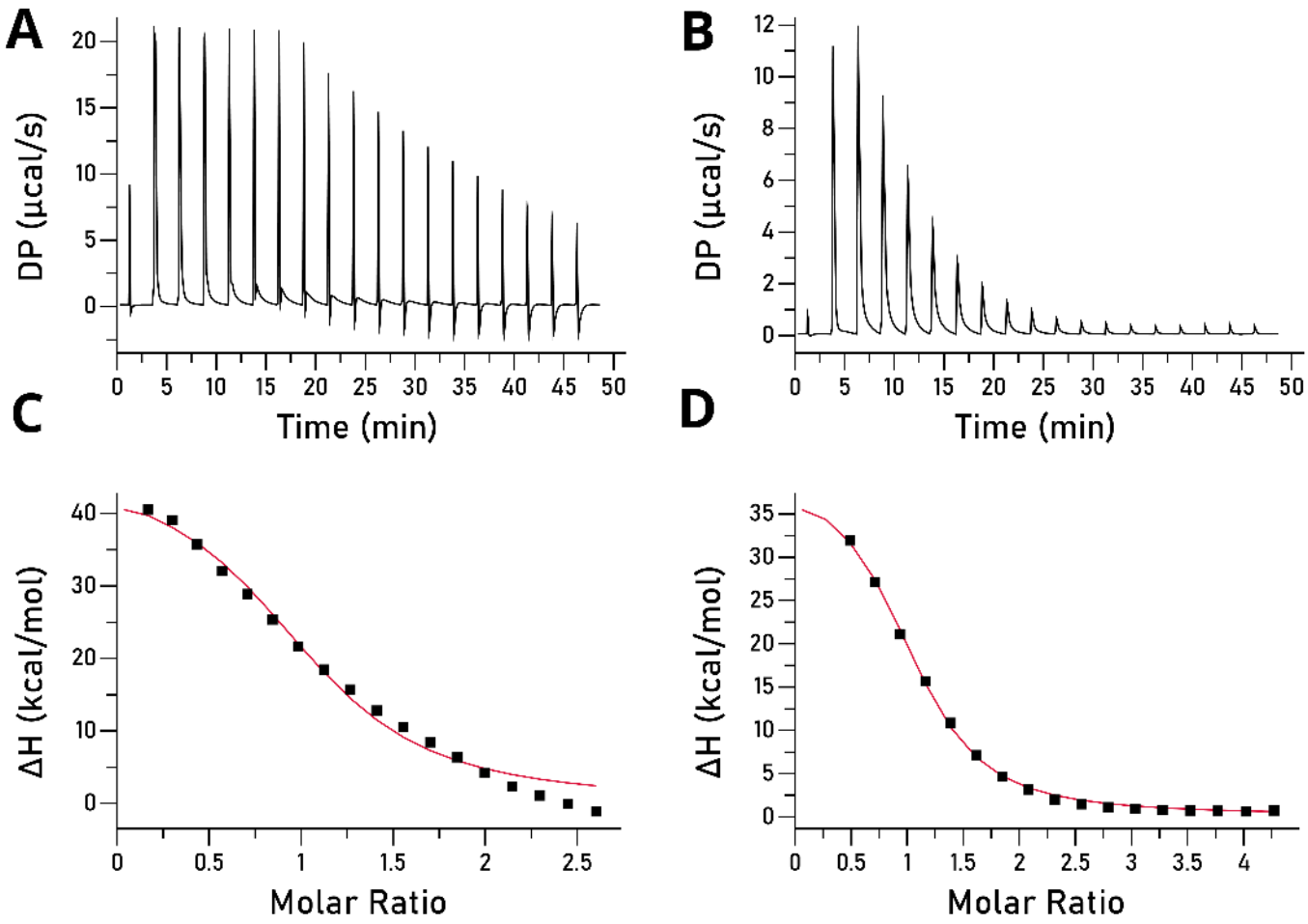

Fig. S4 Results from Isothermal Calorimetry (ITC) for peptide C3.15 displaying the baseline-corrected thermogram and Wiseman plot in the absence (A and C) and presence (B and D) of ACET.

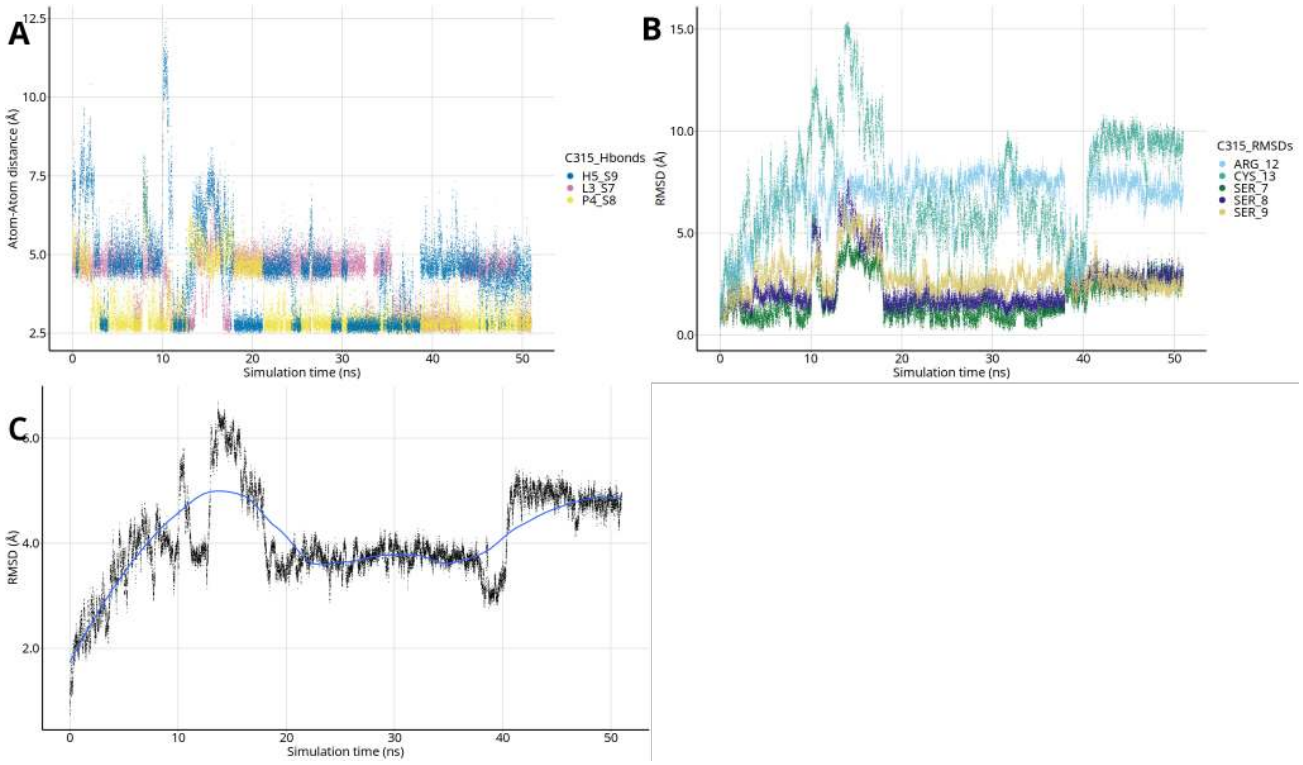

Fig. S6 Time series plots for peptide C3.15 indicative of (A) a hydrogen bond network formed between three pairs of residues (L3-S7, P4-S8 and H5-S9) (B) higher RMSDs and, thus, greater movement for R12-C13 as compared to S7-S9 and (C) overall RMSD, indicative of structural convergence.

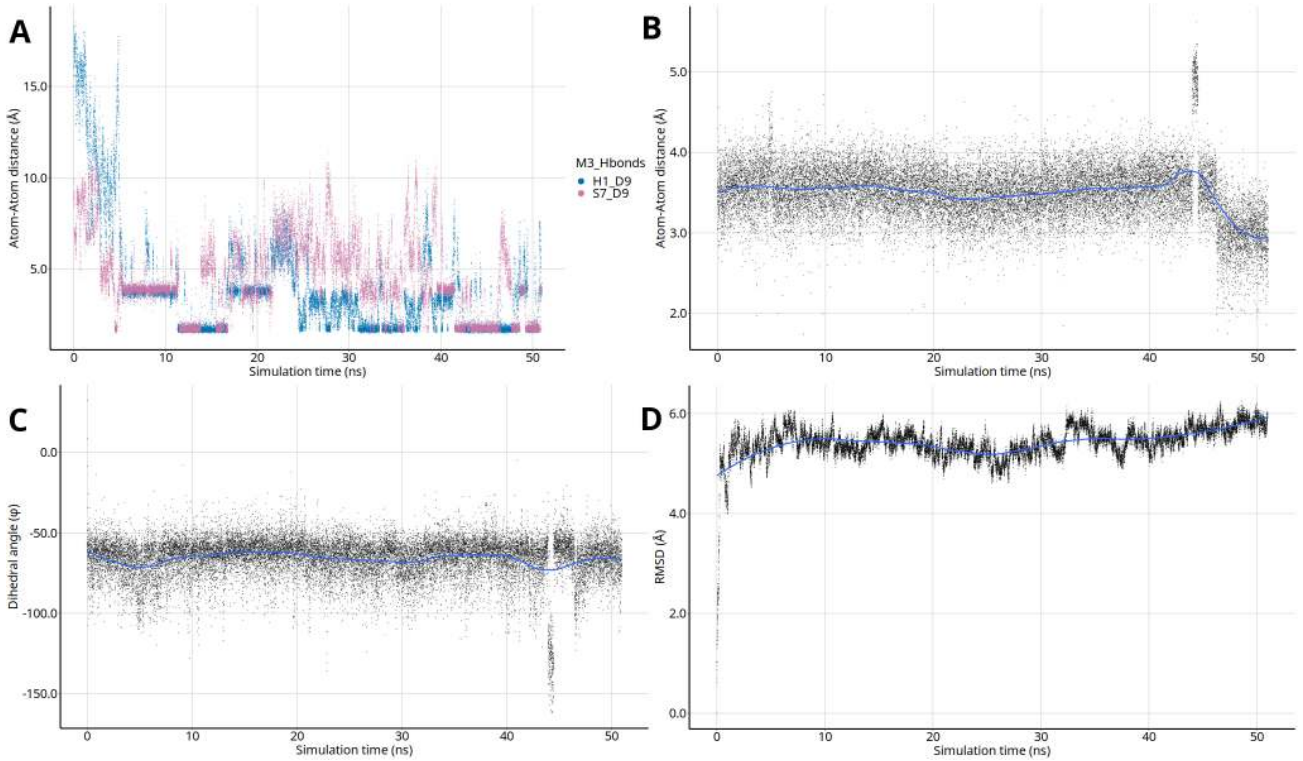

Fig. S5 Time series plots for peptide M3 indicative of (A) a hydrogen bond network formed between H1-D9-S7 (B) formation of a hydrogen bond between the backbone carbonyl of I5 and the amide NH of S7, indicative of an β-I turn at the junction point of I5-Q6-S7 (C) dihedral angle (φ) for Q6 (D) overall RMSD, indicative of structural convergence.

Table S1 Top-10 hydrogen bonds formed in *hbond* analysis of classical MD simulations, peptides M3 and C3.15. Descriptive data are displayed including the number (Frames) and proportion (Frac) of frames each a particular hydrogen-bond was present, the average distance (AvgDist, Å) and angle (AvgAng, θ) for each bond.

Peptide M3						
Acceptor	**DonorH**	**Donor**	**Frames**	**Frac**	**AvgDist**	**AvgAng**
ILE_5@O	HSP_4@HN	HSP_4@N	43001	0.86	2.7876	153.6221
HSP_1@OY	ASP_9@HN	ASP_9@N	14442	0.2888	2.85	156.4311
ASP_9@OD2	HSP_1@HD1	HSP_1@ND1	11527	0.2305	2.7002	163.2632
ASP_9@OD1	HSP_1@HD1	HSP_1@ND1	11232	0.2246	2.699	163.3429
HSP_1@OY	CYS_8@HN	CYS_8@N	9433	0.1887	2.8177	145.6622
ASP_9@OD2	SER_7@HG1	SER_7@OG	8117	0.1623	2.6897	161.147
ASP_9@OD1	SER_7@HG1	SER_7@OG	6821	0.1364	2.6903	160.9112
CYS_8@O	HSP_10@HD1	HSP_10@ND1	3940	0.0788	2.7892	161.9004
HSP_10@O	HSP_10@HD1	HSP_10@ND1	1921	0.0384	2.8204	143.7124
CYS_8@O	SER_7@HG1	SER_7@OG	1906	0.0381	2.7517	155.3118
Peptide C3.15						
Acceptor	**DonorH**	**Donor**	**Frames**	**Frac**	**AvgDist**	**AvgAng**
TYR_2@O	GLN_6@HN	GLN_6@N	35876	0.7175	2.848	162.6847
PRO_4@O	SER_8@HG1	SER_8@OG	25201	0.504	2.7635	161.4867
LEU_3@O	SER_7@HN	SER_7@N	23937	0.4787	2.8646	157.5196
PRO_4@O	SER_8@HN	SER_8@N	20400	0.408	2.8646	154.5552
LEU_3@O	SER_7@HG1	SER_7@OG	18082	0.3616	2.7676	161.4471
ASN_1@O	HSP_5@HN	HSP_5@N	13814	0.2763	2.8889	157.662
HSP_5@O	SER_9@HG1	SER_9@OG	10084	0.2017	2.7491	162.4793
GLN_6@O	SER_9@HG1	SER_9@OG	6801	0.136	2.7367	162.4539
SER_7@O	ARG_12@HH22	ARG_12@NH2	6772	0.1354	2.8047	158.8852
HSP_5@O	SER_9@HN	SER_9@N	6332	0.1266	2.871	151.5162

Table S2 Output from cluster analysis of classical MD simulations, peptides M3 and C3.15. Descriptive data are displayed including the number and proportion of frames each cluster centroid is present in and descriptive data regarding the distribution of distances from the centroid of each cluster for each frame within that cluster.

Peptide M3						
Cluster	**Frames**	**Frac**	**AvgDist**	**Stdev**	**Centroid**	**AvgCDist**
c0	42691	0.854	3.707	0.814	20108	4.906
c1	2973	0.059	2.315	0.649	42955	4.85
c2	2599	0.052	3.02	0.921	46807	4.849
c3	1611	0.032	2.782	0.907	805	4.714
c4	126	0.003	1.72	0.614	53	5.146
Peptide C3.15						
Cluster	**Frames**	**Frac**	**AvgDist**	**Stdev**	**Centroid**	**AvgCDist**
c0	27412	0.548	3.515	0.944	11230	4.852
c1	11339	0.227	3.572	0.807	41010	4.573
c2	7281	0.146	3.449	0.994	47012	5.250
c3	2540	0.051	3.041	0.940	44151	4.780
c4	1428	0.029	2.960	0.777	36871	5.110

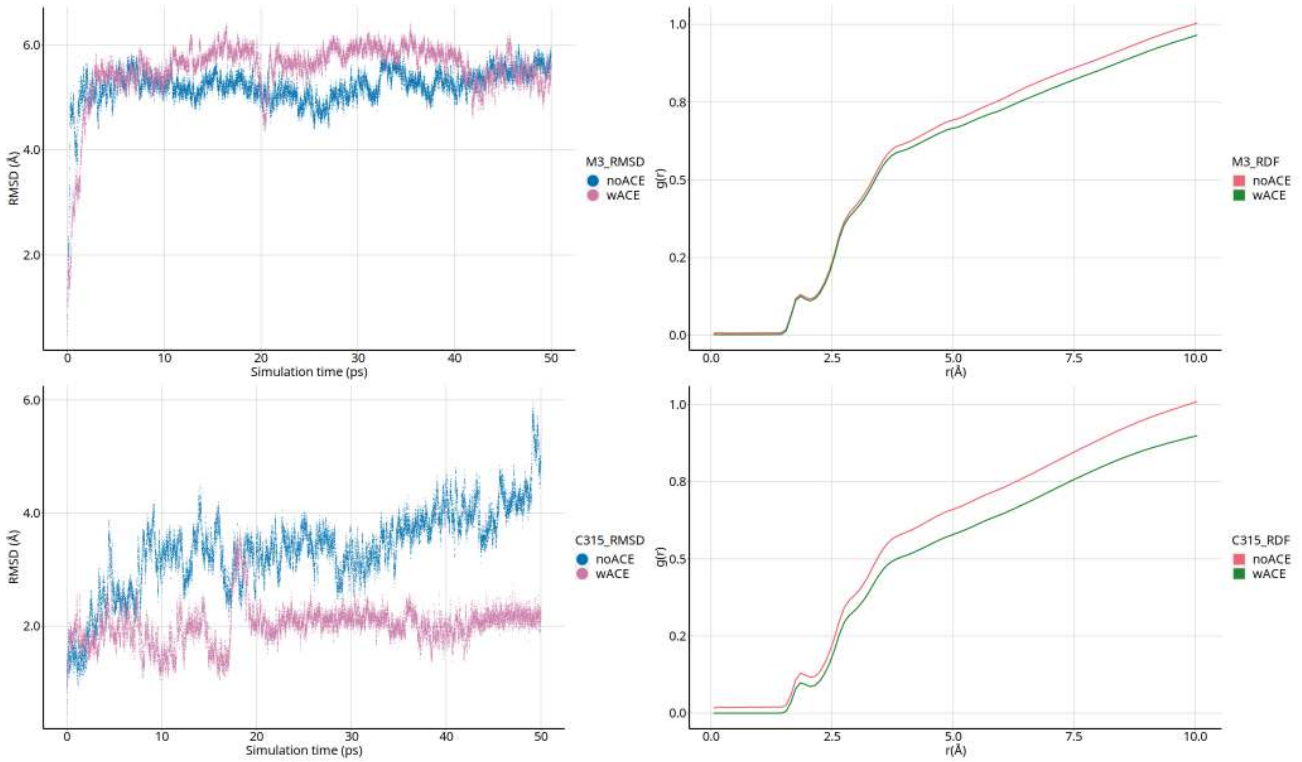

Fig. S7 Calculated Root-Mean-Square Deviation (RMSD) and Radial Pair Distribution Function (RDF) for peptides M3 and C3.15 in the presence and absence of ACET. Differences in the RMSDs for C3.15 can largely be explained by interactions between ACET and the C-terminal residue (R12). The central hydrogen bond network remained unaffected by the presence of ACET.

6.1 Role of acetate in classical simulations

To investigate the effect of acetate, classical simulations were run on peptides M3 (HTCHIQSCDHLA) and C3.15 (NYLPHQSSSPSR) with acetate concentrations that reflected those of experiment (10mM acetate. solvated TIP3 water box, 150mM NaCl $\times$ three repeats). Acetates were placed within hydrogen-bond distance of the peptide ($<$ 3Å) in both cases.

Simulations were run for 50ns with the Root-Mean-Square Deviation (RMSD) and Radial Pair Distribution Function (RDF) calculated for both peptides. Particularly in the case of M3, the authors determined no convincing differences either in calculated RMSDs nor RDFs with respect to the metal binding site.

Differences in the RMSDs for peptide C3.15 were primarily due to movement of peptide residues at the C-terminal in the absence of acetate, where no significant hydrogen-bond structure is present. When acetate was added, results from the simulation suggested an interaction was present with the charged terminal residue (R12). The hydrogen-bond network at the core of the peptide, however, remained undisturbed for the duration of the simulation. Additionally, as confirmed by the ITC portion of the study, affinity was unaffected by the presence of acetate.

Cluster analyses were also conducted and hydrogen-bond patterns calculated and analysed from simulation trajectories. As compared to Table S2 in the SI of the manuscript, we determined that there were no convincing differences in the most frequent clusters when acetate was present with respect to the likely metal binding site. Calculated RMSDs for aligned no acetate/acetate structures for the highest ranked cluster centroid showed little difference overall for peptide M3 (RMSD=1.72Å) and C3.15 (RMSD=0.44Å). Differences can again be largely explained by residues distant to the likely metal binding site.

With respect to calculated hydrogen bonds, when compared to Table S1 in the SI of the manuscript, we determined that there were no convincing differences in the hydrogen bonding patterns when acetate was present at the experimental concentration. Even though there were frames (~40%) where there were hydrogen-bonds present between peptide residues for C3.15 and an acetate, overall proportions of other hydrogen bonds did not differ markedly from simulations where

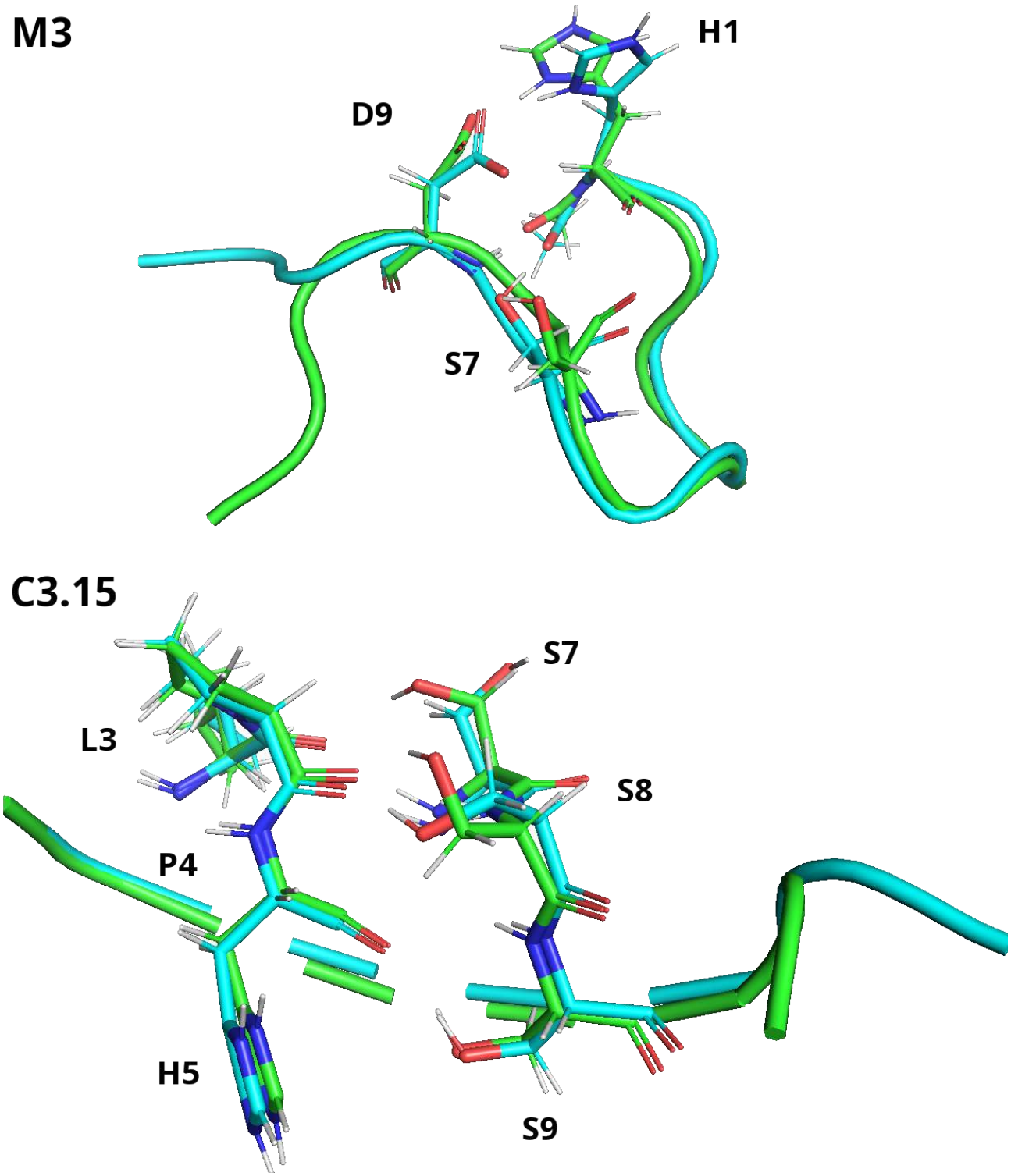

Fig. S8 A depiction of the most frequent cluster centroid (c0) for M3 and C3.15 in the presence and absence of acetate. The c0 centroid for simulations with 10mM acetate is **green** and the c0 centroid for simulations without acetate is **blue**. The central hydrogen bond network remained undisturbed by the presence of ACET.

Table S3 Output from cluster analysis of classical MD simulations, peptides M3 and C3.15 in the presence of acetate. Descriptive data are displayed including the number and proportion of frames each cluster centroid is present in and descriptive data regarding the distribution of distances from the centroid of each cluster for each frame within that cluster.

Peptide M3						
Cluster	**Frames**	**Frac**	**AvgDist**	**Stdev**	**Centroid**	**AvgCDist**
c0	17677	0.707	2.903	0.765	16924	4.909
c1	5054	0.202	3.138	0.801	22094	4.748
c2	955	0.038	2.956	1.032	388	5.32
c3	786	0.031	2.306	0.632	23958	5.245
c4	528	0.021	1.98	0.56	1303	5.186
Peptide C3.15						
Cluster	**Frames**	**Frac**	**AvgDist**	**Stdev**	**Centroid**	**AvgCDist**
c0	18789	0.752	1.862	0.382	15298	2.779
c1	4749	0.19	1.95	0.44	5404	2.864
c2	774	0.031	1.758	0.428	9346	3.362
c3	430	0.017	1.784	0.451	9610	2.988
c4	258	0.01	1.205	0.272	752	3.176

Table S4 Output from cluster analysis of classical MD simulations, peptides M3 and C3.15. Descriptive data are displayed including the number and proportion of frames each cluster centroid is present in and descriptive data regarding the distribution of distances from the centroid of each cluster for each frame within that cluster.

Peptide M3 - with acetate (10mM)						
Acceptor	**DonorH**	**Donor**	**Frames**	**Frac**	**AvgDist**	**AvgAng**
ILE_5@O	HSP_4@HN	HSP_4@N	14484	0.5794	2.8026	155.6786
HSP_1@O	CYS_8@HN	CYS_8@N	8820	0.3528	2.8497	158.6657
HSP_1@OY	ASP_9@HN	ASP_9@N	8576	0.343	2.841	162.5111
ASP_9@OD2	HSP_1@HD1	HSP_1@ND1	6704	0.2682	2.6899	162.4949
ASP_9@OD1	HSP_1@HD1	HSP_1@ND1	4184	0.1674	2.7071	162.5557
CYS_8@O	SER_7@HG1	SER_7@OG	2145	0.0858	2.7763	154.69
ASP_9@OD1	HSP_10@HN	HSP_10@N	1955	0.0782	2.7946	148.8723
GLN_6@OE1	GLN_6@HN	GLN_6@N	1745	0.0698	2.8403	150.9438
SER_7@OG	HSP_10@HN	HSP_10@N	1261	0.0504	2.8825	160.5243
SER_7@OG	HSP_4@HE2	HSP_4@NE2	1219	0.0488	2.8297	162.3693
Peptide C3.15 - with acetate (10mM)						
Acceptor	**DonorH**	**Donor**	**Frames**	**Frac**	**AvgDist**	**AvgAng**
TYR_2@O	GLN_6@HN	GLN_6@N	19392	0.7757	2.8334	163.108
PRO_4@O	SER_8@HN	SER_8@N	12621	0.5048	2.8579	155.6123
LEU_3@O	SER_7@HN	SER_7@N	12503	0.5001	2.8654	159.9319
PRO_4@O	SER_8@HG1	SER_8@OG	10662	0.4265	2.7621	160.266
ACET_15@O1	HSP_5@HD1	HSP_5@ND1	10465	0.4186	2.6752	165.4171
ACET_15@O1	ARG_12@HH22	ARG_12@NH2	10172	0.4069	2.7212	164.4748
ACET_15@O2	ARG_12@HH12	ARG_12@NH1	9978	0.3991	2.7233	165.6241
ASN_1@O	HSP_5@HN	HSP_5@N	9737	0.3895	2.8697	158.9804
HSP_5@O	SER_9@HG1	SER_9@OG	9100	0.364	2.7486	163.1797
LEU_3@O	SER_7@HG1	SER_7@OG	7713	0.3085	2.7646	161.449

acetate was absent.

Qualitatively, in both cases, despite being initially placed within hydrogen bond distance of the peptide, acetates tended to transition from being within hydrogen-bonding distance of the peptides to the bulk water phase. This is reflected in the calculated RDF where the probability of an acetate being found close to either peptide over the course of the simulation was, relatively, lower (Figure S9).

Further ITC experiments where acetate was added to both peptides in the absence of Ga^{3+} determined no notable energy changes indicative of peptide:acetate interactions.

The authors therefore concluded the structure of each peptide with respect to the metal binding site was qualitatively the same in the presence or absence of acetate at the experimental concentration.

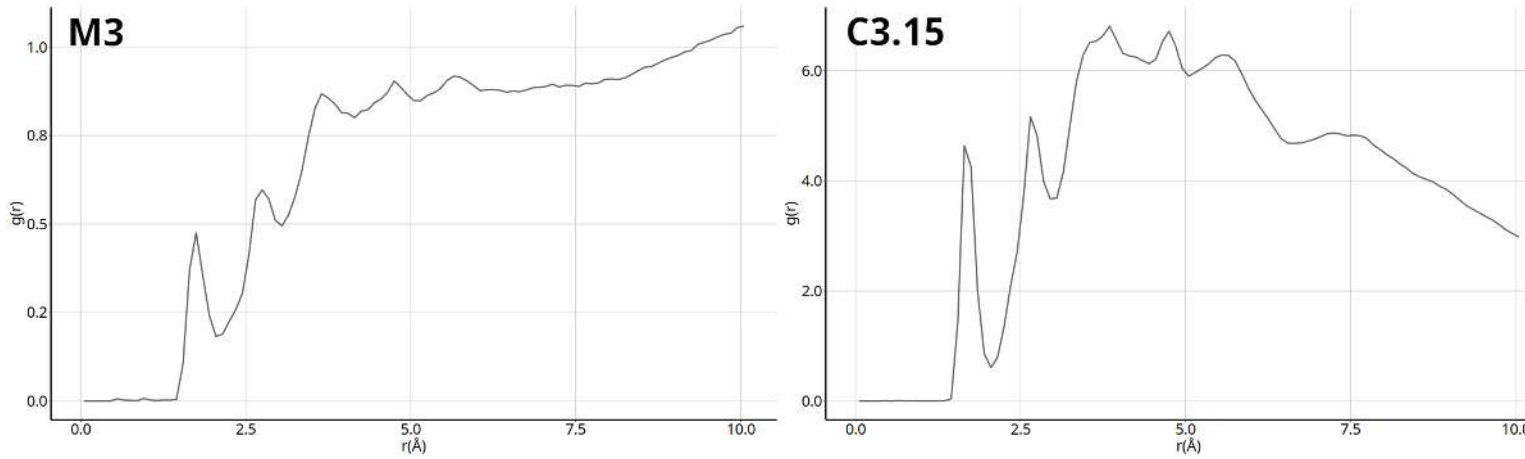

Fig. S9 Radial Distribution Function (RDF) of acetates for peptides M3 and C3.15. Over the course of simulations, probabilities of finding acetate molecules within hydrogen bonding distance (< 3 Å) were relatively lower than the probabilities of acetate molecules being found further away from the peptide and, thus, in bulk solvent.

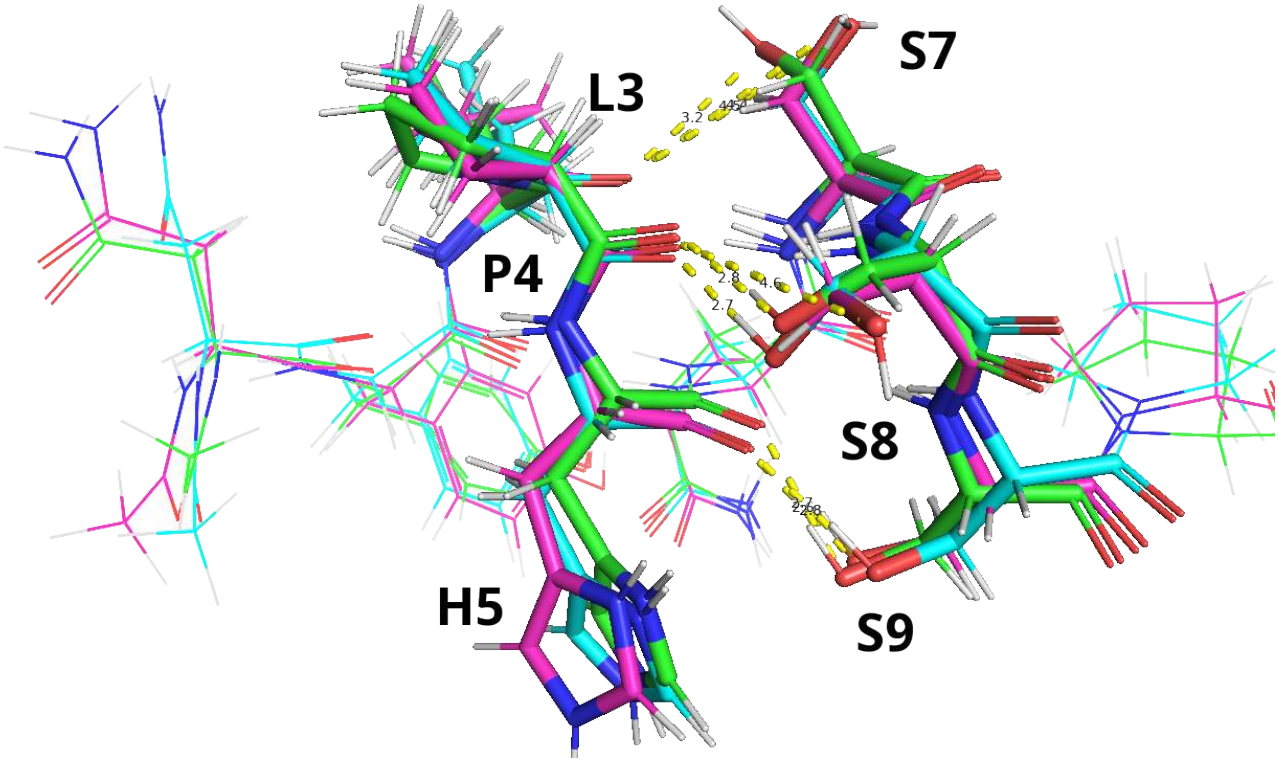

Fig. S10 Structures for c0-c2 are depicted (stick representation) for cluster0 (**green**), cluster1 (**blue**) and cluster2 (magenta). The proportion of simulation frames for each cluster can be found in Table S2 of the SI. In that table, one can find that the proportions of frames for all five of clusters 0-4 are 54.8%, 22.7%, 14.6%, 5.1% and 2.9%, respectively. Combined, clusters c0-c2 comprise 92.1% of all simulation frames. Structures were aligned and calculated RMSDs between the centroid of the most frequent cluster (cluster0) as compared to the centroids of cluster1 and cluster2 show very small differences ($RMSD_{c0\text{-}c1}$=0.61Å, $RMSD_{c0\text{-}c2}$=0.57Å). The three major interactions identified in the manuscript (L3-S7, P4-S8, H5-S9) were all within h-bond distance (heavy-atom) in the case of cluster0 whereas P4-S8 and H5-S9 were preserved for cluster1 and only H5-S9 for cluster2. The overall structure of the peptide, however, was maintained in each centroid and the central h-bond network involving backbone groups preserved for much of the simulations, despite the flexible nature of the peptides generally. Thus, we believe it was reasonable to take cluster0 as the most representative solution structure of the peptide for further calculations.

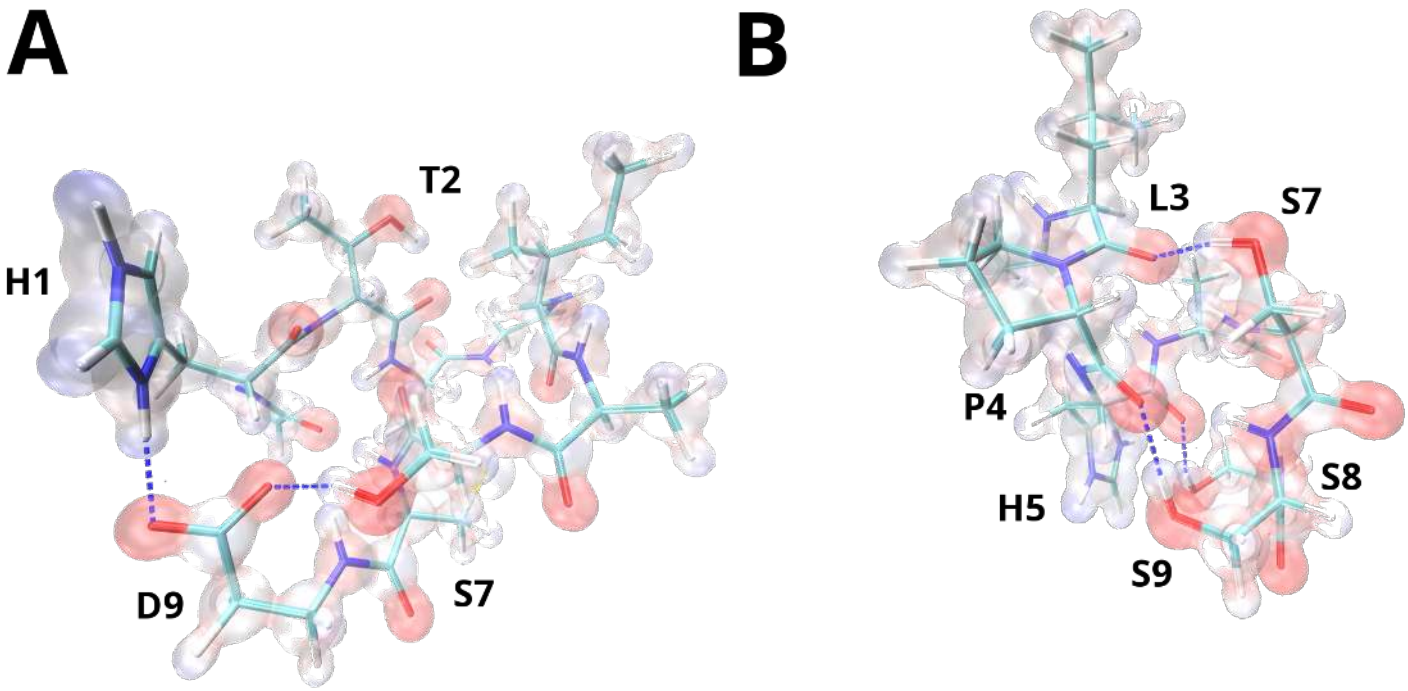

Fig. S11 Molecular Electrostatic Potential (MESP) for peptides M3 (A) and C3.15 (B). Electrostatic potential was mapped to an isosurface of ρ=0.05 and are depicted with the Red White Blue scheme (-ve (-0.01) $\rightarrow$ +ve (0.2)). Both optimised structures are depicted with the stick representation and hydrogen bonds depicted with blue dashed lines.

Table S5 Calculated Fuzzy Bond Orders (FBO) for peptide M3 in the absence of ACET

Bond number	X...Y	FBO	Bond number	X...Y	FBO
1	1(C) 2(O)	1.74509932	67	51(C) 53(H)	0.92539187
2	1(C) 3(H)	0.93628421	68	51(C) 54(C)	1.0658505
3	1(C) 4(N)	1.23292791	69	54(C) 55(H)	0.90445006
4	2(O) 4(N)	0.07225924	70	54(C) 56(H)	0.89584649
5	2(O) 50(H)	0.0974983	71	54(C) 57(C)	0.98933356
6	4(N) 5(H)	0.91020237	72	57(C) 58(O)	1.1814452
7	4(N) 6(C)	0.91198313	73	57(C) 59(O)	1.66183315
8	6(C) 7(H)	0.86581763	74	58(O) 59(O)	0.05943075
9	6(C) 8(C)	1.05099343	75	58(O) 60(Ga)	0.48093334
10	6(C) 20(C)	0.90475686	76	59(O) 86(H)	0.10790691
11	8(C) 9(H)	0.89632158	77	60(Ga) 79(O)	0.62054294
12	8(C) 10(H)	0.8810386	78	60(Ga) 85(O)	0.57731589
13	8(C) 13(C)	1.0526396	79	60(Ga) 88(O)	0.48880108
14	11(C) 12(H)	0.99314494	80	60(Ga) 102(O)	0.54311393
15	11(C) 13(C)	1.52397947	81	60(Ga) 104(O)	0.58739211
16	11(C) 14(N)	1.18306144	82	61(O) 62(H)	0.8781933
17	13(C) 16(N)	1.18760744	83	61(O) 63(H)	0.9487604
18	13(C) 18(C)	0.06458529	84	61(O) 94(H)	0.17002042
19	14(N) 15(H)	0.90426796	85	61(O) 97(H)	0.15558044
20	14(N) 16(N)	0.05258752	86	62(H) 76(O)	0.16270363
21	14(N) 18(C)	1.36846573	87	64(O) 65(H)	0.85698426
22	16(N) 17(H)	0.82744341	88	64(O) 66(H)	0.94184602
23	16(N) 18(C)	1.3134746	89	64(O) 89(H)	0.20301366
24	17(H) 58(O)	0.1461036	90	64(O) 105(H)	0.18834999
25	18(C) 19(H)	0.96326359	91	65(H) 90(O)	0.18857647
26	20(C) 21(O)	1.68673258	92	67(O) 68(H)	0.94337899
27	20(C) 22(N)	1.40451232	93	67(O) 69(H)	0.93743816
28	20(C) 23(H)	0.05025398	94	67(O) 71(H)	0.13515399
29	21(O) 22(N)	0.08224663	95	67(O) 108(H)	0.21304473
30	21(O) 100(H)	0.15028759	96	70(O) 71(H)	0.89835676
31	22(N) 23(H)	0.88787177	97	70(O) 72(H)	0.95016162
32	22(N) 24(C)	0.94817501	98	70(O) 80(H)	0.26491934
33	24(C) 25(H)	0.95939394	99	73(O) 74(H)	0.93816282
34	24(C) 26(H)	0.96401229	100	73(O) 75(H)	0.94335728
35	24(C) 27(H)	0.96551241	101	73(O) 98(H)	0.15517305
36	28(C) 29(O)	1.82757234	102	73(O) 106(H)	0.18620766
37	28(C) 30(H)	0.93499134	103	76(O) 77(H)	0.31784826
38	28(C) 31(N)	1.22000283	104	76(O) 78(H)	0.83044128
39	29(O) 31(N)	0.07513776	105	76(O) 86(H)	0.86457258
40	29(O) 46(H)	0.08068733	106	77(H) 82(O)	0.71665411
41	31(N) 32(H)	0.91326326	107	79(O) 80(H)	0.7865684
42	31(N) 33(C)	0.93767836	108	79(O) 81(H)	0.74767821
43	33(C) 34(H)	0.89319428	109	81(H) 93(O)	0.27663402
44	33(C) 35(C)	1.02078042	110	82(O) 83(H)	0.93059027
45	33(C) 40(C)	0.8986528	111	82(O) 84(H)	0.76754427
46	35(C) 36(H)	0.91461875	112	84(H) 99(O)	0.26218552
47	35(C) 37(H)	0.92978965	113	85(O) 87(H)	0.76503093
48	35(C) 38(O)	0.98321272	114	85(O) 103(H)	0.80866657
49	38(O) 39(H)	0.86671865	115	87(H) 96(O)	0.29062932
50	38(O) 95(H)	0.14304755	116	88(O) 89(H)	0.82656707
51	39(H) 59(O)	0.11781994	117	88(O) 107(H)	0.91556615
52	40(C) 41(O)	1.72224279	118	90(O) 91(H)	0.88915362
53	40(C) 42(N)	1.29902772	119	90(O) 92(H)	0.94771844
54	41(O) 42(N)	0.06190204	120	90(O) 101(H)	0.18870486
55	41(O) 78(H)	0.17586214	121	91(H) 96(O)	0.13707345
56	42(N) 43(H)	0.89541995	122	93(O) 94(H)	0.88980352
57	42(N) 44(C)	0.95748312	123	93(O) 95(H)	0.90191109
58	44(C) 45(H)	0.9109325	124	96(O) 97(H)	0.88115661
59	44(C) 46(H)	0.8994163	125	96(O) 98(H)	0.88485742
60	44(C) 47(C)	0.95207674	126	99(O) 100(H)	0.84859823
61	47(C) 48(O)	1.89941743	127	99(O) 101(H)	0.84060121
62	47(C) 49(N)	1.26110402	128	99(O) 103(H)	0.23086952
63	48(O) 49(N)	0.07513981	129	102(O) 108(H)	0.82828893
64	49(N) 50(H)	0.8699689	130	102(O) 109(H)	0.91849942
65	49(N) 51(C)	0.93026229	131	104(O) 105(H)	0.83755855
66	51(C) 52(H)	0.93075213	132	104(O) 106(H)	0.8396089

Table S6 Calculated Fuzzy Bond Orders (FBO) for peptide M3 in the presence of ACET

Bond number	X...Y	FBO	Bond number	X...Y	FBO	Bond number	X...Y	FBO
1	1(C) 2(O)	1.85474306	64	28(C) 33(C)	0.06588853	127	60(Ga) 73(O)	0.88918984
2	1(C) 3(H)	0.81418162	65	29(O) 30(H)	0.0745608	128	60(Ga) 79(O)	0.74926135
3	1(C) 4(N)	1.4112076	66	29(O) 31(N)	0.22406463	129	60(Ga) 82(O)	0.83147578
4	1(C) 6(C)	0.06610005	67	29(O) 33(C)	0.05426727	130	60(Ga) 94(C)	0.06945804
5	2(O) 3(H)	0.06970784	68	30(H) 31(N)	0.05545378	131	60(Ga) 96(O)	0.87431751
6	2(O) 4(N)	0.21469202	69	31(N) 32(H)	0.80888017	132	60(Ga) 98(O)	0.78567681
7	2(O) 6(C)	0.0558882	70	31(N) 33(C)	1.08031514	133	61(O) 62(H)	0.74342286
8	2(O) 42(N)	0.05095736	71	31(N) 35(C)	0.08941387	134	61(O) 63(H)	0.87752198
9	2(O) 49(N)	0.070632	72	31(N) 40(C)	0.09251392	135	61(O) 82(O)	0.11623981
10	2(O) 50(H)	0.06393885	73	33(C) 34(H)	0.74566105	136	61(O) 83(H)	0.14460498
11	3(H) 4(N)	0.05168796	74	33(C) 35(C)	1.00993649	137	61(O) 87(O)	0.11091743
12	4(N) 5(H)	0.80374492	75	33(C) 38(O)	0.0985947	138	61(O) 98(O)	0.09110897
13	4(N) 6(C)	1.09423243	76	33(C) 40(C)	0.93446457	139	61(O) 99(H)	0.10043661
14	4(N) 8(C)	0.07642643	77	33(C) 41(O)	0.09440544	140	62(H) 87(O)	0.10486184
15	4(N) 20(C)	0.06129762	78	33(C) 42(N)	0.06645593	141	64(O) 65(H)	0.87643621
16	4(N) 22(N)	0.05950646	79	35(C) 36(H)	0.79295317	142	64(O) 66(H)	0.7915103
17	6(C) 7(H)	0.70539199	80	35(C) 37(H)	0.82267339	143	64(O) 67(O)	0.11473941
18	6(C) 8(C)	1.00181603	81	35(C) 38(O)	1.24610468	144	64(O) 68(H)	0.09989339
19	6(C) 13(C)	0.06392743	82	35(C) 40(C)	0.05455651	145	64(O) 79(O)	0.11199463
20	6(C) 20(C)	0.96144468	83	36(H) 38(O)	0.050373	146	64(O) 97(H)	0.14899016
21	6(C) 21(O)	0.09993023	84	38(O) 39(H)	0.69266375	147	64(O) 98(O)	0.09935255
22	6(C) 22(N)	0.0711891	85	38(O) 59(O)	0.11374547	148	66(H) 98(O)	0.06000985
23	6(C) 58(O)	0.05462888	86	38(O) 84(O)	0.10109996	149	67(O) 68(H)	0.76828182
24	8(C) 9(H)	0.82348937	87	38(O) 86(H)	0.09041283	150	67(O) 69(H)	0.88969862
25	8(C) 10(H)	0.78111528	88	39(H) 59(O)	0.09228402	151	67(O) 73(O)	0.12704347
26	8(C) 11(C)	0.07109306	89	40(C) 41(O)	1.7159623	152	67(O) 74(H)	0.1836148
27	8(C) 13(C)	1.08304802	90	40(C) 42(N)	1.42073142	153	70(O) 71(H)	0.57493258
28	8(C) 16(N)	0.06135609	91	40(C) 44(C)	0.06256597	154	70(O) 72(H)	0.62522377
29	8(C) 20(C)	0.06767499	92	41(O) 42(N)	0.21838588	155	70(O) 76(O)	0.1439894
30	11(C) 12(H)	0.85594746	93	41(O) 70(O)	0.13049782	156	70(O) 80(H)	0.64349693
31	11(C) 13(C)	1.5032225	94	41(O) 72(H)	0.15566529	157	70(O) 91(C)	0.05993914
32	11(C) 14(N)	1.29627976	95	42(N) 43(H)	0.76944825	158	70(O) 96(O)	0.05378885
33	11(C) 16(N)	0.12118389	96	42(N) 44(C)	1.12033445	159	71(H) 76(O)	0.20815753
34	11(C) 18(C)	0.14859684	97	42(N) 47(C)	0.06628585	160	73(O) 74(H)	0.62392302
35	13(C) 14(N)	0.1221958	98	44(C) 45(H)	0.8262421	161	73(O) 75(H)	0.63003804
36	13(C) 16(N)	1.24250834	99	44(C) 46(H)	0.78084811	162	73(O) 84(O)	0.11433986
37	13(C) 18(C)	0.14194768	100	44(C) 47(C)	0.98612725	163	75(H) 84(O)	0.15820077
38	14(N) 15(H)	0.79973702	101	44(C) 48(O)	0.11966003	164	76(O) 77(H)	0.87504385
39	14(N) 16(N)	0.16420967	102	44(C) 49(N)	0.07757854	165	76(O) 78(H)	0.71674555
40	14(N) 18(C)	1.45451296	103	47(C) 48(O)	1.84316759	166	76(O) 87(O)	0.11733244
41	16(N) 17(H)	0.66592336	104	47(C) 49(N)	1.3765675	167	78(H) 87(O)	0.11876832
42	16(N) 18(C)	1.43394594	105	47(C) 51(C)	0.06575861	168	79(O) 81(H)	0.79794494
43	16(N) 58(O)	0.0966751	106	48(O) 49(N)	0.2153946	169	79(O) 82(O)	0.0589931
44	17(H) 58(O)	0.09318366	107	48(O) 51(C)	0.05988394	170	79(O) 97(H)	0.66208334
45	18(C) 19(H)	0.83334718	108	49(N) 50(H)	0.70885758	171	82(O) 83(H)	0.66836839
46	20(C) 21(O)	1.65456302	109	49(N) 51(C)	1.11541341	172	82(O) 101(H)	0.63732689
47	20(C) 22(N)	1.48565838	110	49(N) 54(C)	0.07987363	173	84(O) 85(H)	0.88205633
48	20(C) 24(C)	0.07349151	111	51(C) 52(H)	0.79693802	174	84(O) 86(H)	0.75453521
49	21(O) 22(N)	0.20376525	112	51(C) 53(H)	0.82894069	175	87(O) 88(H)	0.74720981
50	21(O) 24(C)	0.0597001	113	51(C) 54(C)	1.083828	176	87(O) 89(H)	0.88078209
51	21(O) 82(O)	0.11926085	114	51(C) 57(C)	0.05453191	177	90(H) 91(C)	0.81815046
52	21(O) 87(O)	0.11650198	115	54(C) 55(H)	0.80666018	178	91(C) 92(H)	0.80614968
53	21(O) 88(H)	0.08639198	116	54(C) 56(H)	0.78355322	179	91(C) 93(H)	0.87657606
54	21(O) 101(H)	0.13659317	117	54(C) 57(C)	1.02325311	180	91(C) 94(C)	1.06396902
55	22(N) 23(H)	0.77924879	118	54(C) 58(O)	0.1011666	181	91(C) 95(O)	0.12146915
56	22(N) 24(C)	1.15719532	119	54(C) 59(O)	0.08904704	182	91(C) 96(O)	0.09266195
57	24(C) 25(H)	0.86086346	120	57(C) 58(O)	1.36646909	183	94(C) 95(O)	1.72489662
58	24(C) 26(H)	0.81367045	121	57(C) 59(O)	1.70911508	184	94(C) 96(O)	1.39077541
59	24(C) 27(H)	0.8838384	122	57(C) 60(Ga)	0.07112006	185	95(O) 96(O)	0.2024914
60	24(C) 76(O)	0.05927492	123	58(O) 59(O)	0.19126393	186	95(O) 98(O)	0.13504605
61	28(C) 29(O)	1.91137371	124	58(O) 60(Ga)	0.7849899	187	95(O) 100(H)	0.18921775
62	28(C) 30(H)	0.82025305	125	59(O) 70(O)	0.12367568	188	98(O) 99(H)	0.70888966
63	28(C) 31(N)	1.40422243	126	59(O) 80(H)	0.1114994	189	98(O) 100(H)	0.58965859

Table S7 Calculated Fuzzy Bond Orders (FBO) for peptide C3.15 in the absence of ACET

Bond number	X...Y	FBO	Bond number	X...Y	FBO	Bond number	X...Y	FBO
1	1(N) 15(C)	1.08614353	69	10(N) 133(H)	0.83601822	137	24(C) 25(C)	1.36791312
2	1(N) 16(C)	0.09553315	70	11(N) 12(N)	0.05372058	138	24(C) 26(C)	1.375557
3	1(N) 17(C)	0.06595733	71	11(N) 47(C)	0.06895248	139	24(C) 27(C)	0.09268948
4	1(N) 18(C)	0.08638587	72	11(N) 48(C)	1.32732845	140	24(C) 28(C)	0.09244673
5	1(N) 20(C)	1.37278029	73	11(N) 52(C)	1.07943153	141	24(C) 29(C)	0.07941683
6	1(N) 67(O)	0.20236403	74	11(N) 53(C)	0.05884266	142	25(C) 26(C)	0.09148637
7	1(N) 82(H)	0.80573033	75	11(N) 54(C)	0.06931097	143	25(C) 27(C)	1.45139633
8	2(N) 18(C)	0.09904274	76	11(N) 73(O)	0.20171011	144	25(C) 28(C)	0.09475285
9	2(N) 19(C)	1.44181338	77	11(N) 134(H)	0.73819394	145	25(C) 29(C)	0.09268025
10	2(N) 66(O)	0.2386314	78	12(N) 13(N)	0.0676587	146	25(C) 95(H)	0.83883703
11	2(N) 86(H)	0.85025434	79	12(N) 52(C)	0.0713403	147	26(C) 27(C)	0.09144727
12	2(N) 87(H)	0.84845671	80	12(N) 53(C)	1.35122678	148	26(C) 28(C)	1.4507871
13	3(N) 15(C)	0.06496994	81	12(N) 55(C)	1.07245903	149	26(C) 29(C)	0.0935544
14	3(N) 17(C)	1.36105715	82	12(N) 56(C)	0.06051879	150	26(C) 96(H)	0.85063006
15	3(N) 21(C)	1.08442976	83	12(N) 57(C)	0.07541056	151	27(C) 28(C)	0.08617793
16	3(N) 22(C)	0.05968122	84	12(N) 72(O)	0.05213946	152	27(C) 29(C)	1.33443164
17	3(N) 23(C)	0.09679449	85	12(N) 75(O)	0.20935799	153	27(C) 69(O)	0.11970575
18	3(N) 65(O)	0.20003874	86	12(N) 139(H)	0.70546937	154	27(C) 97(H)	0.83622518
19	3(N) 67(O)	0.06198413	87	13(N) 55(C)	0.0689667	155	28(C) 29(C)	1.33515494
20	3(N) 91(H)	0.76014145	88	13(N) 56(C)	1.3420504	156	28(C) 69(O)	0.13024525
21	4(N) 21(C)	0.06692398	89	13(N) 58(C)	1.08077934	157	28(C) 98(H)	0.84898657
22	4(N) 22(C)	1.36653154	90	13(N) 59(C)	0.05996771	158	29(C) 69(O)	1.30735813
23	4(N) 30(C)	1.07927112	91	13(N) 60(C)	0.07184212	159	30(C) 31(C)	0.95053192
24	4(N) 31(C)	0.06732175	92	13(N) 64(C)	0.06279057	160	30(C) 32(C)	1.01280798
25	4(N) 32(C)	0.07320921	93	13(N) 77(O)	0.20915087	161	30(C) 33(C)	0.05514702
26	4(N) 67(O)	0.07326298	94	13(N) 144(H)	0.73015007	162	30(C) 70(O)	0.09571198
27	4(N) 68(O)	0.19842305	95	14(N) 58(C)	0.06341678	163	30(C) 101(H)	0.74803083
28	4(N) 100(H)	0.68875325	96	14(N) 59(C)	1.35472919	164	31(C) 32(C)	0.06699295
29	5(N) 30(C)	0.05896186	97	14(N) 61(C)	1.0631471	165	31(C) 36(C)	0.06043095
30	5(N) 31(C)	1.46771131	98	14(N) 62(C)	0.07477661	166	31(C) 40(C)	0.06048109
31	5(N) 36(C)	0.99649628	99	14(N) 63(C)	0.07823406	167	31(C) 70(O)	1.42441297
32	5(N) 37(C)	0.05763937	100	14(N) 64(C)	1.06993153	168	31(C) 81(Ga)	0.07132558
33	5(N) 38(C)	0.06364912	101	14(N) 79(O)	0.21520641	169	32(C) 33(C)	1.03367047
34	5(N) 39(C)	0.07122349	102	15(C) 17(C)	0.94313583	170	32(C) 34(C)	0.08940242
35	5(N) 40(C)	1.02213078	103	15(C) 18(C)	1.02416729	171	32(C) 35(C)	0.07098637
36	5(N) 70(O)	0.1624632	104	15(C) 19(C)	0.05625554	172	32(C) 102(H)	0.77192986
37	6(N) 36(C)	0.06325972	105	15(C) 20(C)	0.06014228	173	32(C) 103(H)	0.78912193
38	6(N) 37(C)	1.40704362	106	15(C) 65(O)	0.10344976	174	33(C) 34(C)	1.09564795
39	6(N) 41(C)	1.06840833	107	15(C) 66(O)	0.05382301	175	33(C) 35(C)	1.09626388
40	6(N) 42(C)	0.06189739	108	15(C) 83(H)	0.76635202	176	33(C) 104(H)	0.78888559
41	6(N) 43(C)	0.07373503	109	16(C) 20(C)	1.08189833	177	34(C) 35(C)	0.08685277
42	6(N) 65(O)	0.06538541	110	16(C) 67(O)	0.12314987	178	34(C) 105(H)	0.88128604
43	6(N) 71(O)	0.19822319	111	16(C) 88(H)	0.85383153	179	34(C) 106(H)	0.89254435
44	6(N) 118(H)	0.70522696	112	16(C) 89(H)	0.88259257	180	34(C) 107(H)	0.87961809
45	7(N) 8(N)	0.15640032	113	16(C) 90(H)	0.86423065	181	35(C) 108(H)	0.87169633
46	7(N) 43(C)	0.06244759	114	17(C) 21(C)	0.05983076	182	35(C) 109(H)	0.86921467
47	7(N) 44(C)	1.24281384	115	17(C) 65(O)	1.76407492	183	35(C) 110(H)	0.88762068
48	7(N) 45(C)	0.12383715	116	18(C) 19(C)	1.00737755	184	36(C) 37(C)	0.95359778
49	7(N) 46(C)	1.42186657	117	18(C) 66(O)	0.10716411	185	36(C) 38(C)	1.00955828
50	7(N) 122(H)	0.78699672	118	18(C) 84(H)	0.81502917	186	36(C) 39(C)	0.06907021
51	8(N) 44(C)	0.11960357	119	18(C) 85(H)	0.81780586	187	36(C) 71(O)	0.10201604
52	8(N) 45(C)	1.29125152	120	19(C) 66(O)	1.83131585	188	36(C) 111(H)	0.73662403
53	8(N) 46(C)	1.44700247	121	20(C) 67(O)	1.75874211	189	37(C) 38(C)	0.07697404
54	8(N) 74(O)	0.1079198	122	20(C) 88(H)	0.05024353	190	37(C) 41(C)	0.06369387
55	8(N) 125(H)	0.66347233	123	20(C) 90(H)	0.05195265	191	37(C) 71(O)	1.70057299
56	9(N) 11(N)	0.05275248	124	21(C) 22(C)	0.94415672	192	38(C) 39(C)	1.07012855
57	9(N) 41(C)	0.06252007	125	21(C) 23(C)	1.00796318	193	38(C) 40(C)	0.07613518
58	9(N) 42(C)	1.36932022	126	21(C) 24(C)	0.06279144	194	38(C) 112(H)	0.83522641
59	9(N) 47(C)	1.06463955	127	21(C) 68(O)	0.10476961	195	38(C) 113(H)	0.83739208
60	9(N) 48(C)	0.05977498	128	21(C) 92(H)	0.76383773	196	39(C) 40(C)	1.05850956
61	9(N) 49(C)	0.07667269	129	22(C) 23(C)	0.06412602	197	39(C) 65(O)	0.0574127
62	9(N) 68(O)	0.08618514	130	22(C) 30(C)	0.06128581	198	39(C) 114(H)	0.84748265
63	9(N) 72(O)	0.19595965	131	22(C) 68(O)	1.75202002	199	39(C) 115(H)	0.79610246
64	9(N) 126(H)	0.68103945	132	23(C) 24(C)	1.06518304	200	40(C) 116(H)	0.74541243
65	10(N) 50(C)	0.08742455	133	23(C) 25(C)	0.08076782	201	40(C) 117(H)	0.78091701
66	10(N) 51(C)	1.46825008	134	23(C) 26(C)	0.07907796	202	41(C) 42(C)	0.93838019
67	10(N) 74(O)	0.23474093	135	23(C) 93(H)	0.82189992	203	41(C) 43(C)	0.9932862
68	10(N) 132(H)	0.83461008	136	23(C) 94(H)	0.81504197	204	41(C) 44(C)	0.05920024

Table S8 Calculated Fuzzy Bond Orders (FBO) for peptide C3.15 in the absence of ACET (cont.)

Bond number	X...Y	FBO	Bond number	X...Y	FBO
205	41(C) 72(O)	0.1077043	273	59(C) 64(C)	0.05526344
206	41(C) 119(H)	0.75563105	274	59(C) 79(O)	1.8120257
207	42(C) 43(C)	0.05367669	275	60(C) 73(O)	0.05207731
208	42(C) 47(C)	0.06249129	276	60(C) 80(O)	1.25967812
209	42(C) 72(O)	1.73821716	277	60(C) 146(H)	0.82028787
210	43(C) 44(C)	1.08288187	278	60(C) 147(H)	0.78723585
211	43(C) 45(C)	0.06835603	279	61(C) 62(C)	1.07316324
212	43(C) 65(O)	0.05832389	280	61(C) 63(C)	0.0774825
213	43(C) 120(H)	0.76451714	281	61(C) 64(C)	0.05176096
214	43(C) 121(H)	0.82607717	282	61(C) 79(O)	0.08253738
215	44(C) 45(C)	1.48242971	283	61(C) 149(H)	0.83585939
216	44(C) 46(C)	0.13678038	284	61(C) 150(H)	0.83576498
217	45(C) 46(C)	0.1410172	285	62(C) 63(C)	1.08006322
218	45(C) 123(H)	0.78156876	286	62(C) 64(C)	0.07875857
219	46(C) 80(O)	0.07169712	287	62(C) 151(H)	0.87324416
220	46(C) 124(H)	0.81941222	288	62(C) 152(H)	0.85789858
221	47(C) 48(C)	0.9401299	289	63(C) 64(C)	1.07316995
222	47(C) 49(C)	1.01025661	290	63(C) 153(H)	0.85505288
223	47(C) 50(C)	0.06381866	291	63(C) 154(H)	0.86706382
224	47(C) 73(O)	0.10757538	292	64(C) 73(O)	0.05243837
225	47(C) 127(H)	0.74193572	293	64(C) 155(H)	0.81395529
226	48(C) 49(C)	0.08111961	294	64(C) 156(H)	0.78685879
227	48(C) 52(C)	0.05896552	295	65(O) 118(H)	0.05287055
228	48(C) 73(O)	1.82805553	296	67(O) 100(H)	0.06587907
229	49(C) 50(C)	1.08234748	297	68(O) 126(H)	0.07590692
230	49(C) 51(C)	0.06063677	298	69(O) 74(O)	0.05399864
231	49(C) 128(H)	0.81173659	299	69(O) 99(H)	0.79028627
232	49(C) 129(H)	0.80205029	300	70(O) 81(Ga)	0.80910103
233	50(C) 51(C)	1.01065311	301	71(O) 78(O)	0.09047747
234	50(C) 74(O)	0.10694443	302	71(O) 143(H)	0.06691762
235	50(C) 130(H)	0.78887516	303	71(O) 165(O)	0.12110575
236	50(C) 131(H)	0.77888525	304	71(O) 167(H)	0.09295712
237	51(C) 74(O)	1.74615717	305	72(O) 80(O)	0.09833413
238	52(C) 53(C)	0.94684567	306	72(O) 148(H)	0.07274084
239	52(C) 54(C)	1.02123529	307	74(O) 125(H)	0.10393062
240	52(C) 73(O)	0.05837251	308	76(O) 81(Ga)	0.84456108
241	52(C) 75(O)	0.10886504	309	76(O) 138(H)	0.52510475
242	52(C) 76(O)	0.07745553	310	76(O) 165(O)	0.13972449
243	52(C) 135(H)	0.74207112	311	78(O) 141(H)	0.05641054
244	53(C) 54(C)	0.05414142	312	78(O) 143(H)	0.74309823
245	53(C) 55(C)	0.06070591	313	80(O) 147(H)	0.05144308
246	53(C) 75(O)	1.83963687	314	80(O) 148(H)	0.71862135
247	54(C) 75(O)	0.05160301	315	81(Ga) 157(O)	0.90451785
248	54(C) 76(O)	1.0796804	316	81(Ga) 162(O)	0.82862831
249	54(C) 81(Ga)	0.05349403	317	81(Ga) 172(O)	0.78152906
250	54(C) 136(H)	0.79376909	318	81(Ga) 175(O)	0.78046008
251	54(C) 137(H)	0.80335412	319	138(H) 165(O)	0.2250945
252	55(C) 56(C)	0.9505471	320	157(O) 158(H)	0.78985353
253	55(C) 57(C)	1.01177238	321	157(O) 168(H)	0.54174735
254	55(C) 75(O)	0.05492006	322	157(O) 169(O)	0.14568926
255	55(C) 77(O)	0.10588281	323	159(O) 160(H)	0.85997323
256	55(C) 78(O)	0.09452378	324	159(O) 161(H)	0.86027804
257	55(C) 140(H)	0.75813485	325	159(O) 162(O)	0.12434166
258	56(C) 57(C)	0.0552406	326	159(O) 164(H)	0.17235336
259	56(C) 58(C)	0.06026046	327	159(O) 169(O)	0.10909735
260	56(C) 77(O)	1.84317954	328	159(O) 171(H)	0.09030576
261	57(C) 77(O)	0.05500727	329	162(O) 163(H)	0.79030494
262	57(C) 78(O)	1.26382176	330	162(O) 164(H)	0.62281681
263	57(C) 141(H)	0.8275168	331	162(O) 175(O)	0.05342765
264	57(C) 142(H)	0.81493629	332	165(O) 166(H)	0.82979521
265	58(C) 59(C)	0.94586863	333	165(O) 167(H)	0.71837457
266	58(C) 60(C)	1.00668463	334	168(H) 169(O)	0.23458305
267	58(C) 77(O)	0.05574579	335	169(O) 170(H)	0.85849063
268	58(C) 79(O)	0.12111841	336	169(O) 171(H)	0.75550761
269	58(C) 80(O)	0.10058383	337	172(O) 173(H)	0.78112977
270	58(C) 145(H)	0.75674534	338	172(O) 174(H)	0.78350055
271	59(C) 60(C)	0.07162977	339	175(O) 176(H)	0.79529904
272	59(C) 61(C)	0.06597888	340	175(O) 177(H)	0.79466749

Table S9 Calculated Fuzzy Bond Orders (FBO) for peptide C3.15 in the presence of ACET

Bond number	X...Y	FBO	Bond number	X...Y	FBO
1	1(N) 15(C)	1.11083313	73	11(N) 52(C)	1.10361102
2	1(N) 16(C)	0.09773641	74	11(N) 53(C)	0.06000115
3	1(N) 17(C)	0.06839732	75	11(N) 54(C)	0.07282045
4	1(N) 18(C)	0.09019943	76	11(N) 73(O)	0.20629643
5	1(N) 20(C)	1.40415292	77	11(N) 76(O)	0.06585245
6	1(N) 67(O)	0.208578	78	11(N) 134(H)	0.73690519
7	1(N) 82(H)	0.80719472	79	12(N) 13(N)	0.0612835
8	2(N) 18(C)	0.10128176	80	12(N) 52(C)	0.07107849
9	2(N) 19(C)	1.48109762	81	12(N) 53(C)	1.38050803
10	2(N) 66(O)	0.24460593	82	12(N) 55(C)	1.09926783
11	2(N) 86(H)	0.85088767	83	12(N) 56(C)	0.0616843
12	2(N) 87(H)	0.84947764	84	12(N) 57(C)	0.08061652
13	3(N) 15(C)	0.06660639	85	12(N) 75(O)	0.21756775
14	3(N) 17(C)	1.39057674	86	12(N) 139(H)	0.71958398
15	3(N) 21(C)	1.11076403	87	13(N) 55(C)	0.07094612
16	3(N) 22(C)	0.06206543	88	13(N) 56(C)	1.37905457
17	3(N) 23(C)	0.099387	89	13(N) 58(C)	1.10554925
18	3(N) 65(O)	0.20573266	90	13(N) 59(C)	0.06118827
19	3(N) 67(O)	0.06951692	91	13(N) 60(C)	0.07241349
20	3(N) 91(H)	0.76147883	92	13(N) 64(C)	0.06263332
21	4(N) 21(C)	0.06971795	93	13(N) 77(O)	0.21476697
22	4(N) 22(C)	1.40177196	94	13(N) 144(H)	0.72233226
23	4(N) 30(C)	1.09956116	95	14(N) 58(C)	0.06471685
24	4(N) 31(C)	0.06989101	96	14(N) 59(C)	1.384851
25	4(N) 32(C)	0.07617498	97	14(N) 61(C)	1.08663909
26	4(N) 67(O)	0.07060665	98	14(N) 62(C)	0.077768
27	4(N) 68(O)	0.20574553	99	14(N) 63(C)	0.08110642
28	4(N) 100(H)	0.69431201	100	14(N) 64(C)	1.09108431
29	5(N) 30(C)	0.06067518	101	14(N) 79(O)	0.22115029
30	5(N) 31(C)	1.46792901	102	15(C) 17(C)	0.95722985
31	5(N) 36(C)	1.02855333	103	15(C) 18(C)	1.0410873
32	5(N) 37(C)	0.05932211	104	15(C) 19(C)	0.05752883
33	5(N) 38(C)	0.06479336	105	15(C) 20(C)	0.0630487
34	5(N) 39(C)	0.07624195	106	15(C) 65(O)	0.10695393
35	5(N) 40(C)	1.05258867	107	15(C) 66(O)	0.05332434
36	5(N) 70(O)	0.17416757	108	15(C) 83(H)	0.77600227
37	6(N) 36(C)	0.06670777	109	16(C) 20(C)	1.09807688
38	6(N) 37(C)	1.43864128	110	16(C) 67(O)	0.12681249
39	6(N) 41(C)	1.09790477	111	16(C) 88(H)	0.85650718
40	6(N) 42(C)	0.06380379	112	16(C) 89(H)	0.88881907
41	6(N) 43(C)	0.07625734	113	16(C) 90(H)	0.87191727
42	6(N) 65(O)	0.06477033	114	17(C) 21(C)	0.0634013
43	6(N) 71(O)	0.2022444	115	17(C) 65(O)	1.82846122
44	6(N) 118(H)	0.7071441	116	18(C) 19(C)	1.02606797
45	7(N) 8(N)	0.16266222	117	18(C) 66(O)	0.10883213
46	7(N) 43(C)	0.06319089	118	18(C) 84(H)	0.82211455
47	7(N) 44(C)	1.27172818	119	18(C) 85(H)	0.82429817
48	7(N) 45(C)	0.13021	120	19(C) 66(O)	1.88992075
49	7(N) 46(C)	1.4546361	121	20(C) 67(O)	1.82626957
50	7(N) 122(H)	0.78867666	122	20(C) 88(H)	0.05215868
51	8(N) 44(C)	0.12614256	123	21(C) 22(C)	0.95870824
52	8(N) 45(C)	1.32321515	124	21(C) 23(C)	1.02707425
53	8(N) 46(C)	1.48171222	125	21(C) 24(C)	0.06518027
54	8(N) 74(O)	0.11595844	126	21(C) 68(O)	0.10860867
55	8(N) 125(H)	0.65387025	127	21(C) 92(H)	0.77174085
56	9(N) 11(N)	0.05152161	128	22(C) 23(C)	0.06680686
57	9(N) 41(C)	0.0640985	129	22(C) 30(C)	0.06372821
58	9(N) 42(C)	1.40145094	130	22(C) 68(O)	1.81862918
59	9(N) 47(C)	1.08732257	131	23(C) 24(C)	1.0830532
60	9(N) 48(C)	0.06243748	132	23(C) 25(C)	0.08247594
61	9(N) 49(C)	0.07933983	133	23(C) 26(C)	0.08052615
62	9(N) 68(O)	0.08671579	134	23(C) 93(H)	0.83056272
63	9(N) 72(O)	0.20419084	135	23(C) 94(H)	0.82089234
64	9(N) 126(H)	0.68446137	136	24(C) 25(C)	1.39076907
65	10(N) 50(C)	0.09106595	137	24(C) 26(C)	1.3991034
66	10(N) 51(C)	1.5044472	138	24(C) 27(C)	0.09695775
67	10(N) 74(O)	0.24009486	139	24(C) 28(C)	0.09678594
68	10(N) 132(H)	0.83674219	140	24(C) 29(C)	0.08201923
69	10(N) 133(H)	0.83763825	141	25(C) 26(C)	0.09589827
70	11(N) 12(N)	0.05627103	142	25(C) 27(C)	1.47513186
71	11(N) 47(C)	0.07257802	143	25(C) 28(C)	0.09782086
72	11(N) 48(C)	1.36999347	144	25(C) 29(C)	0.09733539

Table S10 Calculated Fuzzy Bond Orders (FBO) for peptide C3.15 in the presence of ACET (cont.)

Bond number	X...Y	FBO	Bond number	X...Y	FBO
217	44(C) 45(C)	1.5091394	287	61(C) 150(H)	0.8414889
218	44(C) 46(C)	0.14448046	288	62(C) 63(C)	1.10010191
219	45(C) 46(C)	0.14935472	289	62(C) 64(C)	0.08224645
220	45(C) 123(H)	0.79420432	290	62(C) 151(H)	0.87831331
221	46(C) 80(O)	0.0715308	291	62(C) 152(H)	0.86370218
222	46(C) 124(H)	0.82313639	292	63(C) 64(C)	1.09139193
223	47(C) 48(C)	0.95643503	293	63(C) 153(H)	0.86069354
224	47(C) 49(C)	1.02809302	294	63(C) 154(H)	0.87181603
225	47(C) 50(C)	0.06588007	295	64(C) 73(O)	0.05397446
226	47(C) 72(O)	0.05303908	296	64(C) 155(H)	0.80994291
227	47(C) 73(O)	0.10912739	297	64(C) 156(H)	0.79086485
228	47(C) 127(H)	0.75416547	298	67(O) 100(H)	0.06036897
229	48(C) 49(C)	0.08724805	299	68(O) 126(H)	0.07180822
230	48(C) 52(C)	0.06301866	300	69(O) 99(H)	0.78728515
231	48(C) 72(O)	0.05175568	301	70(O) 81(Ga)	0.77653064
232	48(C) 73(O)	1.88017828	302	70(O) 172(O)	0.06293483
233	49(C) 50(C)	1.10024417	303	71(O) 78(O)	0.09821333
234	49(C) 51(C)	0.06517308	304	71(O) 143(H)	0.07301466
235	49(C) 128(H)	0.81390289	305	71(O) 165(O)	0.12375889
236	49(C) 129(H)	0.80852701	306	71(O) 167(H)	0.09110295
237	50(C) 51(C)	1.02692329	307	72(O) 80(O)	0.0981292
238	50(C) 74(O)	0.10902933	308	72(O) 148(H)	0.07011263
239	50(C) 130(H)	0.79685968	309	74(O) 125(H)	0.10828115
240	50(C) 131(H)	0.78912553	310	76(O) 81(Ga)	0.84075646
241	51(C) 74(O)	1.80690824	311	76(O) 138(H)	0.57337489
242	52(C) 53(C)	0.9610197	312	76(O) 165(O)	0.13858899
243	52(C) 54(C)	1.03018529	313	78(O) 141(H)	0.0558635
244	52(C) 73(O)	0.05531603	314	78(O) 143(H)	0.72600439
245	52(C) 75(O)	0.11877101	315	80(O) 147(H)	0.05168137
246	52(C) 76(O)	0.08196872	316	80(O) 148(H)	0.70774483
247	52(C) 135(H)	0.76216139	317	81(Ga) 157(O)	0.98173023
248	53(C) 54(C)	0.06121422	318	81(Ga) 162(O)	0.9050872
249	53(C) 55(C)	0.06384362	319	81(Ga) 172(O)	0.80617006
250	53(C) 75(O)	1.9156957	320	81(Ga) 179(C)	0.08000916
251	54(C) 76(O)	1.11738562	321	81(Ga) 180(O)	1.02597441
252	54(C) 81(Ga)	0.05483439	322	138(H) 165(O)	0.18136589
253	54(C) 136(H)	0.79966418	323	157(O) 158(H)	0.71799317
254	54(C) 137(H)	0.8192533	324	157(O) 165(O)	0.08055456
255	55(C) 56(C)	0.9657316	325	157(O) 168(H)	0.55836823
256	55(C) 57(C)	1.0292343	326	157(O) 169(O)	0.15049512
257	55(C) 75(O)	0.0608184	327	158(H) 165(O)	0.07203423
258	55(C) 77(O)	0.11007519	328	159(O) 160(H)	0.68004925
259	55(C) 78(O)	0.09857249	329	159(O) 161(H)	0.85686063
260	55(C) 140(H)	0.76114175	330	159(O) 162(O)	0.15193206
261	56(C) 57(C)	0.05811772	331	159(O) 164(H)	0.20472061
262	56(C) 58(C)	0.06423651	332	159(O) 169(O)	0.1224734
263	56(C) 77(O)	1.89912135	333	159(O) 171(H)	0.10053582
264	57(C) 77(O)	0.05293227	334	159(O) 181(O)	0.13082091
265	57(C) 78(O)	1.30047012	335	160(H) 181(O)	0.12464815
266	57(C) 141(H)	0.83460653	336	162(O) 163(H)	0.79577985
267	57(C) 142(H)	0.82397768	337	162(O) 164(H)	0.57064231
268	58(C) 59(C)	0.96119999	338	165(O) 166(H)	0.84161997
269	58(C) 60(C)	1.02340465	339	165(O) 167(H)	0.70657213
270	58(C) 77(O)	0.05714222	340	168(H) 169(O)	0.20820475
271	58(C) 79(O)	0.1244392	341	169(O) 170(H)	0.85838356
272	58(C) 80(O)	0.10360991	342	169(O) 171(H)	0.73317023
273	58(C) 145(H)	0.76625901	343	172(O) 173(H)	0.78797695
274	59(C) 60(C)	0.07304303	344	172(O) 174(H)	0.79257988
275	59(C) 61(C)	0.06932105	345	172(O) 180(O)	0.05069759
276	59(C) 64(C)	0.05729544	346	175(H) 176(C)	0.8711333
277	59(C) 79(O)	1.87117349	347	175(H) 179(C)	0.05183519
278	60(C) 73(O)	0.05541735	348	176(C) 177(H)	0.88959429
279	60(C) 80(O)	1.29535832	349	176(C) 178(H)	0.87196945
280	60(C) 146(H)	0.8283046	350	176(C) 179(C)	1.08592884
281	60(C) 147(H)	0.79396477	351	176(C) 180(O)	0.12360533
282	61(C) 62(C)	1.09155876	352	176(C) 181(O)	0.12467693
283	61(C) 63(C)	0.08125742	353	178(H) 179(C)	0.05247271
284	61(C) 64(C)	0.05419896	354	179(C) 180(O)	1.42691143
285	61(C) 79(O)	0.08475899	355	179(C) 181(O)	1.84624074
286	61(C) 149(H)	0.84162966	356	180(O) 181(O)	0.21624977

Table S11 Normalised ($-|MCI|^{1/n}$) and un-normalised (MCI) three-centre bond orders for peptides M3 and C3.15 in the absence and presence of ACET. Only three-centre bonds involving ligands for Ga^{3+} are displayed. Three-centre bonds directly involving Ga^{3+} were only present when ACET is also a ligand.

M3 without ACET					*M3 with ACET*				
Atom 1	Atom 2	Atom 3	MCI	$-\|MCI\|^{1/n}$	Atom 1	Atom 2	Atom 3	MCI	$-\|MCI\|^{1/n}$
16	17	58 (S9)	-0.049239	-0.36652	16	17	58 (HOH)	-0.044868	-0.35534
58 (S9)	17	16	-0.043621	-0.35202	58 (HOH)	17	16	-0.039034 -0.33922	
54	57	58 (S9)	-0.038463	-0.33756	58 (HOH)	57	54	-0.050767 -0.37028	
58 (S9)	57	54	-0.053171	-0.37603	57	58 (HOH)	59	-0.158946 -0.54169	
57	58 (S9)	59	-0.16516	-0.54866	59	58 (HOH)	57	-0.16043 -0.54337	
59	58 (S9)	57	-0.164202	-0.5476	67	73 (HOH)	74	0.077578 -0.42649	
70	79 (HOH)	80	-0.075402	-0.42247	74	73 (HOH)	67	-0.070199 -0.41252	
80	79 (HOH)	70	-0.069676	-0.41149	73 (HOH)	75	84	-0.066965 -0.40608	
79 (HOH)	81	93	-0.080503	-0.43179	84	75	73 (HOH)	-0.061341 -0.39438	
93	81	79 (HOH)	-0.073455	-0.4188	64	79 (HOH)	97	-0.065634 -0.40338	
85 (HOH)	87	96	-0.087527	-0.444	97	79 (HOH)	64	-0.060498 -0.39257	
96	87	85 (HOH)	-0.076921	-0.42529	21	82 (HOH)	101	-0.050149 -0.36877	
85 (HOH)	99	103	-0.056182	-0.383	101	82 (HOH)	21	-0.047556 -0.3623	
103	99	85 (HOH)	-0.063489	-0.39893	61	82 (HOH)	83	-0.064471 -0.40098	
64	88 (HOH)	89	-0.059183	-0.3897	83	82 (HOH)	61	-0.059584 -0.39058	
89	88 (HOH)	64	-0.056892	-0.38461	**96 (ACET)**	**94**	**60 (Ga)**	**0.03832 0.33714**	
90	99	101 (HOH)	-0.053344	-0.37644	91	94	96 (ACET)	-0.04354 -0.3518	
101 (HOH)	99	90	-0.047726	-0.36273	96 (ACET)	94	91	-0.060432 -0.39242	
67	102 (HOH)	108	-0.056716	-0.38421	94	95	96 (ACET)	-0.193295 -0.57819	
108	102 (HOH)	67	-0.052306	-0.37398	96 (ACET)	95	94	-0.197988 -0.58284	
					61	98 (HOH)	99	-0.037165 -0.33372	
					99	98 (HOH)	61	-0.036412 -0.33145	
					95	98 (HOH)	100	-0.08071 -0.43216	
					100	98 (HOH)	95	-0.081268 -0.43315	
C3.15 without ACET					*C3.15 with ACET*				
Atom 1	Atom 2	Atom 3	MCI	$-\|MCI\|^{1/n}$	Atom 1	Atom 2	Atom 3	MCI	$-\|MCI\|^{1/n}$
5	31	70 (L3)	-0.147452	-0.5283	5	31	70 (L3)	-0.156572	-0.53898
70 (L3)	31	5	-0.162574	-0.54578	70 (L3)	31	5	-0.171613	-0.55571
30	31	70 (L3)	-0.043924	-0.35283	30	31	70 (L3)	-0.041192	-0.34536
70 (L3)	31	30	-0.056633	-0.38402	70 (L3)	31	30	-0.054745	-0.37971
81	**70 (L3)**	**31**	**0.037267**	**0.33402**	**81**	**70 (L3)**	**31**	**0.037986**	**0.33616**
76 (S7)	138	165	-0.083651	-0.43734	76 (S7)	54	52	-0.031896	-0.31714
165	138	76 (S7)	-0.073198	-0.41831	76 (S7)	138	165	-0.086172	-0.44169
157 (HOH)	168	169	-0.096009	-0.4579	165	138	76 (S7)	-0.076427	-0.42437
169	168	157 (HOH)	-0.090583	-0.44911	157 (HOH)	168	169	-0.106956	-0.47468
159	162 (HOH)	164	-0.067715	-0.40759	169	168	157 (HOH)	-0.095746	-0.45748
164	162 (HOH)	159	-0.063991	-0.39998	159 (HOH)	162	164	-0.104916	-0.47164
					164	162	159 (HOH)	-0.097754	-0.46066
					180 (ACET)	**179**	**81 (Ga)**	**0.034206**	**0.32461**
					176	179	180 (ACET)	-0.043703	-0.35224
					180 (ACET)	179	176	-0.062131	-0.39607
					179	180 (ACET)	181	-0.199374	-0.58419
					181	180 (ACET)	179	-0.19289	-0.57779

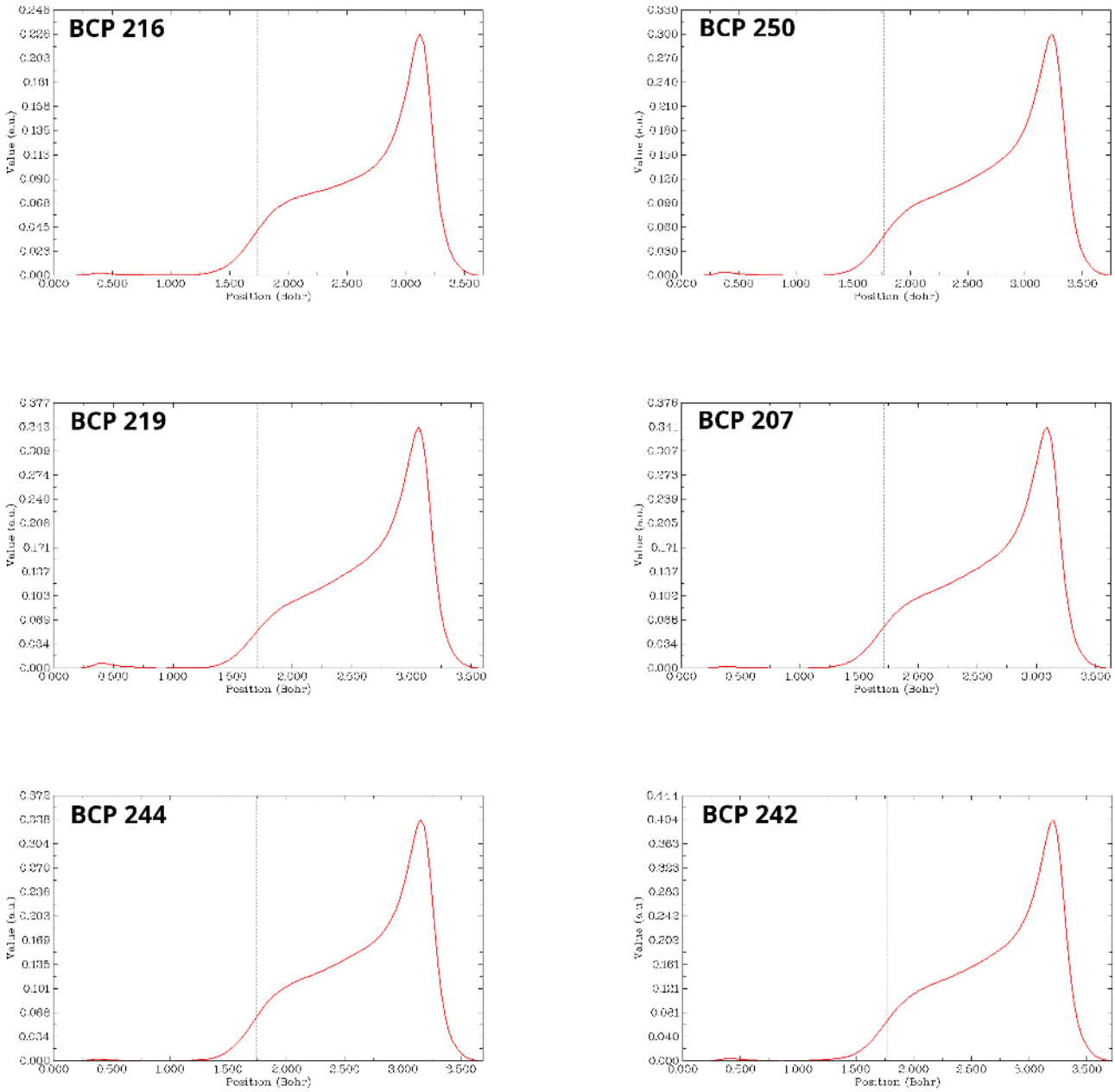

Fig. S12 Bond ellipticity plots for each BCP of ligands interacting directly with Ga^{3+} when complexed with peptide M3 and without ACET. Key and binding energies for labelled BCPs can be found in Table 3 of the main text.

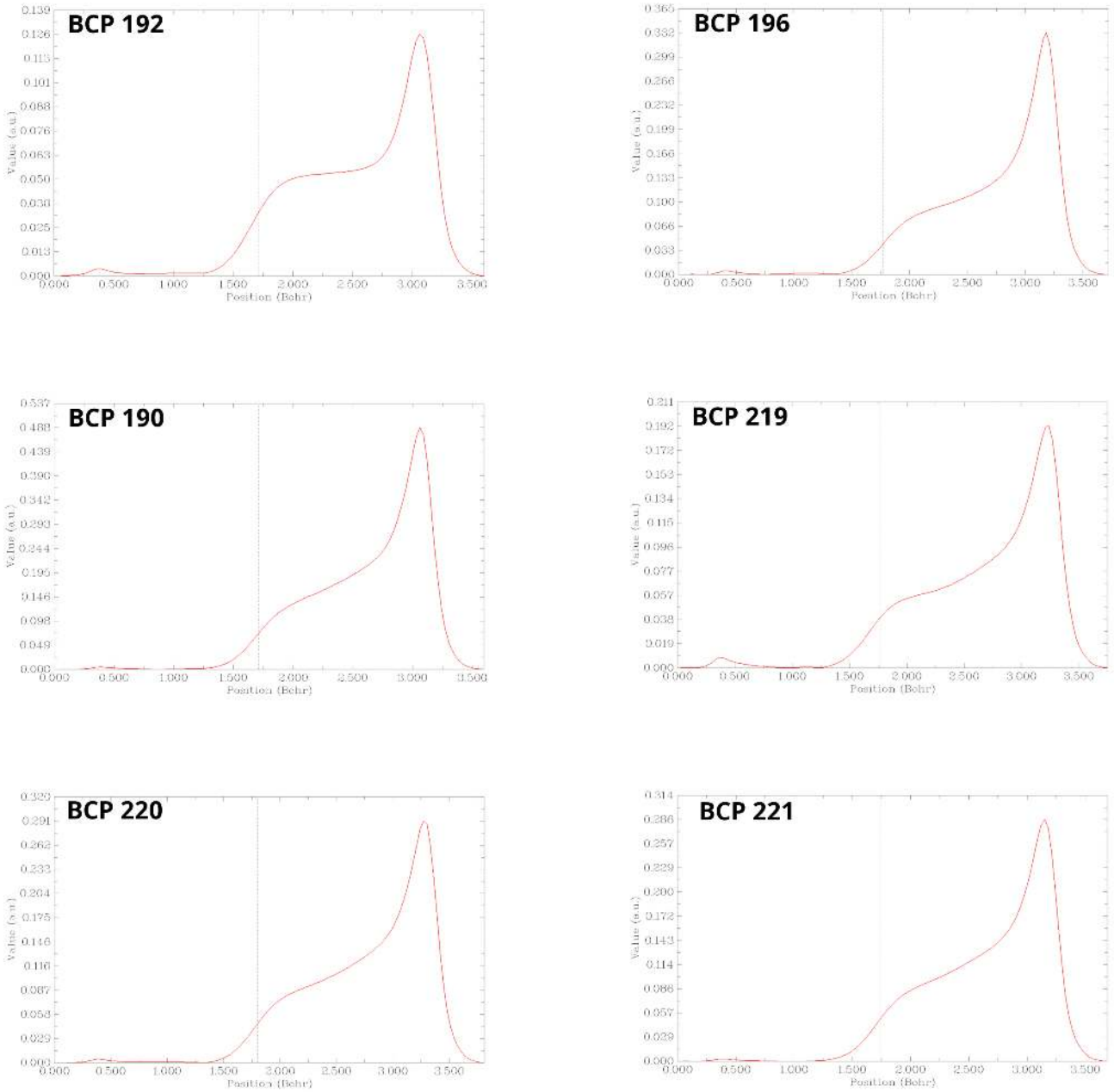

Fig. S13 Bond ellipticity plots for each BCP of ligands interacting directly with Ga^{3+} when complexed with peptide M3 and with ACET as a ligand. Key and binding energies for labelled BCPs can be found in Table 3 of the main text.

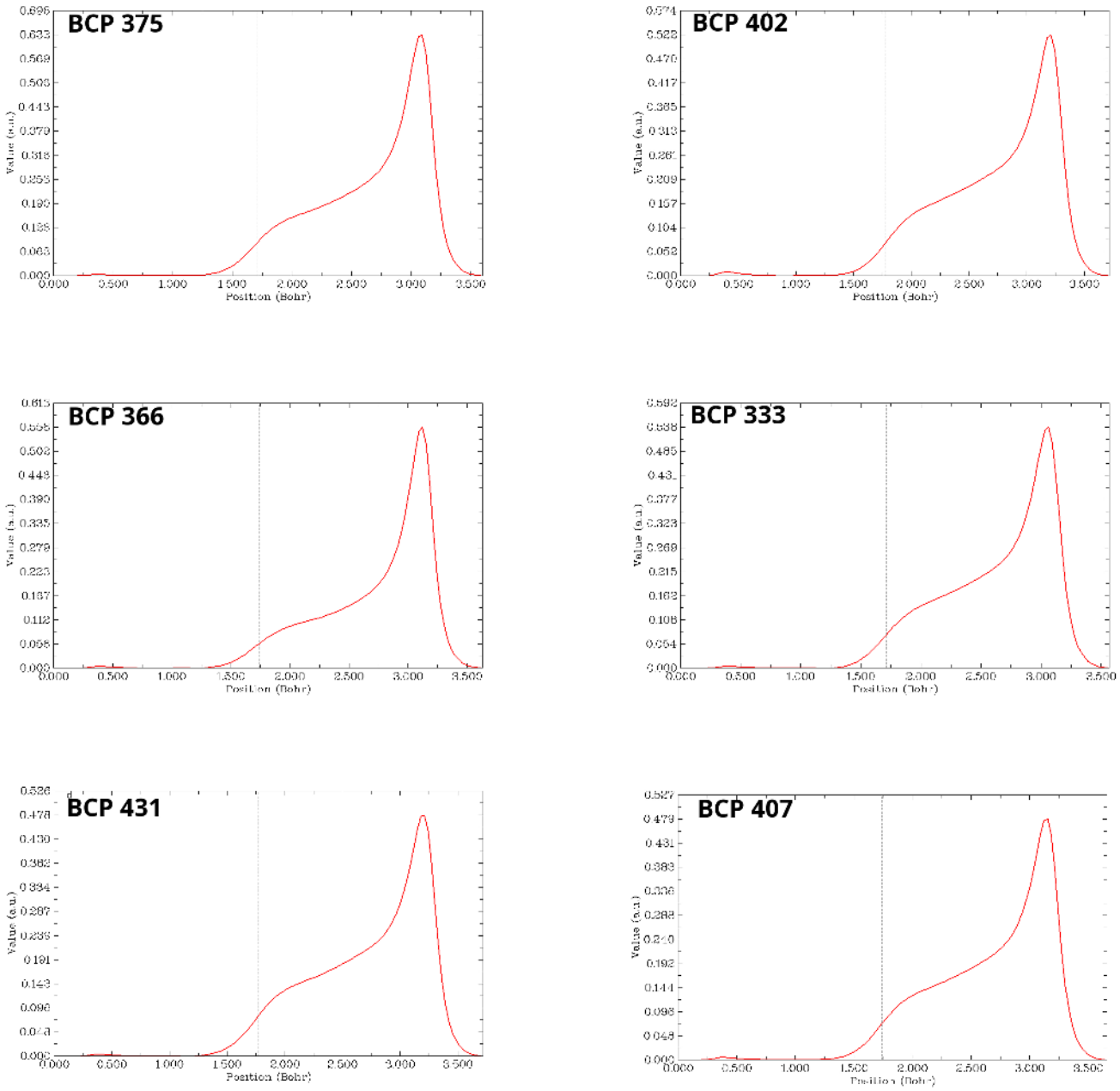

Fig. S14 Bond ellipticity plots for each BCP of ligands interacting directly with Ga^{3+} when complexed with peptide C3.15 and without ACET. Key and binding energies for labelled BCPs can be found in Table 3 of the main text.

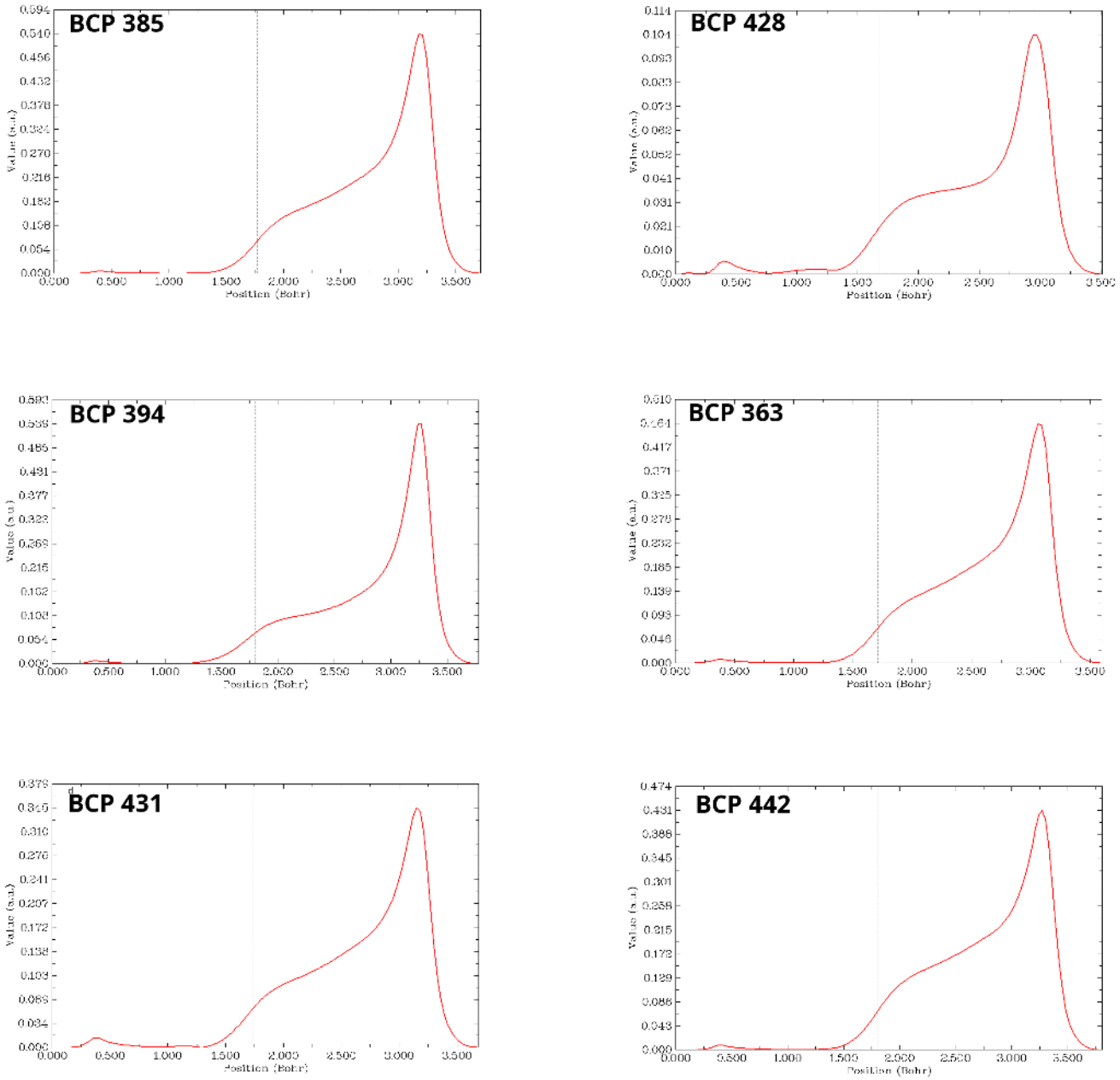

Fig. S15 Bond ellipticity plots for each BCP of ligands interacting directly with Ga^{3+} when complexed with peptide C3.15 and with ACET as a ligand. Key and binding energies for labelled BCPs can be found in Table 3 of the main text.

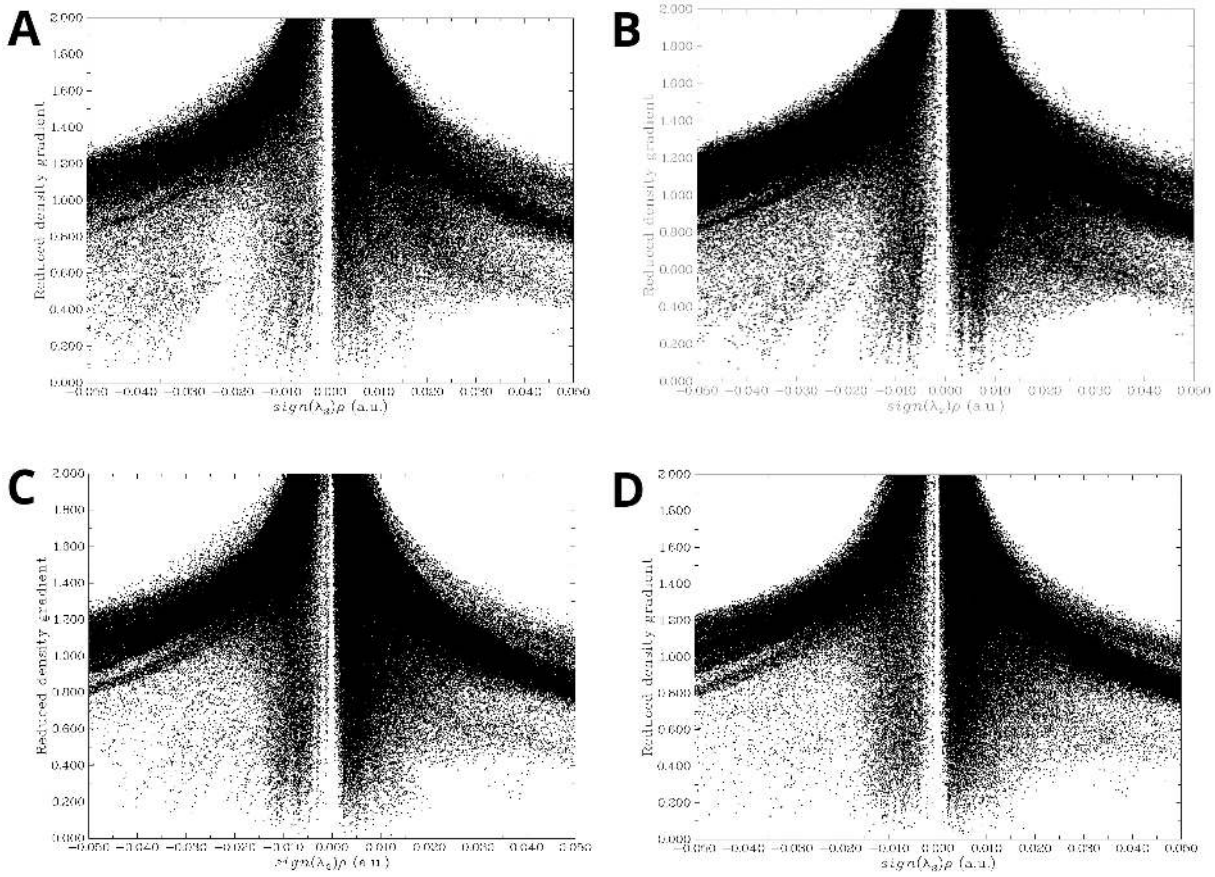

Fig. S16 Scatter plots of RDG for peptide M3 (A) without ACET (B) with ACET and peptide C3.15 without ACET (C) and with ACET (D). Of note is the region in plot A where there are fewer points in the $sign(\lambda_2\rho)$ region corresponding to non-bonded interactions such as vdW forces.

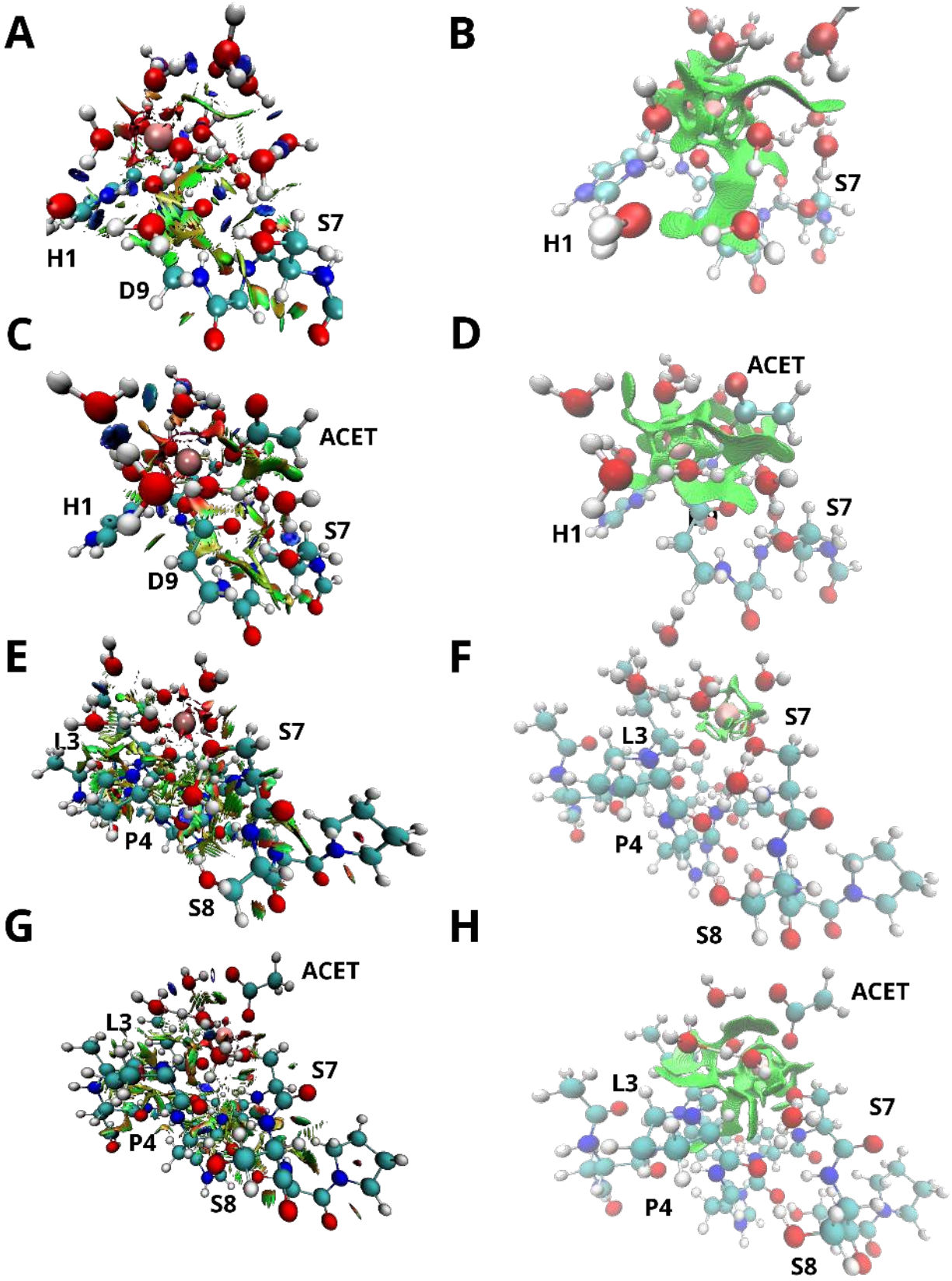

Fig. S17 NCI plots (left) and the largest integrated RDG domains (right) for peptide M3 without ACET (A and B) and with ACET (C and D) present, peptide C3.15 without ACET (E and F) and with ACET (G and H) ACET present. Selected residues and Ga^{3+} atom (pink spheres) are displayed, blue discs of RDG density are indicative of favourable hydrogen bonding, green regions indicative of weaker vdW interactions with regions regions assumed to be unfavourable for binding.

Table S12 q_{bind} indices for domains derived from integration and clustering of RDG isosurfaces for peptides M3 and C3.15 with and without acetate present.

M3 without ACET			*M3 with ACET*		
Domain	**q_{bind} (a.u.)**	**type**	**Domain**	**q_{bind} (a.u.)**	**type**
13	-0.00292906	NH...C=O	8	-0.00414614	NH...C=O
17	-0.00755583	NH...C=O (H1-D9)	14	-0.00718921	NH...C=O
23	-0.00717977	HOH...C=O	17	-0.00327423	HOH...C=O
26	-0.00678304	HOH...HOH	19	-0.0058662	HOH...C=O
27	-0.00579789	HOH...HOH	24	0.00074875	HOH...C=O
29	-0.00585405	HOH...C=O (D9)	30	-0.00571438	HOH...C=O
30	-0.00279833	HOH...C=O	32	-0.00550723	HOH...HOH
31	-0.00605514	OH...C=O (S7-D9)	34	-0.00701454	OH...C=O (S7-D9)
32	0.00140308	HOH...HOH	35	-0.00734349	HOH...HOH
36	-0.00556573	HOH...HOH	38	-0.00476539	HOH...HOH
37	-0.00478412	HOH...HOH	41	-0.0059732	HOH...HOH
41	-0.00082314	HOH...HOH	43	-0.00598465	HOH...OH (S7)
42	-0.00705266	HOH...HOH	44	-0.00011422	HOH...HOH
44	-0.00757126	HOH...HOH	46	-0.00603208	HOH...HOH
46	-0.00599294	HOH...OH (S7)	47	-0.00279051	HOH...HOH
48	-0.00746276	HOH...HOH	48	0.00128872	HOH...C=O (ACE)
51	0.00210854	HOH...HOH			
52	-0.0074817	HOH...HOH			
53	0.00092933	HOH...HOH			
55	-0.00709723	HOH...HOH			
56	-0.00731666	HOH...HOH			
58	-0.00578205	HOH...HOH			
59	-0.00678678	HOH...HOH			
61	-0.00649777	HOH...HOH			
C3.15 without ACET			*C3.15 with ACET*		
Domain	**q_{bind} (a.u.)**	**type**	**Domain**	**q_{bind} (a.u.)**	**type**
1	-0.00493396	NH...C=O	2	-0.007175	NH...C=O
18	-0.00334227	OH...C=O	11	-0.00511451	OH...C=O
27	-0.00325102	NH...C=O	16	-0.00485494	NH...C=O
29	-0.00191524	NH...C=O	19	-0.00170064	NH...C=O
31	-0.00077542	NH...C=O	20	-0.00279231	NH...C=O
32	-0.00181249	NH...C=O	30	-0.00515668	OH...C=O
33	-0.00296991	NH...C=O	36	-0.00697074	HOH...C=O
49	-0.0027996	OH...C=O	52	0.00066663	HOH...HOH
58	-0.00477246	HOH...C=O	55	-0.00719841	HOH...HOH
79	-0.00144816	HOH...HOH	56	-0.00445976	HOH...HOH
81	-0.00349659	HOH...HOH			

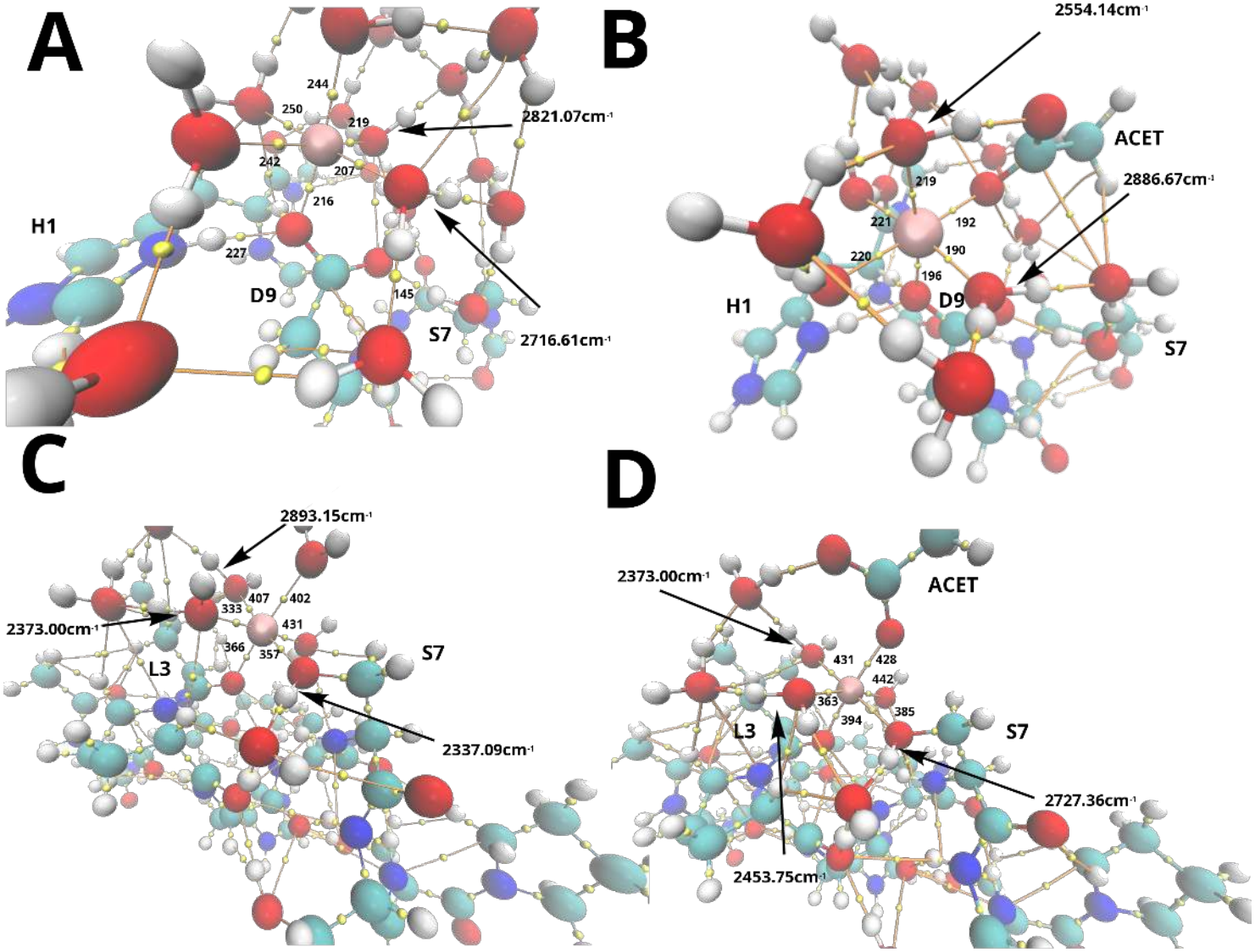

Fig. S18 Optimised structures for peptide M3 (CPK representation) depicted without ACET (A) and with ACET (B) and peptide C3.15 without ACET (C) and with ACET (D). Selected (3, -1) interactions (yellow spheres) and Ga^{3+} (pink sphere) are depicted. Calculated bond paths (orange lines) are also depicted. Key and binding energies for labelled BCPs can be found in Table 3

Table S13 Medium-range cross peaks in the NOESY spectrum for residues in the Ga^{3+}-free M3 peptide. Medium-range cross peaks include correlation of atoms of residue i to residues i + 1, i + 2 and i + 3. Peak intensities have been evaluated from the relative data height to very strong, strong, medium and weak.

Peak	δ_1 (ppm)	δ_2 (ppm)	Intensity	Peak	δ_1 (ppm)	δ_2 (ppm)	Intensity
T2 MG2 – H4 HD2	1.134	7.311	weak	Q6 QG – S7 HN	2.437	7.966	weak
C3 HA – H4 HN	4.702	9.093	weak	S7 HA – C8 HN	4.414	8.290	strong
C3 HA – I5 HN	4.704	7.708	weak	S7 HA – D9 HN	4.414	8.259	weak
C3 HBa – I5 HN	3.232	7.707	weak	S7 HBa – C8 HN	3.933	8.290	weak
C3 HN – T2 HB	8.739	4.069	weak	S7 HBa – D9 HN	3.856	8.256	very weak
H4 HA – I5 HN	4.887	7.707	medium	S7 HBb – C8 HN	3.854	8.291	weak
H4 HBa – I5 HN	3.164	7.709	weak	S7 HBb – D9 HN	3.926	8.262	very weak
H4 HBa – I5 MG2	3.160	0.950	weak	S7 HN – I5 HB	7.967	2.087	weak
H4 HBb – I5 HN	3.429	7.706	weak	S7 HN – I5 HG1b	7.966	1.318	medium
H4 HBb – I5 MG2	3.429	0.951	weak	S7 HN – I5 MD	7.966	0.903	weak
H4 HN – I5 HN	9.090	7.705	very weak	S7 HN – I5 MG2	7.964	0.952	weak
I5 HA – Q6 HN	4.407	8.493	strong	S7 HN – Q6 HA	7.966	4.125	medium
I5 HG1a – Q6 HN	1.156	8.493	weak	S7 HN – Q6 HN	7.966	8.493	medium
I5 HG1a – S7 HN	1.156	7.967	weak	S7 HN – Q6 QB	7.965	2.124	medium
I5 HG1a – C8 HN	1.154	8.288	very weak	S7 HN – C8 HN	7.966	8.292	medium
I5 HG1b – Q6 HN	1.319	8.493	weak	C8 HA – S7 HN	4.701	7.966	very weak
I5 HG1b – S7 HN	1.318	7.967	medium	C8 HBa – D9 HN	3.145	8.260	medium
I5 HG1b – C8 HN	1.320	8.290	weak	C8 HBb – D9 HN	3.288	8.259	medium
I5 HN – C3 HBa	7.711	3.234	very weak	C8 HN – I5 HG1b	8.290	1.317	weak
I5 HN – H4 HBa	7.709	3.167	weak	C8 HN – S7 HA	8.289	4.413	weak
I5 HN – H4 HBb	7.710	3.429	very weak	C8 HN – S7 HBa	8.293	3.935	very weak
I5 HN – H4 HN	7.708	9.092	weak	C8 HN – S7 HBb	8.284	3.854	very weak
I5 HN – Q6 HN	7.707	8.493	medium	C8 HN – S7 HN	8.293	7.967	medium
I5 HN – C8 HBb	7.706	3.284	very weak	D9 HA – H10 HN	4.540	8.368	medium
I5 MD – H4 HD2	0.903	7.310	weak	D9 HA – C8 HN	4.541	8.291	very weak
I5 MD – Q6 HN	0.905	8.494	weak	D9 HN – H10 HBa	8.256	3.186	weak
I5 MD – S7 HN	0.907	7.968	weak	D9 HN – H10 HBb	8.253	3.311	very weak
I5 MG2 – H4 HD2	0.953	7.311	weak	D9 HN – H10 HN	8.260	8.368	medium
I5 MG2 – Q6 HN	0.955	8.493	medium	D9 QB – H10 HN	2.643	8.369	medium
I5 MG2 – S7 HN	0.951	7.967	weak	D9 QB – C8 HN	2.635	8.290	weak
Q6 HA – S7 HN	4.126	7.967	medium	H10 HA – L11 HN	4.689	8.258	strong
Q6 HA – C8 HN	4.126	8.292	weak	H10 HN – D9 HA	8.370	4.538	very weak
Q6 HA – D9 HN	4.122	8.260	very weak	H10 HN – D9 HN	8.362	8.256	medium
Q6 HN – I5 HA	8.491	4.406	weak	H10 HN – D9 QB	8.367	2.641	weak
Q6 HN – I5 HB	8.492	2.090	medium	L11 HA – A12 HN	4.340	7.918	medium
Q6 HN – I5 HG1b	8.493	1.317	weak	L11 HBb – A12 HN	1.627	7.921	weak
Q6 HN – I5 HN	8.492	7.706	weak	L11 HG – A12 HN	1.581	7.921	weak
Q6 HN – I5 MG2	8.492	0.954	weak	L11 HG – D9 HN	1.570	8.256	medium
Q6 HN – S7 HN	8.493	7.966	medium	L11 HN – A12 HN	8.255	7.918	weak
Q6 QB – S7 HN	2.123	7.966	medium	A12 HN – L11 HA	7.917	4.338	weak
Q6 QG – I5 MG2	2.442	0.953	weak	A12 HN – L11 HN	7.918	8.256	medium

Table S14 Medium-range cross peaks in the NOESY spectrum for residues in the Ga^{3+}-bound M3 peptide. Medium-range cross peaks include correlation of atoms of residue i to residues i + 1, i + 2 and i + 3. Peak intensities have been evaluated from the relative data height to very strong, strong, medium and weak.

Peak	δ_1 (ppm)	δ_2 (ppm)	Intensity	Peak	δ_1 (ppm)	δ_2 (ppm)	Intensity
H1 HA – T2 HN	4.443	8.727	medium	Q6 HA – D9 HN	4.091	8.154	very weak
H1 QB – T2 HN	3.424	8.729	weak	Q6 HA – D9 QB	4.092	2.804	very weak
T2 HA – C3 HBa	4.338	3.180	very weak	Q6 HN – I5 HA	8.557	4.451	weak
T2 HA – C3 HBb	4.340	3.092	very weak	Q6 HN – I5 HB	8.557	2.083	medium
T2 HA – C3 HN	4.331	8.696	strong	Q6 HN – I5 HG1a	8.560	1.155	very weak
T2 HB – C3 HN	4.037	8.695	medium	Q6 HN – I5 HG1b	8.557	1.332	weak
T2 HN – H1 QB	8.727	3.421	weak	Q6 HN – I5 HN	8.559	7.652	weak
T2 MG2 – C3 HN	1.120	8.696	weak	Q6 HN – I5 MG2	8.558	0.951	weak
T2 MG2 – H4 HD2	1.116	7.298	very weak	Q6 HN – S7 HN	8.558	8.006	medium
C3 HA – H4 HN	4.671	9.130	strong	Q6 HN – C8 HN	8.557	8.078	very weak
C3 HA – I5 HN	4.673	7.652	weak	Q6 QB – S7 HN	2.112	8.006	medium
C3 HBb – I5 MG2	3.141	0.945	weak	Q6 QB – C8 HN	2.100	8.081	very weak
C3 HN – T2 HA	8.697	4.329	medium	Q6 QG – I5 MG2	2.441	0.945	weak
C3 HN – T2 HB	8.700	4.035	weak	Q6 QG – S7 HN	2.433	8.007	weak
C3 HN – T2 MG2	8.700	1.120	weak	S7 HA – Q6 HA	4.348	4.084	very weak
C3 HN – H4 HN	8.697	9.128	weak	S7 HA – C8 HN	4.349	8.080	medium
H4 HA – I5 HN	4.902	7.653	medium	S7 HA – D9 HN	4.346	8.156	weak
H4 HBa – I5 HN	3.134	7.653	weak	S7 HBa – I5 MD	3.948	0.887	weak
H4 HBb – I5 HN	3.418	7.653	weak	S7 HBa – C8 HN	3.943	8.080	weak
H4 HBb – I5 MD	3.427	0.886	weak	S7 HBa – D9 HN	3.945	8.150	very weak
H4 HBb – I5 MG2	3.421	0.945	weak	S7 HBb – Q6 QB	3.852	2.111	very weak
H4 HN – C3 HBa	9.130	3.191	weak	S7 HBb – C8 HN	3.859	8.081	weak
H4 HN – C3 HBb	9.131	3.095	weak	S7 HN – I5 HG1a	8.006	1.158	very weak
H4 HN – C3 HN	9.137	8.700	weak	S7 HN – I5 HG1b	8.006	1.333	weak
H4 HN – I5 HG1a	9.133	1.167	very weak	S7 HN – I5 HN	7.984	7.647	very weak
H4 HN – I5 HN	9.130	7.652	medium	S7 HN – I5 MD	8.007	0.890	weak
H4 HN – I5 MG2	9.128	0.948	very weak	S7 HN – I5 MG2	8.003	0.949	weak
I5 HA – T2 MG2	4.447	1.119	very weak	S7 HN – Q6 HA	8.006	4.090	weak
I5 HA – Q6 HN	4.450	8.557	strong	S7 HN – Q6 HN	8.006	8.557	medium
I5 HA – S7 HN	4.449	8.005	weak	S7 HN – Q6 QB	8.004	2.114	medium
I5 HA – C8 HN	4.446	8.086	very weak	S7 HN – Q6 QG	8.011	2.435	very weak
I5 HB – C8 QB	2.087	3.233	very weak	C8 HA – I5 HG1b	4.694	1.328	very weak
I5 HG1a – H4 HN	1.161	9.129	very weak	C8 HA – I5 MD	4.693	0.887	weak
I5 HG1a – Q6 HN	1.165	8.557	weak	C8 HA – D9 HN	4.696	8.155	medium
I5 HG1a – S7 HN	1.168	8.007	weak	C8 HN – I5 HG1b	8.080	1.332	weak
I5 HG1a – C8 HN	1.169	8.085	very weak	C8 HN – I5 MG2	8.076	0.950	very weak
I5 HG1a – C8 QB	1.160	3.237	weak	C8 HN – Q6 HN	8.074	8.559	weak
I5 HG1b – Q6 HN	1.332	8.557	weak	C8 HN – S7 HA	8.082	4.346	weak
I5 HG1b – S7 HN	1.333	8.006	medium	C8 HN – D9 QB	8.080	2.807	very weak
I5 HG1b – C8 HN	1.335	8.081	weak	C8 QB – I5 HB	3.239	2.083	very weak
I5 HG1b – C8 QB	1.332	3.237	weak	C8 QB – I5 HG1a	3.235	1.161	very weak
I5 HN – C3 HBa	7.657	3.194	very weak	C8 QB – I5 HG1b	3.238	1.340	very weak
I5 HN – C3 HBb	7.652	3.095	very weak	C8 QB – I5 HN	3.235	7.654	weak
I5 HN – H4 HBa	7.650	3.136	weak	C8 QB – I5 MG2	3.234	0.950	very weak
I5 HN – H4 HBb	7.654	3.419	very weak	C8 QB – S7 HN	3.239	8.003	very weak
I5 HN – H4 HN	7.654	9.130	medium	C8 QB – D9 HN	3.236	8.155	medium
I5 HN – Q6 HN	7.653	8.557	weak	D9 HA – H10 HN	4.604	8.397	strong
I5 HN – C8 HN	7.649	8.080	very weak	D9 HA – C8 HN	4.600	8.079	very weak
I5 HN – C8 QB	7.654	3.235	weak	D9 HA – C8 QB	4.604	3.237	very weak
I5 MD – Q6 HN	0.889	8.558	weak	D9 HN – C8 QB	8.154	3.236	medium
I5 MD – S7 HN	0.889	8.007	weak	D9 QB – H10 HN	2.804	8.398	weak
I5 MD – C8 HN	0.894	8.083	very weak	H10 HA – L11 HN	4.682	8.173	medium
I5 MD – C8 QB	0.891	3.239	weak	H10 HBa – L11 HN	3.177	8.173	weak
I5 MG2 – H4 HBa	0.952	3.137	weak	H10 HBb – L11 HN	3.291	8.173	weak
I5 MG2 – H4 HBb	0.949	3.418	very weak	H10 HN – L11 HN	8.396	8.169	medium
I5 MG2 – H4 HD2	0.952	7.299	weak	H10 HN – C8 QB	8.394	3.237	very weak
I5 MG2 – H4 HN	0.951	9.130	weak	H10 HN – D9 HN	8.400	8.155	medium
I5 MG2 – Q6 HN	0.949	8.558	medium	H10 HN – D9 QB	8.396	2.805	weak
I5 MG2 – Q6 QG	0.948	2.437	weak	L11 HA – A12 HN	4.336	8.229	medium
I5 MG2 – S7 HN	0.950	8.006	weak	L11 HA – C8 QB	4.339	3.236	very weak
I5 MG2 – C8 HN	0.949	8.079	very weak	L11 HN – H10 HBa	8.168	3.178	weak
Q6 HA – I5 MG2	4.091	0.950	very weak	L11 HN – H10 HBb	8.176	3.296	very weak
Q6 HA – S7 HN	4.090	8.006	medium	L11 HN – H10 HN	8.161	8.396	medium
Q6 HA – C8 HN	4.091	8.080	weak	A12 HN – L11 HA	8.232	4.332	weak

Table S15 Assigned ^{13}C and ^{1}H chemical shifts of identified nuclei for Ga^{3+}-free and Ga^{3+}-bound peptide M3.

Residue	Atom	δ // Ga^{3+}-free (ppm)	δ // Ga^{3+}-bound (ppm)	Residue	Atom	δ // Ga^{3+}-free (ppm)	δ // Ga^{3+}-bound (ppm)
H1	CB	29.329	29.032	Q6	HN	8.496	8.557
H1	HA	4.443	4.441	Q6	QB	2.126	2.114
H1	HD2	7.408	7.430	Q6	QG	2.441	2.436
H1	HE1	8.652	8.703	S7	CB	63.129	62.969
H1	QB	3.415	3.423	S7	HA	4.413	4.348
T2	CB	70.068	70.086	S7	HBa	3.932	3.945
T2	CG2	21.682	21.667	S7	HBb	3.863	3.856
T2	HA	4.357	4.331	S7	HN	7.968	8.005
T2	HB	4.067	4.034	C8	CB	41.916	41.524
T2	HN	8.737	8.727	C8	HA	4.699	4.696
T2	MG2	1.136	1.121	C8	HBa	3.154	8.081
C3	CB	42.273	42.023	C8	HBb	3.286	
C3	HA	4.706	4.668	C8	HN	8.285	3.237
C3	HBa	3.234	3.191	D9	CB	40.453	38.497
C3	HBb	3.118	3.101	D9	HA	4.542	4.601
C3	HN	8.732	8.697	D9	HN	8.258	8.154
H4	CB	29.495	29.529	D9	QB	2.655	2.805
H4	HA	4.892	4.901	H10	CB	28.773	28.706
H4	HBa	3.172	3.138	H10	HA	4.686	4.678
H4	HBb	3.436	3.420	H10	HBa	3.191	3.178
H4	HD2	7.315	7.299	H10	HBb	3.317	3.296
H4	HE1	8.618	8.617	H10	HD2	7.295	7.280
H4	HN	9.099	9.130	H10	HE1	8.616	8.610
I5	CB	39.668	39.882	H10	HN	8.371	8.396
I5	CD	13.600	13.588	L11	CB	42.388	42.409
I5	CG	27.064	26.954	L11	CDa	23.420	23.420
I5	CG2	18.008	17.972	L11	CDb	25.131	24.984
I5	HA	4.412	4.449	L11	CG	26.983	26.919
I5	HB	2.093	2.085	L11	HA	4.345	4.335
I5	HG1a	1.162	1.165	L11	HBa	1.594	1.576
I5	HG1b	1.310	1.334	L11	HBb	1.644	1.627
I5	HN	7.708	7.653	L11	HG	1.574	1.570
I5	MD	0.909	0.890	L11	HN	8.251	8.172
I5	MG2	0.958	0.950	L11	MDa	0.859	0.853
Q6	CA	58.422	58.637	L11	MDb	0.920	0.905
Q6	CB	28.772	28.621	A12	CA	53.620	
Q6	CG	34.039	33.968	A12	CB	20.128	19.331
Q6	HA	4.126	4.090	A12	HA	4.132	4.259
Q6	HEa	7.459	7.553	A12	HN	7.926	8.230
Q6	HEb	6.879	6.868	A12	MB	1.342	1.382

Table S16 Medium-range cross peaks in the NOESY spectrum for residues in the Ga^{3+}-free C3.15 peptide. Medium-range cross peaks include correlation of atoms of residue i to residues i + 1, i + 2 and i + 3. Peak intensities have been evaluated from the relative data height to very strong, strong, medium and weak. Residues with a minor form are noted by 'a' in front of the name of the residue.

Peak	δ_1 (ppm)	δ_2 (ppm)	Intensity	Peak	δ_1 (ppm)	δ_2 (ppm)	Intensity
Y2 HD – L3 HN	7.121	8.144	weak	Q6 HN – S7 HN	8.401	8.507	medium
Y2 QB – L3 HN	2.982	8.144	medium	Q6 QG – S7 HN	2.349	8.511	weak
L3 HA – P4 QD	4.574	3.587	strong	S7 HN – Q6 HA	8.509	4.385	medium
L3 HN – Y2 QB	8.148	2.984	medium	S7 HN – Q6 HBb	8.510	2.110	weak
L3 MD1 – P4 QD	0.880	3.586	weak	S7 HN – Q6 QG	8.509	2.353	weak
L3 QB – P4 QD	1.471	3.584	medium	S8 HA – S9 HN	4.517	8.328	strong
P4 HA – H5 HN	4.295	8.538	strong	S9 HA – P10 HDa	4.791	3.726	strong
P4 HBa – H5 HN	1.798	8.539	medium	S9 HA – P10 HDb	4.791	3.816	strong
P4 HBb – H5 HN	2.253	8.540	weak	P10 HA – S11 HN	4.483	8.387	strong
P4 QD – L3 HA	3.589	4.574	weak	P10 HBa – S11 HN	1.941	8.384	medium
P4 QD – L3 HG	3.579	1.516	weak	P10 HBb – S11 HN	2.314	8.384	medium
P4 QD – L3 HN	3.586	8.149	weak	P10 HDa – S11 HN	3.724	8.385	medium
P4 QD – L3 QB	3.580	1.477	medium	P10 HDb – S11 HN	3.809	8.388	weak
P4 QD – H5 HN	3.579	8.537	weak	P10 QG – S11 HN	2.018	8.384	weak
P4 QG – H5 HN	1.970	8.540	weak	S11 HN – P10 HA	8.389	4.484	medium
aH5 HA – aQ6 HN	4.714	8.585	medium	S11 QB – P10 HA	3.874	4.483	medium
H5 HA – L3 HN	4.637	8.146	strong	S11 QB – C13 HN	3.872	8.068	medium
H5 HA – Q6 HN	4.633	8.408	strong	R12 HA – C13 HN	4.418	8.068	strong
H5 HA – S7 HN	4.640	8.506	weak	R12 HBa – C13 HN	1.791	8.069	medium
H5 HBa – Q6 HN	3.241	8.406	medium	R12 HBb – C13 HN	1.926	8.068	medium
H5 HN – P4 HA	8.538	4.295	medium	R12 HN – C13 HN	8.405	8.069	medium
H5 HN – P4 HBb	8.536	2.254	weak	R12 QG – C13 HN	1.650	8.065	weak
Q6 HA – H5 HN	4.389	8.539	weak	C13 HN – S11 QB	8.068	3.872	weak
Q6 HA – S7 HN	4.389	8.508	strong	C13 HN – R12 HA	8.068	4.419	weak
Q6 HBa – P4 HA	1.987	4.295	weak	C13 HN – R12 HBa	8.070	1.790	weak
Q6 HBa – S7 HN	1.982	8.510	medium	C13 HN – R12 HBb	8.066	1.930	weak
Q6 HBb – S7 HN	2.107	8.508	medium	C13 HN – R12 HN	8.070	8.405	medium
Q6 HN – H5 HN	8.401	8.538	medium				

Table S17 Medium-range cross peaks in the NOESY spectrum for residues in the Ga^{3+}-bound C3.15 peptide. Medium-range cross peaks include correlation of atoms of residue i to residues i + 1, i + 2 and i + 3. Peak intensities have been evaluated from the relative data height to very strong, strong, medium and weak.

Peak	δ_1 (ppm)	δ_2 (ppm)	Intensity	Peak	δ_1 (ppm)	δ_2 (ppm)	Intensity
N1 HA – Y2 HN	4.301	8.606	strong	Q6 HN – H5 HBb	8.416	3.253	weak
N1 HBa – Y2 HN	2.875	8.606	medium	Q6 HN – H5 HN	8.411	8.546	medium
aY2 HA – aL3 HN	4.570	7.887	weak	Q6 HN – S7 HN	8.409	8.510	strong
Y2 HA – L3 HN	4.625	8.139	strong	Q6 QG – S7 HN	2.337	8.511	weak
Y2 HD – L3 HN	7.107	8.139	weak	S7 HA – S8 HN	4.480	8.385	strong
Y2 HN – N1 HA	8.606	4.300	medium	S7 HN – Q6 HA	8.511	4.377	medium
Y2 HN – N1 HBa	8.607	2.870	very weak	S7 HN – Q6 HBa	8.512	1.967	weak
Y2 HN – L3 HN	8.607	8.138	weak	S7 HN – Q6 HBb	8.510	2.089	medium
Y2 QB – L3 HN	2.966	8.139	medium	S7 HN – Q6 HN	8.512	8.413	medium
L3 HA – P4 QD	4.564	3.572	strong	S7 HN – Q6 QG	8.514	2.339	weak
L3 HN – N1 HG1	8.138	7.107	weak	S7 HN – S8 HN	8.511	8.386	medium
L3 HN – Y2 HN	8.142	8.605	medium	S8 HA – S9 HN	4.505	8.329	strong
L3 HN – Y2 QB	8.139	2.968	medium	S8 HN – S7 HN	8.382	8.511	medium
L3 MD1 – P4 QD	0.867	3.573	weak	S8 HN – S9 HN	8.393	8.329	strong
L3 QB – P4 QD	1.462	3.577	medium	S9 HA – P10 HDa	4.778	3.713	medium
L3 QB – H5 HN	1.460	8.546	weak	S9 HN – S8 HA	8.329	4.505	medium
P4 HA – H5 HN	4.281	8.546	strong	P10 HA – S11 HN	4.468	8.371	strong
P4 HA – Q6 HN	4.282	8.416	weak	P10 HBa – S11 HN	1.929	8.370	medium
P4 HBa – H5 HN	1.787	8.546	medium	P10 HBb – S11 HN	2.300	8.371	medium
P4 HBa – Q6 HN	1.788	8.414	weak	P10 HDa – S11 HN	3.711	8.372	medium
P4 HBb – H5 HN	2.239	8.546	medium	P10 HDa – S9 HN	3.710	8.329	weak
P4 QD – L3 HA	3.574	4.563	weak	P10 QG – S11 HN	2.009	8.370	weak
P4 QD – L3 HN	3.577	8.138	weak	S11 HN – P10 HA	8.378	4.469	medium
P4 QD – L3 MD1	3.568	0.862	medium	S11 HN – P10 HBb	8.371	2.304	weak
P4 QD – L3 MD2	3.569	0.891	weak	S11 HN – P10 HDa	8.371	3.709	weak
P4 QD – L3 QB	3.565	1.466	medium	S11 HN – P10 QG	8.372	2.009	weak
P4 QD – H5 HN	3.565	8.545	weak	S11 QB – R12 HBa	3.851	1.781	weak
P4 QG – H5 HN	1.956	8.546	weak	S11 QB – R12 HN	3.855	8.345	medium
aH5 HA – aQ6 HN	4.703	8.580	medium	S11 QB – R12 QG	3.856	1.634	weak
H5 HA – Q6 HN	4.619	8.414	strong	S11 QB – aC13 HN	3.854	8.254	medium
H5 HBa – Q6 HN	3.217	8.414	medium	R12 HA – aC13 HN	4.408	8.254	strong
H5 HBb – Q6 HN	3.249	8.413	medium	R12 HA – C13 HN	4.409	8.215	weak
H5 HN – P4 HA	8.546	4.281	medium	R12 HBa – aC13 HN	1.778	8.254	medium
H5 HN – P4 HBa	8.545	1.784	medium	R12 HBb – aC13 HN	1.907	8.254	medium
H5 HN – P4 HBb	8.546	2.240	weak	R12 QG – aC13 HN	1.637	8.254	medium
H5 HN – Q6 HN	8.548	8.414	medium	aC13 HBa – R12 HN	2.992	8.345	weak
Q6 HA – S7 HN	4.377	8.511	strong	aC13 HN – aR12 HBb	8.258	1.905	medium
Q6 HBa – S7 HN	1.969	8.511	medium	aC13 HN – R12 HA	8.257	4.409	medium
Q6 HBb – S7 HN	2.091	8.510	medium	aC13 HN – R12 HBa	8.257	1.776	weak
Q6 HBb – S8 HN	2.090	8.385	weak	aC13 HN – R12 QG	8.256	1.635	weak
Q6 HN – H5 HBa	8.415	3.212	medium				

Table S18 Assigned ^{13}C and ^{1}H chemical shifts of identified nuclei for Ga^{3+}-free and Ga^{3+}-bound peptide C3.15. Chemical shifts of residues with a minor form are noted by 'a' in front of the name of the residue, 'd' is for further duplicates of C13. Resonances of ambiguous serines are denoted by 'aS11?' and aS?'.

Residue	Atom	δ // Ga^{3+}-free (ppm)	δ // Ga^{3+}-bound (ppm)	Residue	Atom	δ // Ga^{3+}-free (ppm)	δ // Ga^{3+}-bound (ppm)
N1	CB	37.847	37.723	aQ6	HN	8.590	8.580
N1	HA	4.314	4.303	S7	CB	63.929	63.913
N1	HBa	2.888	2.873	S7	HA	4.495	4.479
N1	HBb	2.953	2.947	S7	HBa	3.876	3.860
N1	HG1	6.994	7.010	S7	HBb	3.917	3.899
N1	HG2	7.684	7.673	S7	HN	8.509	8.511
Y2	CB	38.931	38.915	S8	CB	63.929	63.917
Y2	HA	4.642	4.625	S8	HA	4.521	4.507
Y2	HD	7.126	7.109	S8	HN	8.393	8.386
Y2	HE	6.822	6.804	S8	QB	3.894	3.879
Y2	HN	8.612	8.606	S9	CB	63.483	63.465
Y2	QB	2.988	2.970	S9	HA	4.794	4.783
aY2	HA	-	4.571	S9	HBa	3.829	3.812
aY2	HN	-	8.597	S9	HBb	3.874	3.858
aY2	QB	-	3.053	S9	HN	8.330	8.329
L3	CB	42.337	42.330	P10	CB	32.206	32.170
L3	CD1	23.655	23.636	P10	CD	50.843	50.832
L3	CD2	25.183	25.140	P10	CG	27.377	27.357
L3	CG	26.921	26.901	P10	HA	4.483	4.467
L3	HA	4.577	4.564	P10	HBa	1.948	1.934
L3	HG	1.529	1.515	P10	HBb	2.321	2.304
L3	HN	8.145	8.139	P10	HDa	3.732	3.715
L3	MD1	0.881	0.869	P10	HDb	3.822	3.810
L3	MD2	0.909	0.889	P10	QG	2.027	2.012
L3	QB	1.476	1.472	S11	CB	63.920	63.902
aL3	CD2	-	23.130	S11	HN	8.386	8.371
aL3	HA	4.312	4.300	S11	QB	3.874	3.856
aL3	HBa	1.360	1.339	R12	CB	30.922	30.915
aL3	HBb	1.567	1.546	R12	CD	43.397	43.364
aL3	HG	1.488	1.469	R12	CG	27.127	27.079
aL3	HN	7.900	7.887	R12	HA	4.426	4.414
aL3	MD1	0.893	0.875	R12	HBa	1.794	1.780
aL3	MD2	0.784	0.769	R12	HBb	1.934	1.910
P4	CB	32.144	32.125	R12	HE	7.192	7.177
P4	CD	50.546	50.537	R12	HN	8.392	8.350
P4	CG	27.317	27.285	R12	QD	3.215	3.197
P4	HA	4.298	4.283	R12	QG	1.654	1.644
P4	HBa	1.803	1.790	aR12	HBa	1.786	1.768
P4	HBb	2.258	2.241	aR12	Hbb	-	1.903
P4	QD	3.588	3.574	aR12	HN	8.508	8.466
P4	QG	1.972	1.958	C13	CB	42.662	41.933
H5	CB	28.884	28.792	C13	HA	4.476	4.591
H5	HA	4.637	4.620	C13	HBa	2.983	2.996
H5	HBa	3.235	3.216	C13	HBb	3.250	3.275
H5	HBb	3.272	3.252	C13	HN	8.070	8.255
H5	HD2	7.313	7.299	dC13	HA	-	4.585
H5	HE1	8.609	8.605	dC13	HBa	-	2.995
H5	HN	8.540	8.546	dC13	HBb	-	3.273
aH5	HA	4.716	4.704	dC13	HN	-	8.281
aH5	HBa	3.170	3.147	aC13	CB	29.116	28.550
aH5	HBb	3.259	3.236	aC13	HA	4.382	4.489
aH5	HN	8.827	8.825	aC13	HN	8.024	8.212
Q6	CB	29.779	29.774	aC13	QB	2.931	2.952
Q6	CG	33.793	33.754	adC13	HA	-	4.479
Q6	HA	4.393	4.378	adC13	HN	8.054	8.243
Q6	HBa	1.989	1.971	aS11?	HA	4.433	4.418
Q6	HBb	2.110	2.090	aS11?	HN	8.636	8.628
Q6	HE1	6.879	6.866	aS11?	QB	3.920	3.895
Q6	HE2	7.534	7.520	aS?	HA	4.612	4.598
Q6	HN	8.409	8.414	aS?	HN	8.144	3.704
Q6	QG	2.354	2.340	aS?	QB	3.742	3.734
aQ6	HBa	1.977	-	aS?	HN	-	8.131

Table S19 Predicted $^{3}J_{H^{N}\text{-}H^{\alpha}}$ values for nine types of β-turns using published dihedral angles (φ) from deBrevern, et al (Scientific Reports, 6, pp 1-15, 2016)

Type of β-turn	φ of i + 1 and i + 2	$^{3}J_{H^{N}\text{-}H^{\alpha}}$/Hz
I	-60	3.3
	-90	7.7
I'	60	7.3
	90	5.5
II	-60	3.3
	80	6.5
II'	60	7.3
	-80	6.3
VII	-60	3.3
	-120	9.9
IV_1	-120	9.9
	55	7.3
IV_2	-85	7.0
	-125	9.8
IV_3	-71	4.9
	-72	5.0
IV_4	-97	8.5
	-117	9.8

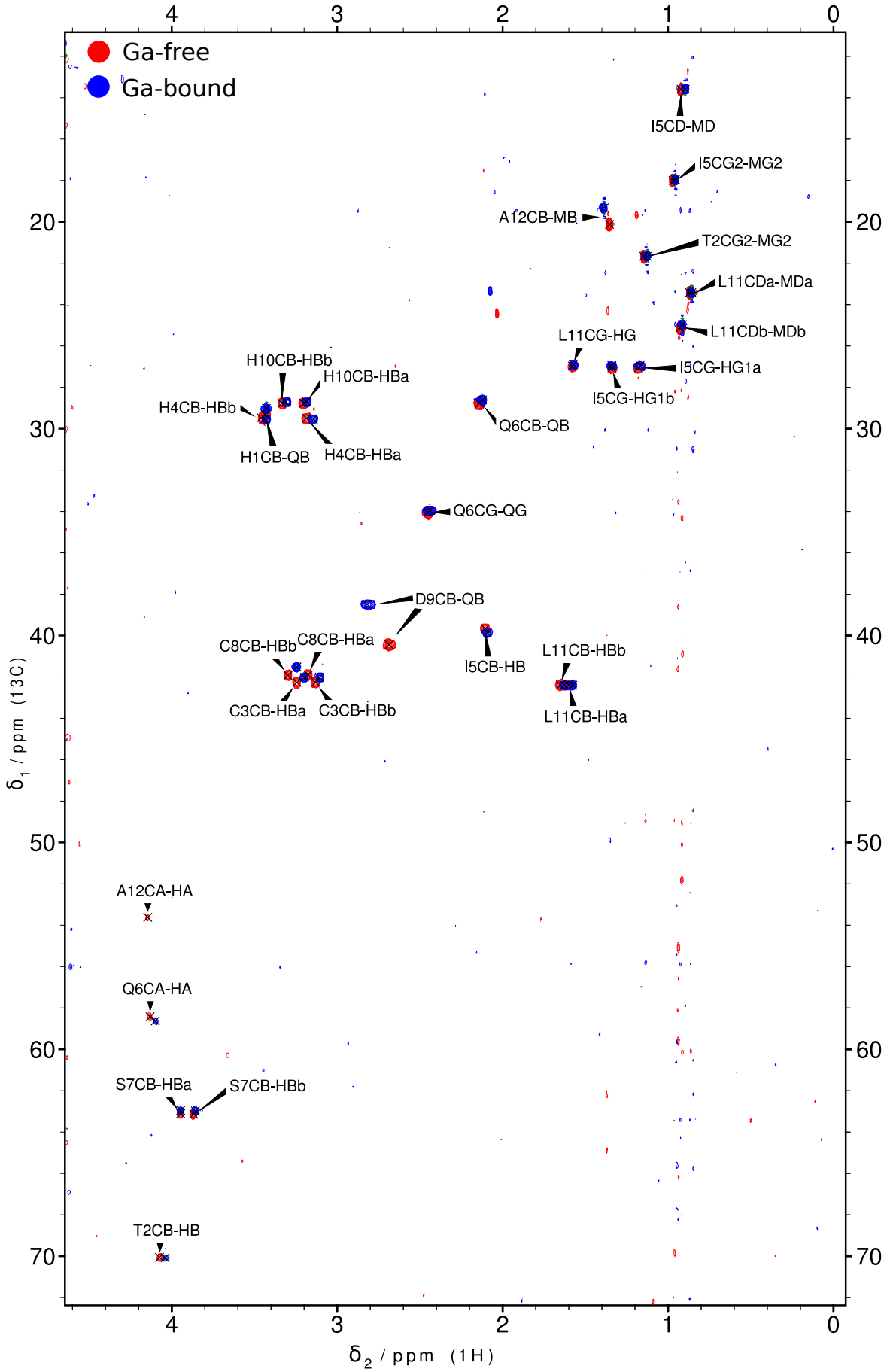

Fig. S19 Overlaid ^{1}H-^{13}C HSQC spectra of the peptide M3. Ga-free form is shown in red, Ga-bound in blue.

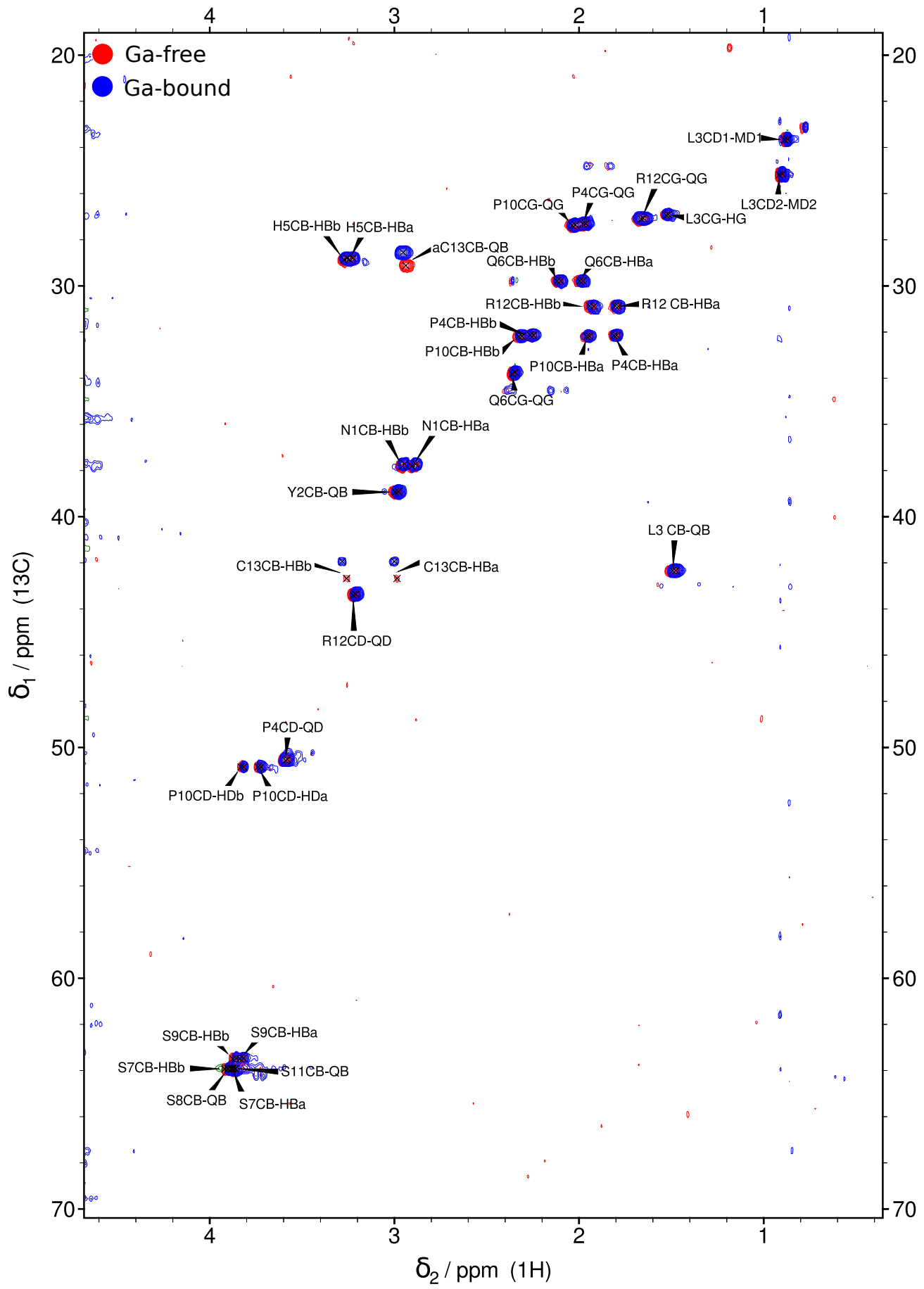

Fig. S20 Overlaid ^{1}H-^{13}C HSQC spectra of the peptide C3.15. Ga-free form is shown in red, Ga-bound in blue.

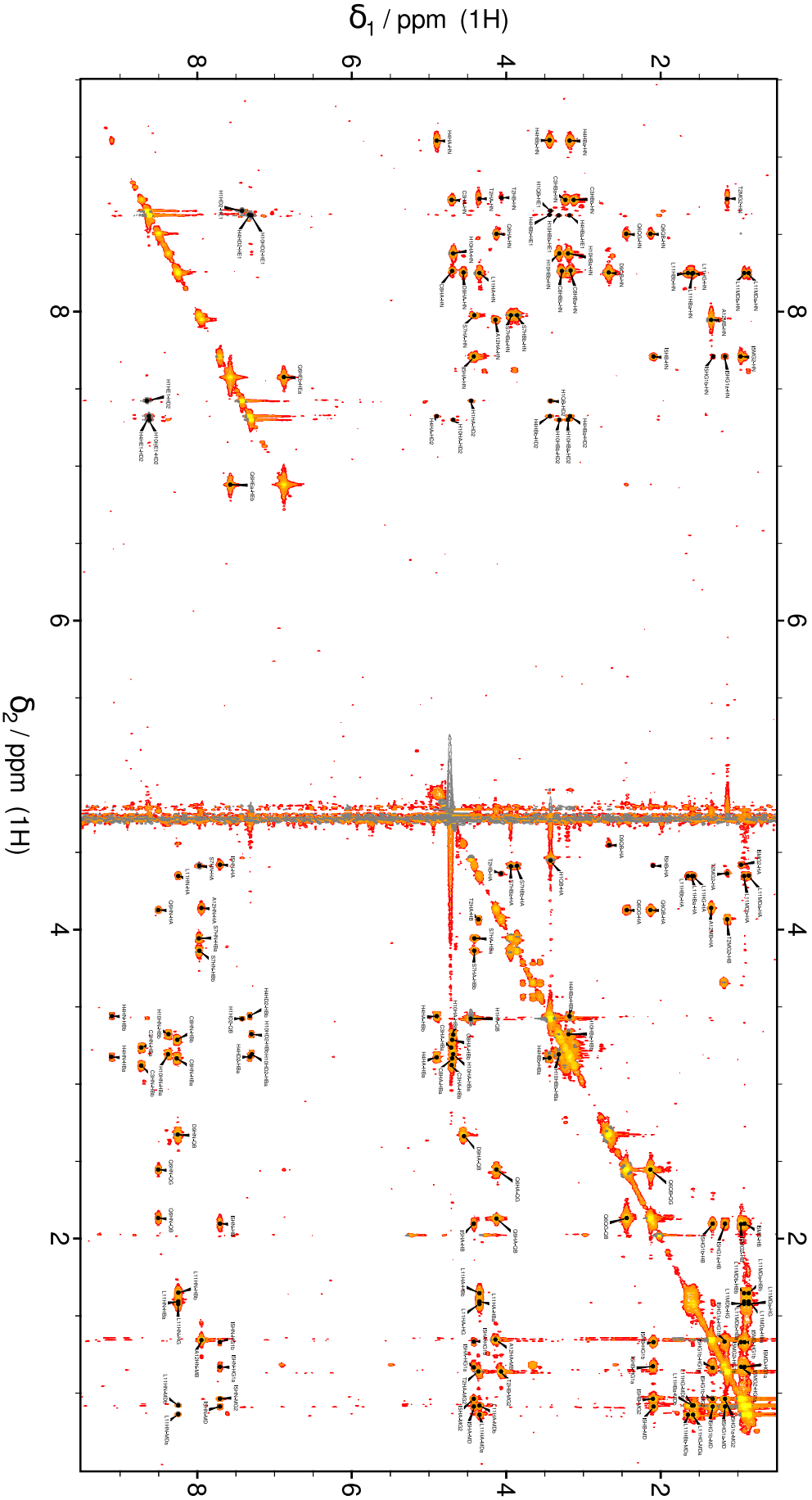

Fig. S21 ^{1}H-^{1}H TOCSY spectra of the peptide M3 Ga^{3+}-free.

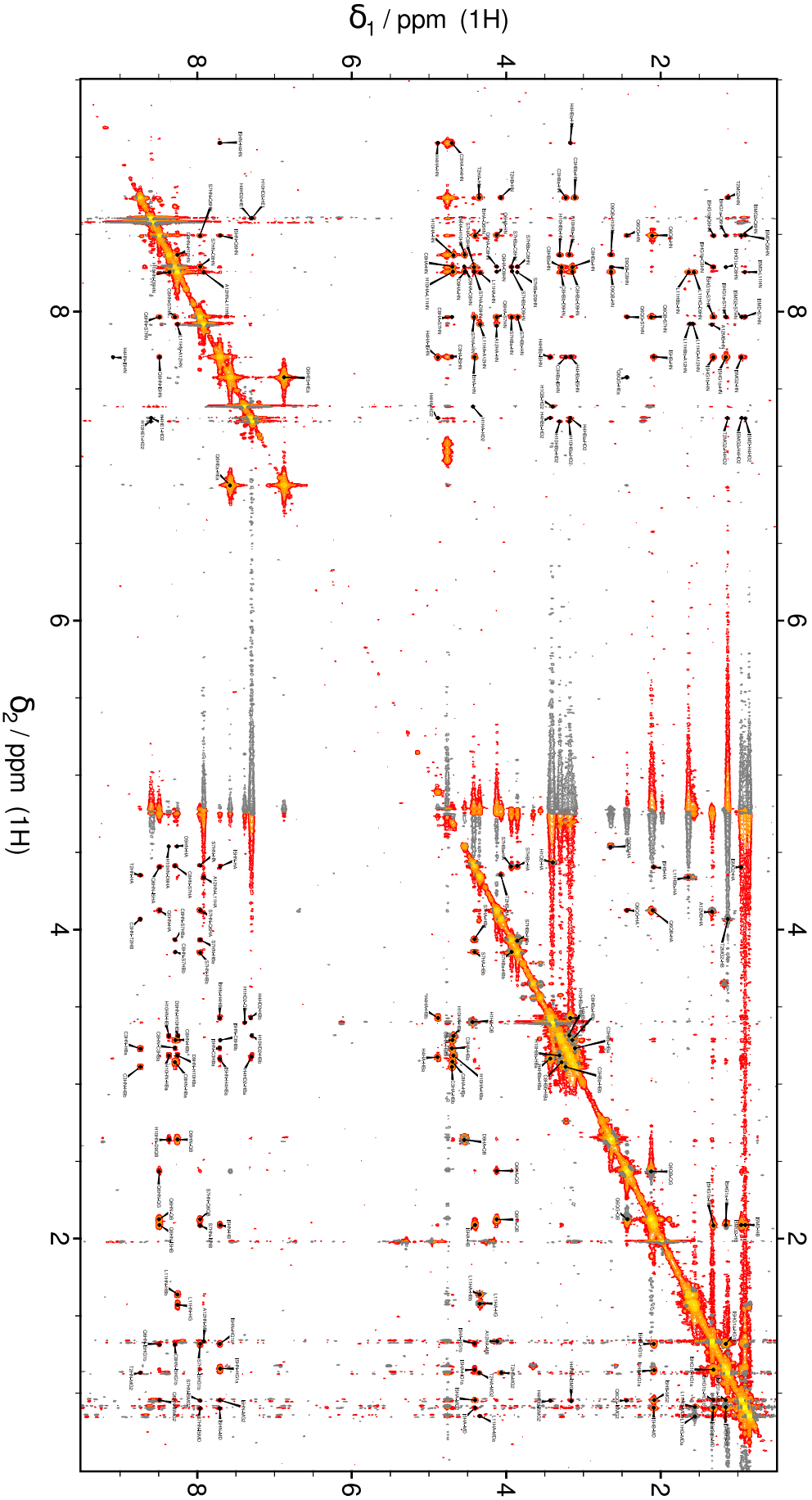

Fig. S22 ^{1}H-^{1}H NOESY spectra of the peptide M3 Ga^{3+}-free.

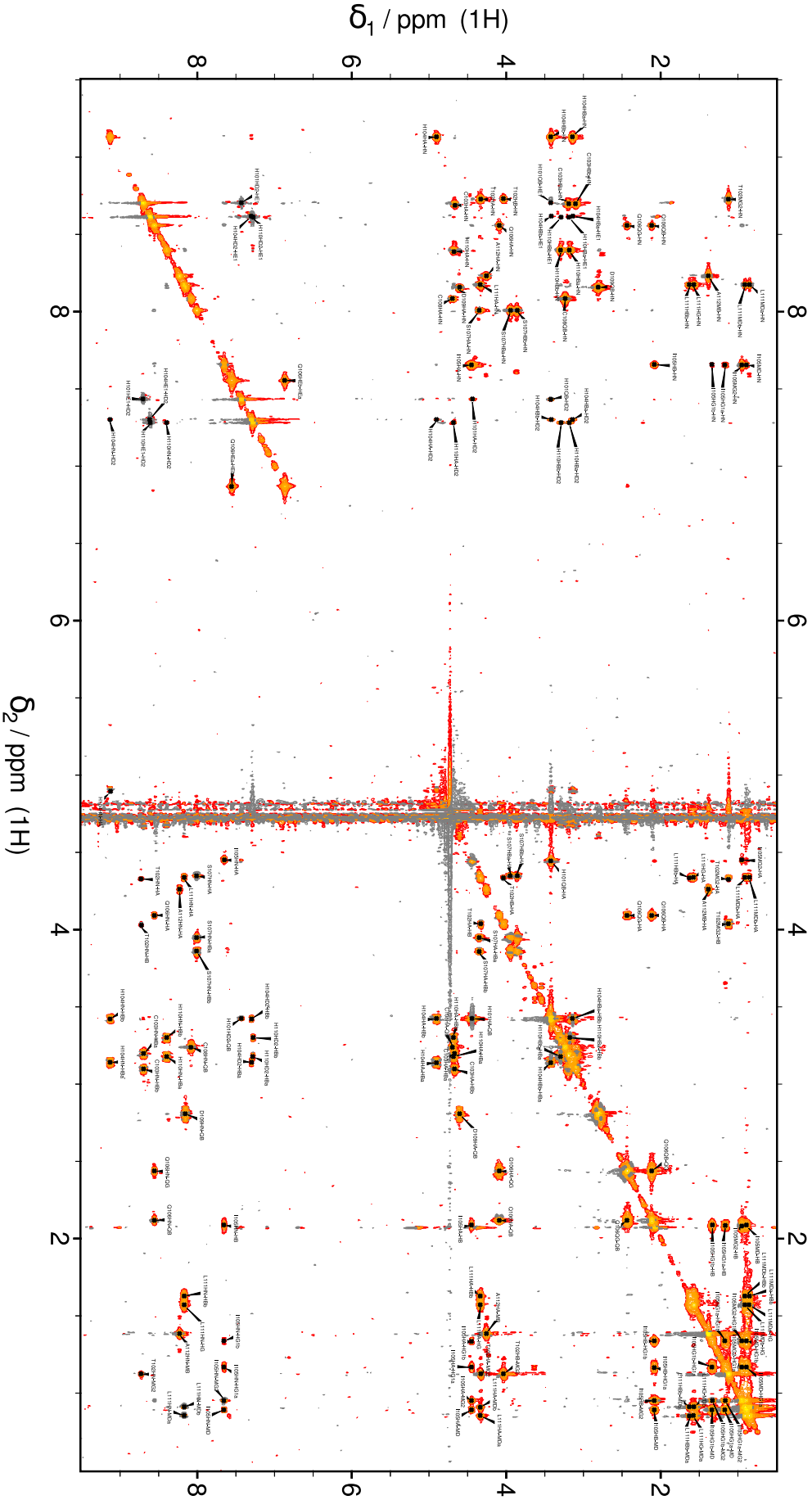

Fig. S23 ^{1}H-^{1}H TOCSY spectra of the peptide M3 Ga^{3+}-bound.

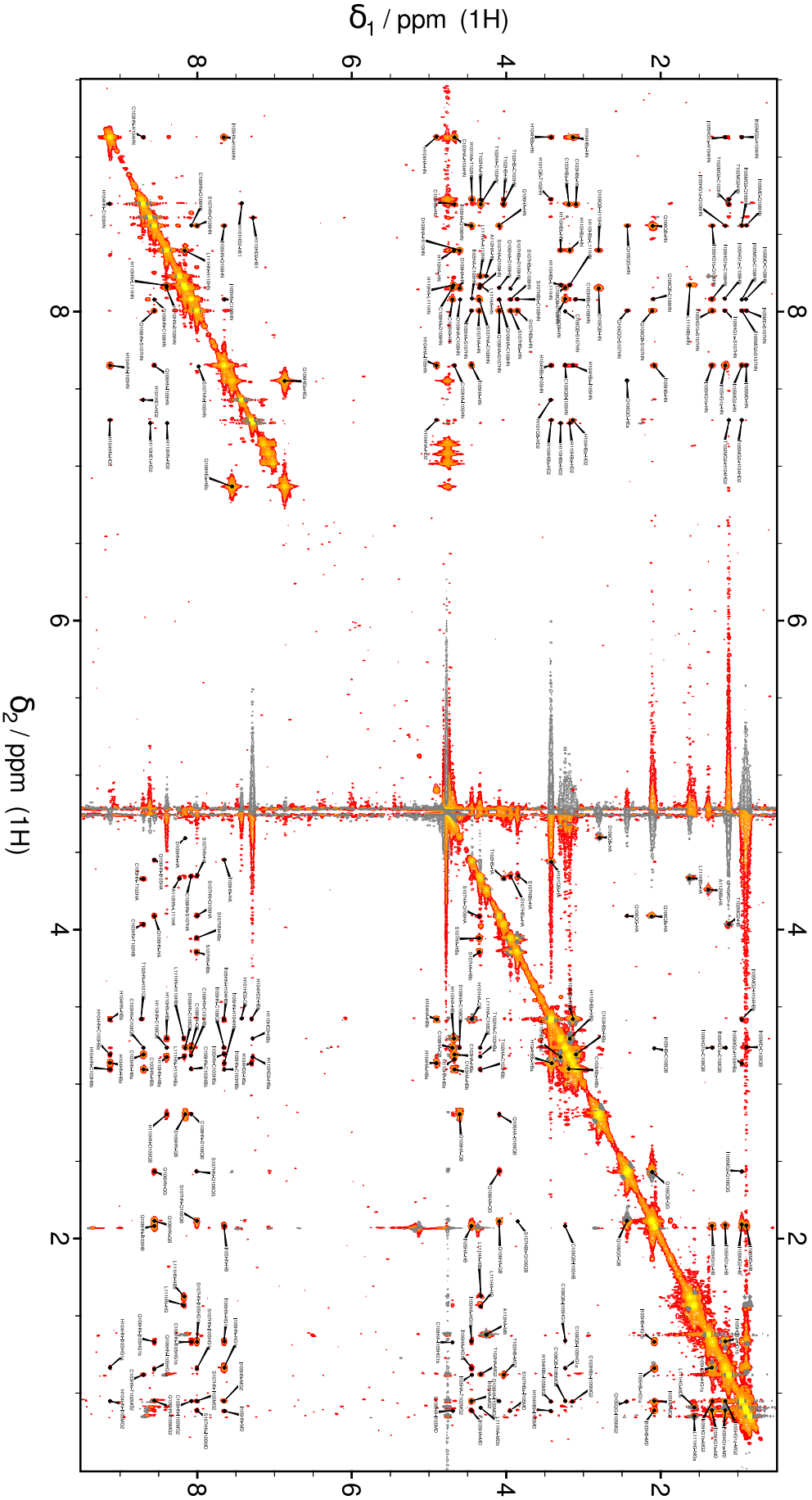

Fig. S24 ^{1}H-^{1}H NOESY spectra of the peptide M3 Ga^{3+}-bound.

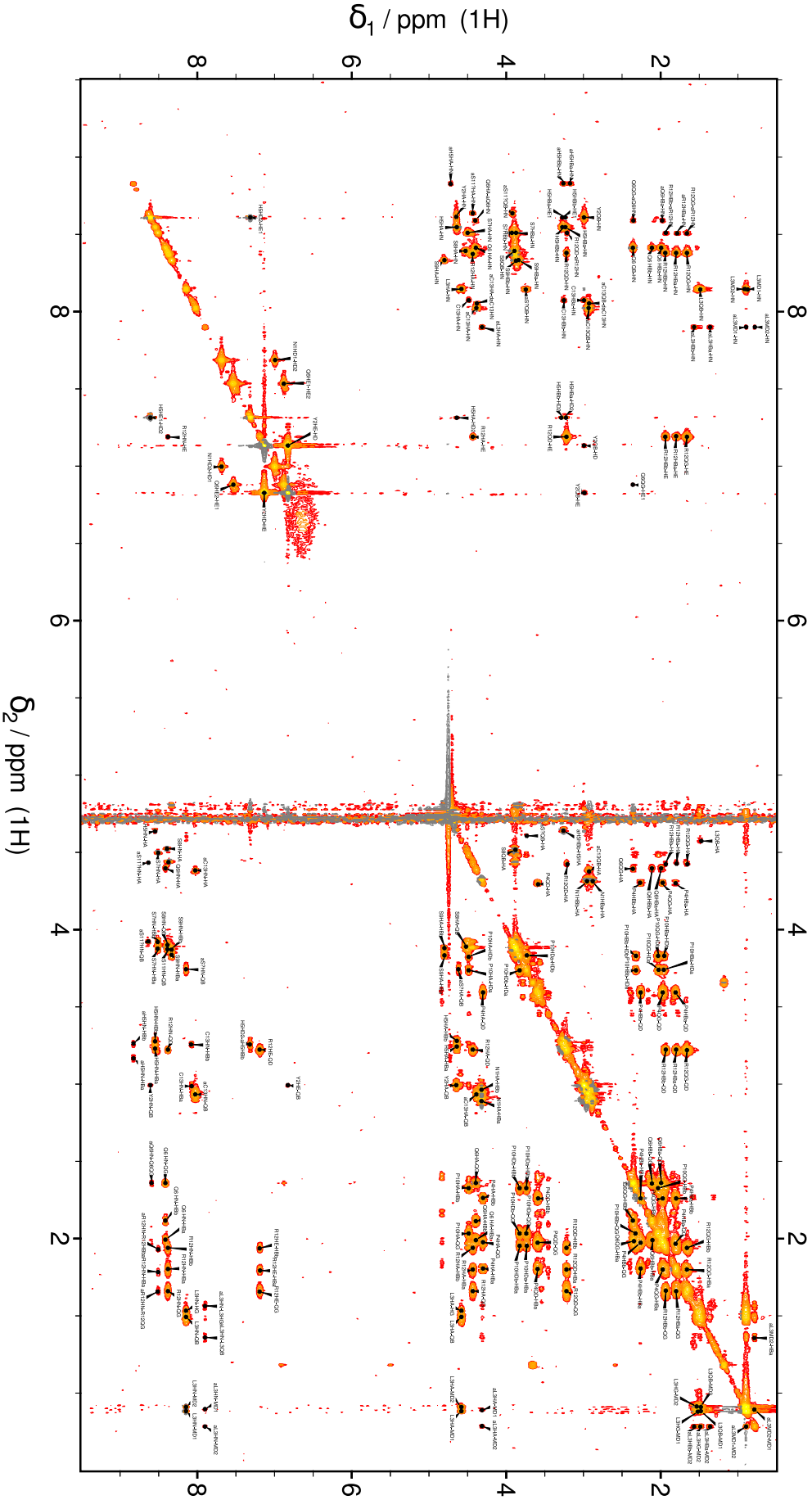

Fig. S25 ^{1}H-^{1}H TOCSY spectra of the peptide C3.15 Ga^{3+}-free.

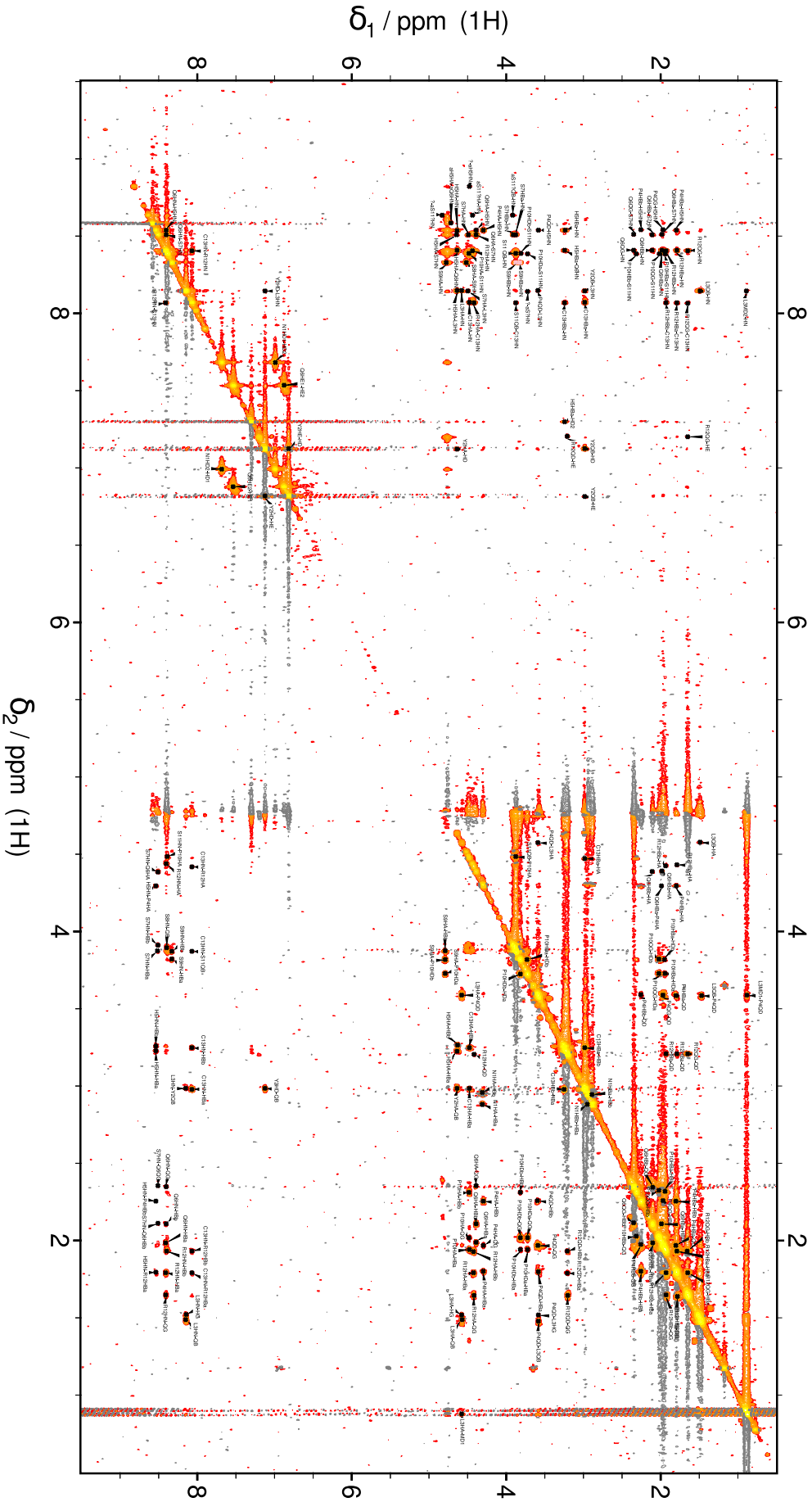

Fig. S26 ^{1}H-^{1}H NOESY spectra of the peptide C3.15 Ga^{3+}-free.

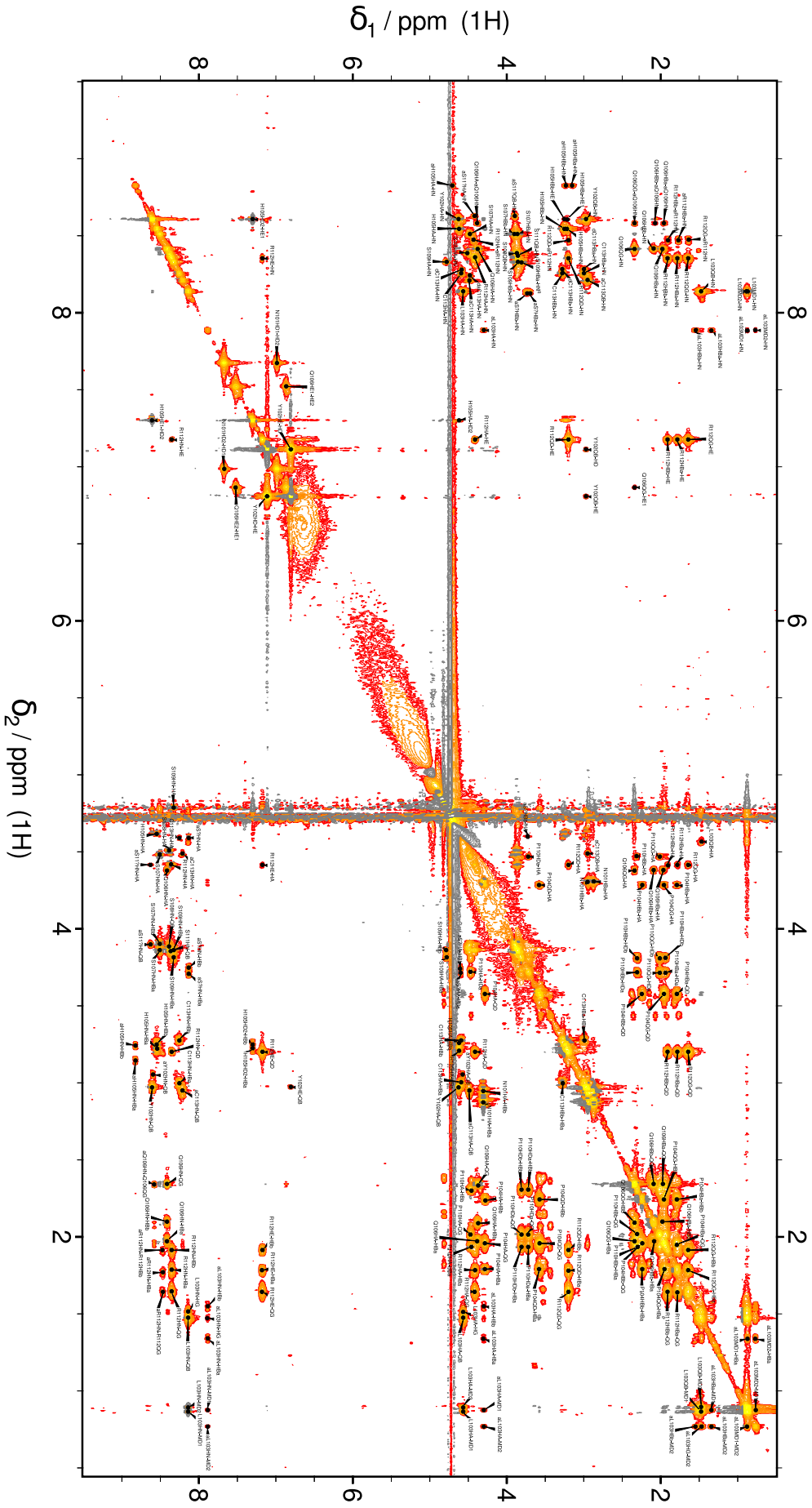

Fig. S27 ^{1}H-^{1}H TOCSY spectra of the peptide C3.15 Ga^{3+}-bound.

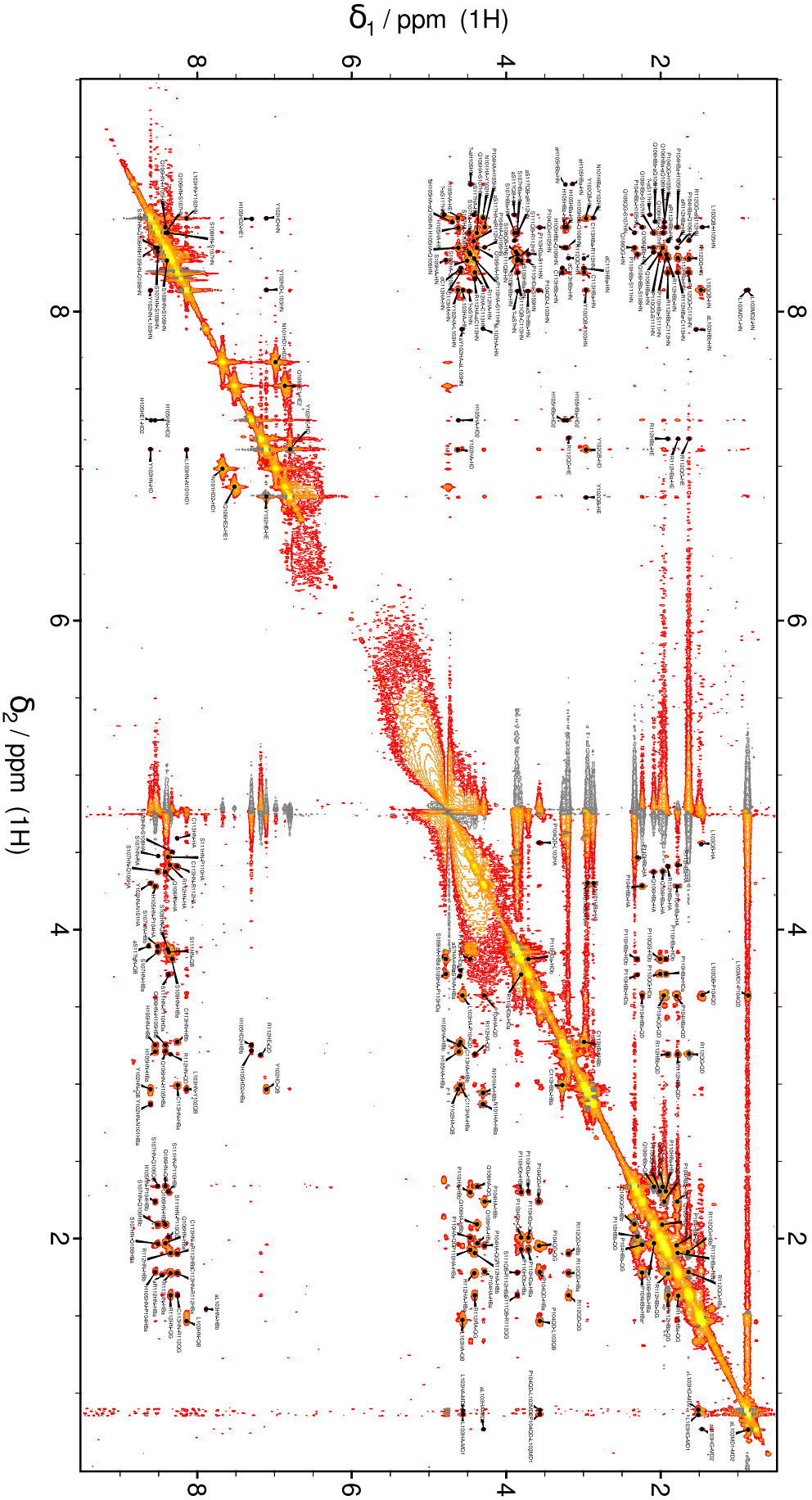

Fig. S28 ^{1}H-^{1}H NOESY spectra of the peptide C3.15 Ga^{3+}-bound.

Notes and references

38 E. F. Pettersen, T. D. Goddard, C. C. Huang, G. S. Couch, D. M. Greenblatt, E. C. Meng and T. E. Ferrin, *J. Comput. Chem.*, 2004, **25**, 1605–1612.

39 B. R. Brooks, C. L. Brooks, III, A. D. Mackerell, Jr., L. Nilsson, R. J. Petrella, B. Roux, Y. Won, G. Archontis, C. Bartels, S. Boresch, A. Caflisch, L. Caves, Q. Cui, A. R. Dinner, M. Feig, S. Fischer, J. Gao, M. Hodoscek, W. Im, K. Kuczera, T. Lazaridis, J. Ma, V. Ovchinnikov, E. Paci, R. W. Pastor, C. B. Post, J. Z. Pu, M. Schaefer, B. Tidor, R. M. Venable, H. L. Woodcock, X. Wu, W. Yang, D. M. York and M. Karplus, *J. Comput. Chem.*, 2009, **0**, 1545–1614.

40 J. C. Meza, *Wiley Interdisciplinary Reviews: Computational Statistics*, 2010, **2**, 719–722.

41 R. Fletcher and C. M. Reeves, *The Computer Journal*, 1964, **7**, 149–538.

42 S. Jo, T. Kim, V. G. Iyer and W. Im, *Journal of Computational Chemistry*, 2008, **29**, 1859–1865.

43 W. L. Jorgensen, J. Chandrasekhar, J. D. Madura, R. W. Impey and K. M. I, *J. Chem. Phys.*, 1983, **79**, 926–935.

44 M. H. M. Olsson, C. R. Søndergaard, M. Rostkowski and J. H. Jensen, *J. Chem. Theory Comput.*, 2011, **7**, 525–537.

45 J. Huang, S. Rauscher, G. Nawrocki, T. Ran, M. Feig, B. L de Groot, H. Grubmüller and A. D. MacKerell, *Nature Methods*, 2017, **14**, 71–73.

46 J.-W. Chu, B. L. Trout and B. R. Brooks, *J. Chem. Phys.*, 2003, **119**, 12708–12717.

47 L. Verlet, *Phys. Rev.*, 1967, **159**, 98–103.

48 J.-P. Ryckaert, G. Ciccotti and H. J. C. Berendsen, *J. Chem. Phys.*, 1977, **23**, 327–341.

49 W. G. Hoover, *Phys. Rev. A*, 1985, **31**, 1695–1697.

50 P. Eastman, J. Swails, J. D. Chodera, R. T. McGibbon, Y. Zhao, K. A. Beauchamp, L.-P. Wang, A. C. Simmonett, M. P. Harrigan, C. D. Stern, R. P. Wiewiora, B. R. Brooks and V. S. Pande, *PLOS Comp. Biol.*, 2017, **13**, 1–17.

51 P. P. Ewald, *Annalen der Physik*, 1921, **369**, 253–287.

52 W. F. V. Gunsteren and H. J. C. Berendsen, *Molecular Simulation*, 1988, **1**, 173–185.

53 D. Roe and T. Cheatham, *J. Chem. Theory Comput.*, 2013, **9**, 3084–3095.

54 D. A. Case, R. M. Betz, D. S. Cerutti *et al.*, *Amber 16, University of California, San Francisco.*, 2016, `http://www.ambermd.org`.

55 W. S. Cleveland and S. J. Devlin, *J. Am. Stat. Soc.*, 1988, **83**, 596–610.

56 *TURBOMOLE V7.0 2015, a development of University of Karlsruhe and Forschungszentrum Karlsruhe GmbH, 1989-2007, TURBOMOLE GmbH, since 2007; available from* `http://www.turbomole.com`.

57 S. Riahi and C. N. Rowley, *Journal of Computational Chemistry*, 2014, **35**, 2076–2086.

58 A. D. Becke, *J. Chem. Phys.*, 1993, **98**, 5648–5652.

59 C. Lee, W. Yang and R. G. Parr, *Phys. Rev. B*, 1988, **37**, 785–789.

60 S. H. Vosko, L. Wilk and M. Nusair, *Canadian Journal of Physics*, 1980, **58**, 1200–1211.

61 P. J. Stephens, F. J. Devlin, C. F. Chabalowski and M. J. Frisch, *J. Phys. Chem.*, 1994, **98**, 11623–11627.

62 F. Weigend, *Phys. Chem. Chem. Phys.*, 2006, **8**, 1057–1065.

63 S. Grimme, J. Antony, S. Ehrlich and H. Krieg, *J. Chem. Phys.*, 2010, **132**, 154104.

64 K. Eichkorn, O. Treutler, H. Öhm, M. Häser and R. Ahlrichs, *Chemical Physics Letters*, 1995, **240**, 283 – 290.

65 R. Bauernschmitt, M. Häser, O. Treutler and R. Ahlrichs, *Chemical Physics Letters*, 1997, **264**, 573 – 578.

66 A. Klamt and G. Schüürmann, *J. Chem. Soc., Perkin Trans. 2*, 1993, 799–805.

67 G. Schaftenaar, E. Vlieg and F. Vfriend, *J. Comput.-Aided Mol. Design*, 2017, **31**, 789–800.

68 T. Lu and F. Chen, *J. Comput. Chem.*, 2012, **33**, 580–592.

69 I. Mayer and P. Salvador, *Chemical Physics Letters*, 2004, **383**, 368 – 375.

70 I. Mayer, *Chemical Physics Letters*, 1983, **97**, 270 – 274.

71 M. Giambiagi, M. S. de Giambiagi and K. C. Mundim, *Structural Chemistry*, 1990, **1**, 423–427.

72 M. Giambiagi, M. S. de Giambiagi, C. D. dos Santos Silva and A. P. de Figueiredo, *Phys. Chem. Chem. Phys.*, 2000, **2**, 3381–3392.

73 P. Bultinck, R. Ponec and S. Van Damme, *J. Phys. Org. Chem.*, 2005, **18**, 706–718.

74 E. Matito, *Phys. Chem. Chem. Phys.*, 2016, **18**, 11839–11846.

75 E. R. Johnson, S. Keinan, P. Mori-Sánchez, J. Garcia-Contreras, C. A. J and W. Yang, *J. Am. Chem. Soc.*, 2010, **132**, 6498–6506.
76 J. Garcia-Contreras and W. Yang, *J. Phys. Chem. A*, 2011, **115**, 12983–12990.
77 R. F. W. Bader, *Chem. Rev.*, 1991, **91**, 893–928.
78 R. F. W. Bader and M. E. Stephens, *J. Am. Chem. Soc.*, 1975, **97**, 7391–7399.
79 A. D. Becke and K. E. Edgecombe, *J. Chem. Phys.*, 1990, **92**, 5397–5403.
80 W. Humphrey, A. Dalke and K. Schulten, *Journal of Molecular Graphics*, 1996, **14**, 33–38.
81 R Core Team, *R: A Language and Environment for Statistical Computing*, R Foundation for Statistical Computing, Vienna, Austria, 2013.
82 H. Wickham, M. Averick, J. Bryan, W. Chang, L. D. McGowan, R. François, G. Grolemund, A. Hayes, L. Henry, J. Hester, M. Kuhn, T. L. Pedersen, E. Miller, S. M. Bache, K. Müller, J. Ooms, D. Robinson, D. P. Seidel, V. Spinu, K. Takahashi, D. Vaughan, C. Wilke, K. Woo and H. Yutani, *Journal of Open Source Software*, 2019, **4**, 1686.
83 F. Delaglio, S. Grzesiek, G. W. Vuister, G. Zhu, J. Pfeifer and B. A, *J. Biomol. NMR*, 1995, **6**, 277–293.
84 W. Lee, M. Tonelli and J. L. Markley, *Bioinformatics*, 2014, **31**, 1325–1327.
85 B. Vögeli, J. Ying, A. Grishaev and A. Bax, *J. Am. Chem. Soc.*, 2007, **129**, 9377 – 9385.